Copyright Warning & Restrictions

The copyright law of the United States (Title 17, United States Code) governs the making of photocopies or other reproductions of copyrighted material.

Under certain conditions specified in the law, libraries and archives are authorized to furnish a photocopy or other reproduction. One of these specified conditions is that the photocopy or reproduction is not to be "used for any purpose other than private study, scholarship, or research." If a, user makes a request for, or later uses, a photocopy or reproduction for purposes in excess of "fair use" that user may be liable for copyright infringement,

This institution reserves the right to refuse to accept a copying order if, in its judgment, fulfillment of the order would involve violation of copyright law.

Please Note: The author retains the copyright while the New Jersey Institute of Technology reserves the right to distribute this thesis or dissertation

Printing note: If you do not wish to print this page, then select "Pages from: first page # to: last page #" on the print dialog screen

ABSTRACT

EFFECT OF POSTURAL TILT ON THE AUTONOMIC NERVOUS SYSTEM IN GULF WAR VETERANS

by
Shrenik Dagli

Time-frequency signal representations characterize signals over a joint time-frequency plane. They combine time-domain and frequency-domain analysis to yield a potentially more revealing picture of the temporal localization of a signal spectrum. Time-frequency distributions (TFDS) of signals map a one-dimensional function of time, x (t), into a two-dimensional function of time and frequency, $\rho(t, f)$. Most TFDs are "time-varying representations" which are similar conceptually to a musical score with time running along one axis and frequency along the other axis.

Many Gulf War Veterans complained of symptoms like unexplainable tiredness. This condition is known as the Gulf War Syndrome. The purpose of the research was to determine the changes occurring in the autonomic nervous system of these veterans under stress. Time frequency analysis of heart rate variability was used as a tool to compare the condition of Gulf War Veterans with Gulf War Syndrome with healthy Veterans.

A total of 27 Gulf War Veterans, 12 healthy and 15 sick, were subjected to a 45 minute tilt test at VA Medical Center, East Orange. Their age group is from 25 to 50 years. The ECG, blood pressure and the respiration of each subject was measured continuously during these 45 minutes.

From the raw ECG data, the interbeat beat intervals were extracted. From this data the power spectrum of heart rate variability, low frequency (LF) and high frequency (parasympathetic) activity (HF) with respect to change in time were obtained. The results were statistically analyzed and comparisons were performed on the data obtained from healthy and sick subjects before and during the tilt. The data were compared based on parameters like the age, low frequency activity (LF), high frequency activity (HF) and the ratio LF/HF.

The results indicated that for the same age group all veterans suffering from gulf war syndrome have lower autonomic activity (i.e. parasympathetic and sympathetic activity) than their healthy counterparts. Also a higher rate of drop in activity level with age of veterans suffering from gulf war syndrome is observed as compared to their healthy counterparts.

All the above indicators lead to the conclusion that veterans suffering from gulf war syndrome show lower autonomic activity in general as compared to healthy veterans, thus indicating a difference in functioning in their autonomic nervous system. This could be attributed to the gulf war syndrome. Our findings suggest that heart rate variability might be one of the indicators to evaluate gulf war syndrome.

EFFECT OF POSTURAL TILT ON THE AUTONOMIC NERVOUS SYSTEM IN GULF WAR VETERANS

by
Shrenik Dagli

A Thesis
Submitted to the Faculty of
New Jersey Institute of Technology
In Partial Fulfillment of the Requirements for the Degree of
Master of Science in Biomedical Engineering

Biomedical Engineering Committee

May 1999

APPROVAL PAGE

EFFECT OF POSTURAL TILT ON AUTONOMIC NERVOUS SYSTEM IN GULF WAR VETERANS

Shrenik Dagli

Dr. Stanley S. Reisman, Dissertation Advisor — Date
Professor of Electrical and Computer Engineering,
New Jersey Institute of Technology, Newark, NJ.

Dr. Peter Engler, Committee Member — Date
Associate Professor of Electrical and Computer Engineering,
New Jersey Institute of Technology, Newark, NJ.

Dr. John J. LaManca, Committee Member — Date
Research Coordinator of the NJ Fatigue Research Center,
Assistant Professor of Neurosciences, VA Medical Center, East Orange, NJ.

BIOGRAPHICAL SKETCH

Author: Shrenik Dagli

Degree: Master of Science

Date: May 1999

Undergraduate and Graduate Education:

- Master of Science in Biomedical Engineering,
  New Jersey Institute of Technology, New Jersey, USA, 1999

- Bachelor of Engineering in Electronics,
  University of Bombay, Bombay, India, 1997

Major: Biomedical Engineering

To my family

ACKNOWLEDGEMENT

I would like to express my gratitude to Dr. Stanley S. Reisman, served as my research supervisor, provided me with valuable guidance, encouragement and reassurance.

Special thanks to Dr. John LaManca for helping me with my research and answering all my questions. I am also grateful to the staff of the VA Medical Center, East Orange for providing me the support and infrastructure required for my research. Thanks to Dr. Engler for participating in my committee.

Finally I would like to thank my parents and all my friends for the invaluable support they gave me.

TABLE OF CONTENTS

TABLE OF CONTENTS
(continued)

Chapter Page

LIST OF FIGURES

Figure **Page**

LIST OF FIGURES
(continued)

Figure **Page**

LIST OF TABLES

Table **Page**

CHAPTER 1

INTRODUCTION

Biomedical engineering is the application of engineering and mathematical principles to medical science. The goal for its advancement is to develop tools for enhanced diagnosis and treatment of ailments that afflict mankind. The following work chronicles the research conducted on the utilization of time-frequency analysis as a non-invasive tool to quantify rapidly changing biological signals. The first step is to investigate the relevant physiology behind the human organs that are of interest.

1.1 The Heart

The cardiovascular system consists of blood vessels and the heart. In 1628, British physiologist William Harvey discovered that the cardiovascular system forms a circle, or circuit, so that blood pumped out of the heart through one set of vessels returns to the heart via a different set of vessels [1]. In actuality, there are really two circuits, both originating and terminating in the heart. Therefore, the heart, illustrated in Figure 1.1, is divided into two functional halves, each half containing two chambers: an atrium and a ventricle. The atrium of each side empties into the ventricle on that side. There is no direct flow between the two atria or the two ventricles in a healthy individual.

Blood is pumped by the pulmonary circuit from the right ventricle through the lungs and

ventricle, through all the tissues of the body except the lungs, and then to the right atrium. In both circuits, the vessels carrying blood away from the heart are called arteries, and those carrying blood from either the lung or all other parts of the body back to the heart are called veins.

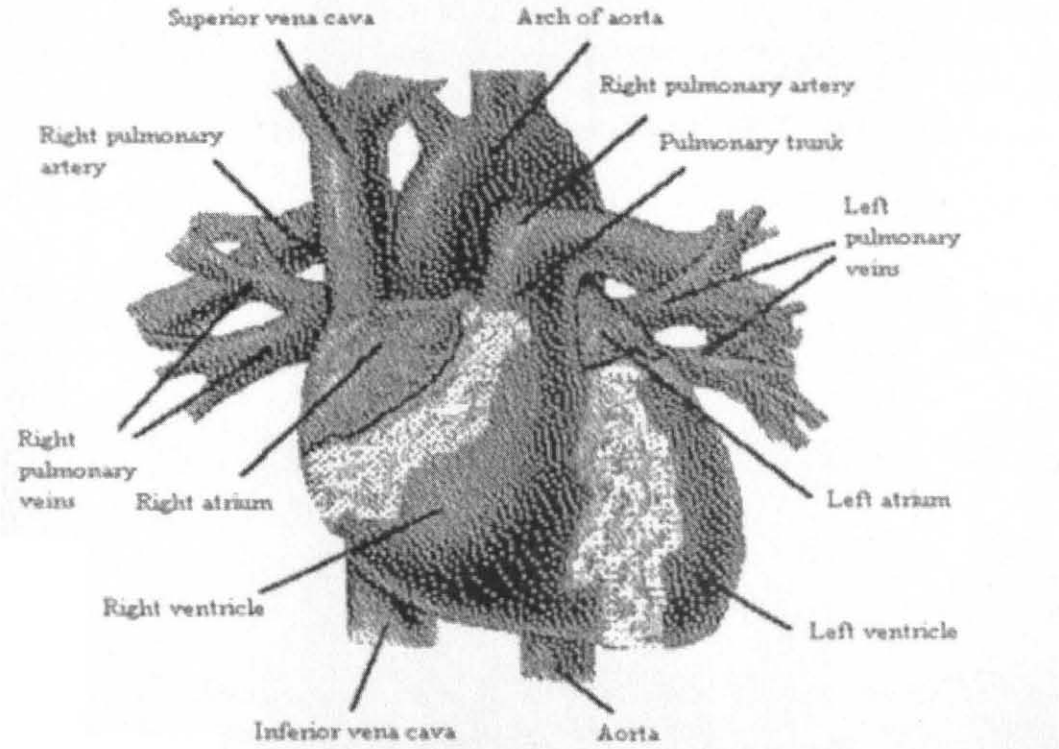

Figure 1.1 The Heart

(From A.J. Vander, J.H. Sherman, and D.S. Luciano, *Human Physiology, 1994*)

The heart is a muscular organ, which is enclosed in a fibrous sac called the pericardium [2]. The walls of the heart are primarily composed of cardiac-muscle cells called the myocardium. Cardiac-muscle cells combine properties of both skeletal muscle and smooth muscle. However, even more important, approximately one percent of the cardiac-muscle fibers have specialized features that are essential for normal heart excitation [1]. They constitute a network known as the conducting system of the heart and are connected to other cardiac-muscle fibers by gap junctions. The gap junctions allow action potentials to spread from one cardiac-muscle cell to another. Thus, the initial excitation of one myocardial cell results in excitation of all cells, which in turn results in the pumping action of the heart. The conducting system of the heart is shown in Figure 1.2.

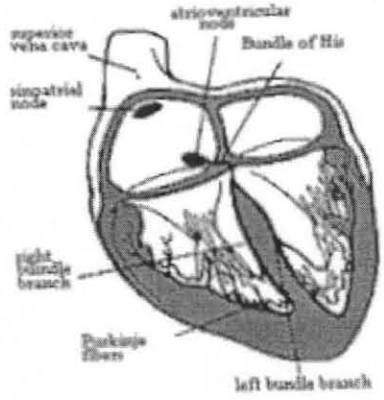

Figure 1.2 The conducting system of the heart
(From A.J. Vander, J.H. Sherman, and D.S. Luciano, *Human Physiology, 1994)*

The initial depolarization normally arises in a small group of conducting-system cells called the sinoatrial (SA) node. The SA node is located in the right atrium near the entrance of the superior vena cava. The SA node has the fastest inherent discharge rate of any of the myocardial cells with pacemaker activity. Therefore, the SA node is the normal pacemaker for the entire heart [1]. The action potential initiated in the SA node spreads throughout the myocardium, passing from cell to cell by way of gap junctions. The spread throughout the right atrium and the left atrium does not depend on fibers of the conducting system. The spread is rapid enough to depolarize the two atria and they contract at essentially the same time.

The spread of the action potential from the atria to the ventricles involves a portion of the conducting system called the atrioventricular (AV) node. The AV node is located at the base of the right atrium. The AV node has an important characteristic that makes the cardiac cycle more efficient. Because of the electrical properties of the cells that make up the AV node, the propagation of action potentials through the AV node results in a delay of approximately 0.1 seconds [1]. This delay allows the atria to finish contracting and, therefore, completely empty their contents of blood into their respective ventricles before ventricular excitation occurs.

Upon leaving the AV node, the action potential then travels to the septum, the wall between the two ventricles, by the conducting-system fibers called the bundle of His [2]. The bundle of His then divides into the left and right bundle branches which eventually leave the septum and enter the walls of their respective ventricles. These fibers then make contact with the Purkinje fibers, which are large conducting cells that

rapidly distribute the action potential throughout most of the ventricles. The rapid conduction along the Purkinje fibers and the distribution of these fibers cause the depolarization of the left and right ventricular cells to occur approximately simultaneously, thus resulting in a single coordinated contraction. Figure 1.3 illustrates the sequence of cardiac excitation within the heart.

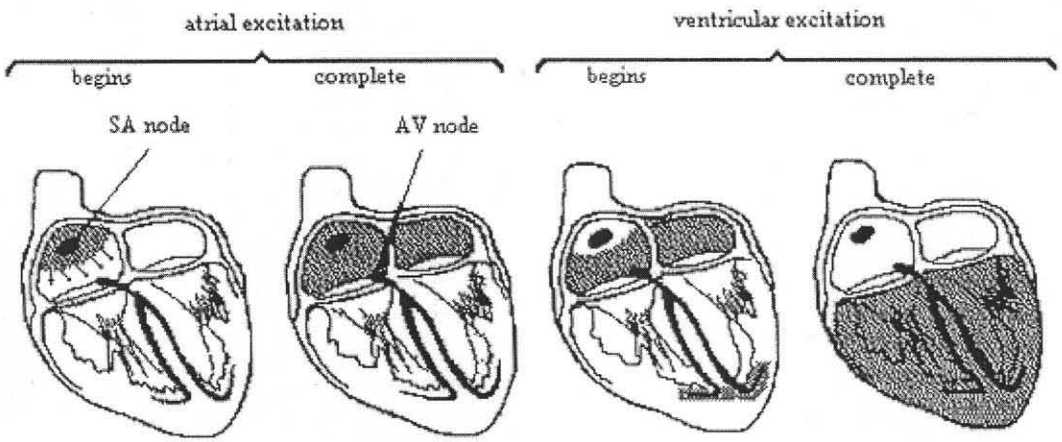

Figure 1.3 The sequence of cardiac excitation
(From A.J. Vander, J.H. Sherman, and D.S. Luciano, *Human Physiology, 1994)*

1.2 The Electrocardiogram

The electrocardiogram (ECG) is primarily a tool for evaluating the electrical events of the heart. The action potentials of cardiac muscles can be viewed as batteries that cause charge to move throughout the body fluids. These moving charges, or currents, represent the sum of the action potentials occurring simultaneously in many individual cells and

can be detected by recording electrodes at the surface of the skin [1]. Figure 1.4 illustrates a typical normal ECG recorded between the right and left wrists for one heartbeat.

The first deflection, the P wave, corresponds to the current flow during atrial depolarization (contraction). The second deflection, the QRS complex, is a result of ventricular depolarization. The third and final deflection is the T wave. The T wave is a result of ventricular repolarization (relaxation). It should be noted that atrial repolarization is usually not evident in the ECG because it occurs at the same time as the QRS complex.

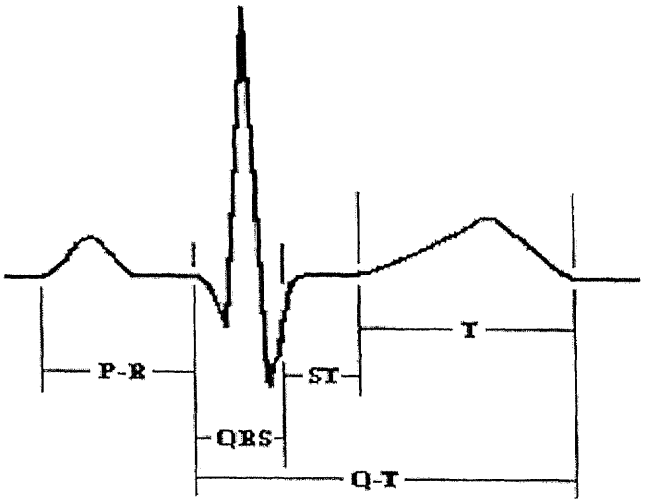

Figure 1.4 Illustration of a typical electrocardiogram

As mentioned earlier, the ECG is a measure of the electrical activity of the heart measured on the skin. The bipolar method of acquiring ECG detects electrical variations at two different locations on the skin and displays the difference to obtain one waveform. Figure 1.5 is an illustration of the standard limb lead connections that form Einthoven's

triangle. In addition, the diagram also shows the names of the respective leads. To record lead I, the negative terminal of ECG monitor is connected to the right arm (RA) and the positive terminal is connected to the left arm (LA). To record lead II, the negative terminal of the ECG monitor is connected to the right arm and the positive terminal is connected to the left leg. To record lead III, the negative terminal of the ECG monitor is connected to the left arm and the positive terminal is connected to the left leg (LL). The reference point or ground is connected to the right leg (RL).

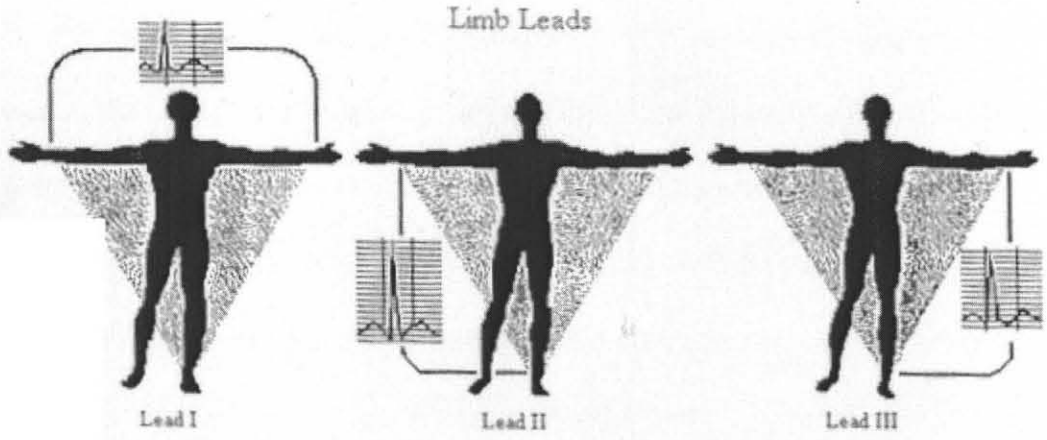

Figure 1.5 Standard ECG limb leads to form Einthoven's triangle

(From F. Netter. *The CIBA Collection of Medical Illustrations Volume 5, The Heart, 1981)*

It is important to note that when electrodes are attached in different configurations, a different waveshape will be obtained for the same electrical events occurring in the heart.

1.3 The Nervous System

Human behavior is controlled and regulated by two major communication systems- the endocrine system and the nervous system. The nervous system can be divided into two separate, but interconnected, parts. The first part consists of the brain and spinal cord and is called the central nervous system. The second part, which consists of nerves that extend from the brain and the spinal cord out to all points of the body, is called the peripheral nervous system.

The peripheral nervous system consists of both an afferent division and efferent division. The afferent division conveys information from primary receptors in the periphery of the body to the central nervous system. The efferent division carries signals from the central nervous system out to the effector cells in the periphery such as muscles and organs. The efferent division is subdivided into a somatic nervous system and an autonomic nervous system. The somatic nervous system consists of all the nerve fibers going from the central nervous system to skeletal-muscle cells. The efferent innervation of all tissues other than skeletal muscle is achieved by the autonomic nervous system [1].

1.3.1 The Autonomic Nervous System

The autonomic nervous system is the part of the nervous system that controls the visceral functions of the body. Regulation of internal activities such as blood pressure, heart rate, gastrointestinal motility, and body temperature, among many others, is performed by the

autonomic nervous system. Autonomic activity is controlled mainly by centers in the spinal cord, brain stem, and hypothalamus. Table 1.1 summarizes the effects of the autonomic nervous system on selected organs [1].

The autonomic nervous system is divided into two anatomical and functional units with opposite properties. The sympathetic nervous system is responsible for creating an increased level of activity in an organism. Anatomically, sympathetic nerves are composed of two neurons: a preganglionic neuron and a postganglionic neuron. These nerves pass from the spinal cord through the white ramus into one of the sympathetic ganglia before reaching their destination as shown in Figure 1.6. Most postganglionic sympathetic nerve endings secrete norepinepherine, a neurotransmitter that activates excitatory receptors, but in some cases can inhibit certain organs. The sympathetic nervous system is also responsible for the alarm or fight-or-flight response. This is caused by a mass discharge of all sympathetic nerve endings [2].

The parasympathetic nervous system, by contrast, generally lowers the activity of an organism, and is associated with a relaxed state. Anatomically, parasympathetic fibers leave the brain through cranial nerves III, V, VII, IX, and X, and the second and third sacral spinal nerves as illustrated in Figure 1.7. Cranial nerve X is also called the vagus nerve, and since the vagus innervates much of the thorax and abdomen, especially the

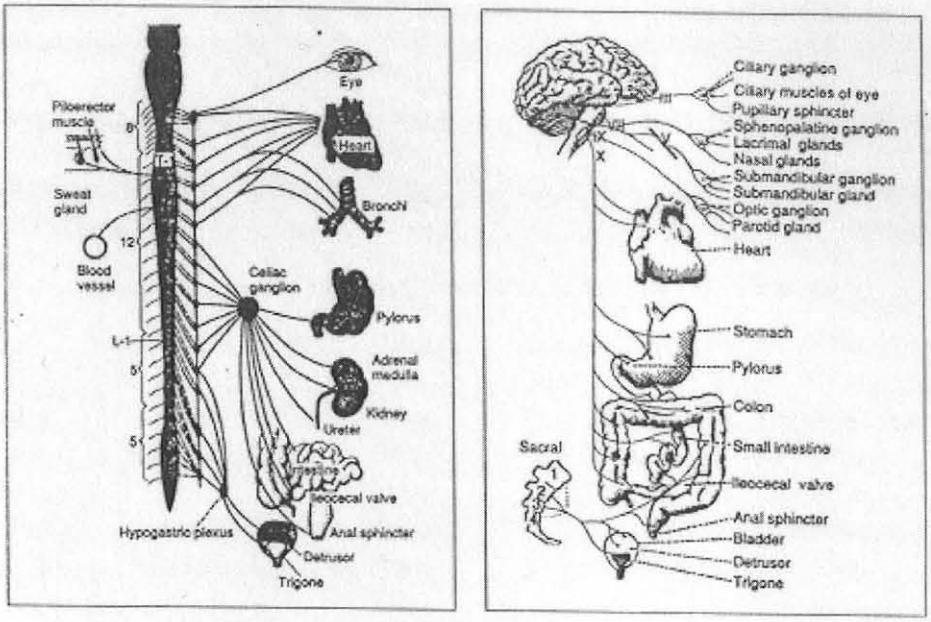

Figure 1.6 The sympathetic nervous system and The parasympathetic nervous system (from Guyton, A. C., Textbook of Medical Physiology, 1991)

heart, for the parasympathetic nervous system, parasympathetic activity is often called vagal activity. All parasympathetic nerve endings secrete acetylcholine. Although acetylcholine generally has an excitatory effect, it is also known to have inhibitory effects as well, such as the slowing of the heart by the vagus nerve [2].

Both the sympathetic and parasympathetic nervous systems are continually active. These basal rates of activity are known as sympathetic and parasympathetic tone. The advantage of tone is that it allows a single nervous system to increase or decrease activity in an organ. Arterioles except those supplying the sex organs are innervated by the sympathetic systems only. For instance, normal sympathetic tone keeps the systemic

arterioles constricted to approximately half their maximum diameter. By changing the degree of sympathetic tone, the diameter of the arterioles can be increased or decreased. Without tone, the sympathetic nervous system can only cause vasoconstriction, never vasodilation.

Table 1.1 Autonomic effects on selected organs of the body
(From A.J. Vander, J.H. Sherman, and D.S. Luciano, *Human Physiology, 1994)*

Effector Organ	Effect of Sympathetic Stimulation	Effect of Parasympathetic Stimulation
Eyes		
Iris muscles	contracts (dilates pupil)	relaxes (constricts pupil)
Ciliary muscle	Relaxes (flattens lens)	Contracts
Heart		
SA node	Increases heart rate	Decreases heart rate
Atria	Increases contractility	Decreases contractility
AV node	Increases conduction velocity	Decreases conduction velocity
Arterioles		
Coronary	Dilates (β_2); constricts (α)	Dilates
Skin	Constricts	None
Skeletal muscle	Dilates (β_2); constricts (α)	None
Abdominal viscera	Dilates (β_2); constricts (α)	None
Salivary glands	Constricts	Dilates
Lungs		
Bronchial Muscle	Relaxes	Contracts
Stomach		
Motility, tone	Decreases	Increases
Sphincters	Contracts	Relaxes

1.3.2 Stress and Behavioral Medicine Research of the Cardiovascular System

Growing interest in behavioral medicine has focused attention on the function and control of the cardiovascular system, partly because of its involuntary responsiveness to emotional and stressful situations. The external manifestations of cardiovascular responses provide objective indications of the changing psychological status of normal

subjects and patients. An expanding array of noninvasive techniques open opportunities for new and exciting research regarding the potential roles of psychological and behavioral factors in the development of dysfunction and disease [32].

In studies of stress, factors such as the context of the research situation, and subtle variations in the instructions presented can have significant effects on the resulting psychological, behavioral, and physiological responses. Specifically, both laboratory and field psychophysiology studies involve procedural elements, from the obtaining of informed consent to payment for participation, that can be significant sources of error variance that remain even if the most stringent experimental controls are instituted [33]. There is considerable evidence that the effects of physical stressors depend strongly on psychological factors, and that specific types of stressors can produce rather specific patterns of response [34][35]. There are numerous ways of dimensionalizing the tasks and stimulus situations that produce different patterns of bodily responses. However, implicit in the description of a stressor as psychological is that the individual's response to a challenging or stressful stimulus depends on the way that stimulus is interpreted or appraised, the context in which that stimulus occurs, and the personal resources available for coping [36][37]. A body of research demonstrates that if situations are viewed as harmful, threatening, or noxious, they can produce substantial physiological responses [34][37]. Conversely, when conditions are designed to change the demands of a stressor, or reduce the psychological threat that might be endangered by potentially aversive procedures, they may produce smaller and perhaps only minimal physiological responses and/or behavioral reaction [37].

1.3.3 Cardiovascular Response to Vigorous Exercise

The cardiovascular system must be capable of adapting rapidly and effectively to changing requirements to enable the relatively small blood volume to serve the vital needs of the millions of cells in the various organs of the human body. Living cells survive, function, and thrive only in stable chemical and physical environments from which they can easily extract the essential nutrients and oxygen while eliminating toxic products derived from their metabolic activities. Many different functions of tissues require different and widely varying blood flow rates under various conditions. An extreme example is the transition from rest to vigorous exercise during which the blood flow through large muscle masses increase many fold in response to their greatly increased metabolic activity and energy release. At the same time, blood flow to the skin is increased to dissipate heat. Despite curtailed blood flow through inactive tissues, the total blood flow through the systemic circulation is increased and the pumping action of the heart is both accelerated and enhanced instantaneously or even in anticipation of exertion. Diverse, integrated patterns of response occur automatically under many different circumstances induced by neural and hormonal control [32].

These involuntary control systems respond to various physical or psychological stresses by cardiovascular responses such as blushing, pallor, rapid pulse, fainting, or "palpitations" of the heart. The autonomic nervous system plays prominent roles in many aspects of cardiovascular response. As stated earlier, the parasympathetic nervous system acts through the vagus nerves to slow heart rate but has little direct influence on the peripheral vascular system. Conversely, the sympathetic nervous system acts to

accelerate heart rate, enhance the force of cardiac contraction, and can produce patterns of peripheral vascular responses that are appropriate for vigorous exertion. Since some of these reactions may emerge in anticipation of exercise, the central nervous system is the logical site of their origin [32]. Peronnet et al. [42] examined the cardiovascular and sympathetic profiles in response to a series of physical and mental challenges during recovery from an acute bout of aerobic exercise.

1.4 Heart Rate Variability

1.4.1 Physiology of Changes in Heart Rate

Change in heart rate is sensitive to changes in body temperature, plasma electrolyte concentrations, and hormone levels [1]. However, the most important influence of beat-to-beat variations of heart rate comes from the autonomic nervous system. More specifically, sympathetic activity increases heart rate, whereas activity in the parasympathetic (vagus) nerves causes the heart rate to decrease. Due to considerably more parasympathetic activity of the SA node than sympathetic activity in the resting state, the normal resting heart rate is below the inherent rate of 100 beats/minute.

The autonomic nervous system innervates the heart in a number of places. The sympathetic nervous system terminates at the SA node, the conduction system, atrial and ventricular myocardium, and coronary vessels. The parasympathetic fibers terminate in the SA and AV nodes, atrial and ventricular musculature. Interplay between the two systems will cause the heart to speed up or slow down, depending on which system is more active. Figure 1.8 illustrates autonomic innervation of the heart [3].

Perhaps the most important site of innervation of the autonomic nervous system on the heart occurs at the SA node. The SA node possesses an inherent discharge rate,

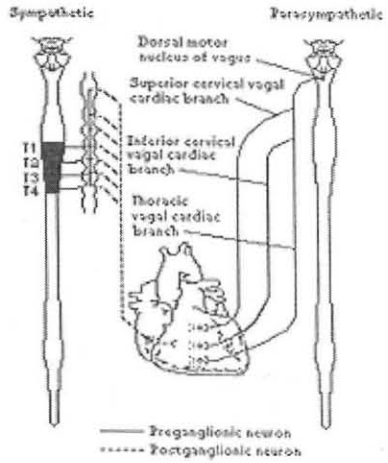

Figure 1.7 Autonomic innervation of the heart (from M.D. Kamath and E.L. Fallen, "Power spectral analysis of heart rate variability," *Crit. Rev. in Biomed. Eng.*, 1993)

often referred to as the pacemaker potential of approximately 100 beats/minute. The pacemaker potential is a slow depolarization of the cells of the SA node. The innervation of the sympathetic and parasympathetic nervous system on the SA node changes the characteristics of depolarization within the SA node cells, thus changing heart rate. Figure 1.9 illustrates these changes due to autonomic innervation [1].

For comparative purposes, the pacemaker potential labeled 'a' is the control. From the figure, one can observe that sympathetic stimulation (curve b) increases the rate of depolarization of the pacemaker potential. As a result, the SA node cells reach the threshold more rapidly, thus increasing the heart rate. Conversely, parasympathetic

stimulation (curve c) decreases the slope of the pacemaker potential. Consequently, the SA node cells reach the threshold more slowly, and heart rate decreases. In addition to decreasing the rate of depolarization of the pacemaker potential, parasympathetic stimulation also hyperpolarizes the plasma membrane of the SA node cells so that the pacemaker potential starts from a more negative membrane

potential. As a result, the time it takes the SA node cells to reach the threshold increases, which in turn decreases heart rate.

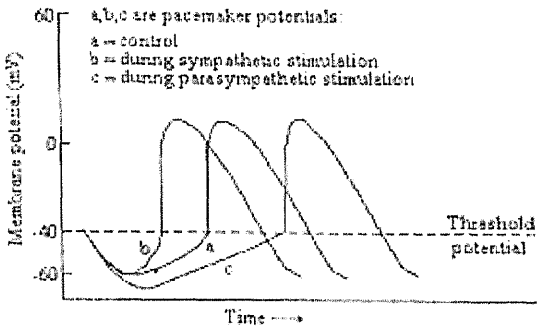

Figure 1.8 Effect of autonomic stimulation on the slope of the pacemaker potential (from A.J. Vander, J.H. Sherman, and D.S. Luciano, *Human Physiology, 1994)*

1.4.2 Heart Rate Variability as a Measure of Autonomic Function

Changes in heart rate usually involve the reciprocal action of the two divisions of the autonomic nervous system. An increased heart rate is usually the result of reduced parasympathetic tone coupled with an increased sympathetic activity. A decrease in heart rate is usually the result of increased parasympathetic tone and a simultaneous decrease in sympathetic tone. Therefore, changes in heart rate reflect the action of the sympathetic and parasympathetic nervous systems on the heart. However, under certain conditions, it is possible for heart rate to change by activity of only one division of the autonomic nervous system, independent of the other division, rather than reciprocal changes in both.

Initially, the effect of the autonomic nervous system on the heart was estimated by utilizing the traditional technique of average heart rate [3]. As a reference, the average heart rate was measured under normal resting conditions. Then the average heart rate was measured under the administration of drugs. The drugs used were atropine, which blocks the effects of the parasympathetic nervous system, and propranolol, which masks the effects of the sympathetic nervous system. A qualitative assessment can then be made of the autonomic nervous system by comparing the reference heart rate to the heart rate during the administration of the drugs. This method looks at the average over time of heart rate. However, when the ECG is looked at on a beat-to-beat basis, rather than over a period of time, fluctuations in the heart rate are observed [3].

1.4.3 Power Spectral Analysis of Heart Rate Variability

Power spectral analysis of heart rate variability is a potentially powerful tool for evaluating the activity of the autonomic nervous system noninvasively. The time domain signal used for computing the heart rate variability power spectrum is known as the interbeat interval (IBI). Spectral analysis of this interval between the R-waves in the ECG results in a graph similar to that shown in Figure 1.10. Three distinct peaks are usually evident. These peaks are defined as a very low frequency peak (0.02 Hz to 0.06 Hz), a low frequency peak (0.06 Hz to 0. 15 Hz), and a high frequency peak (0. 1 5 Hz to 0.4 Hz). Sometimes, a fourth peak is identified as the ultra low frequency peak, which consists of frequencies less than 0.0033 Hz.

Past research in power spectral analysis of heart rate variability correlates the three distinct peaks with certain physiological parameters [3]. The very low frequency band is associated with vasomotor control and temperature control. The low frequency band is associated with baroreceptor-mediated blood pressure control. The high frequency band has been linked with respiration.

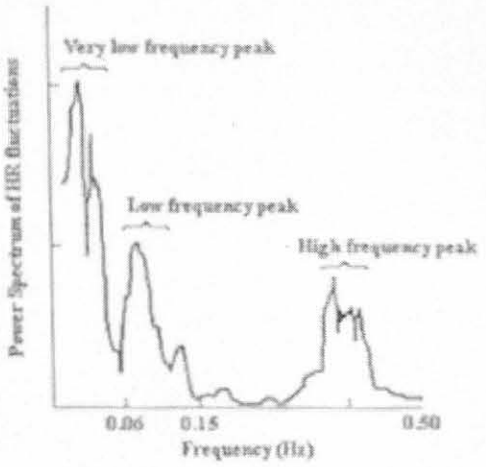

Figure 1.9 Typical power spectrum of HRV

(from M. Kamath and E. Fallen, "Power spectral analysis of heart rate variability," *Crit. Rev. in Biomed. Eng.,* 1993)

To date, the best known and best-defined peak in power spectral analysis of heart rate variability is the high frequency peak. The high frequency peak reflects changes in the interbeat interval that cycles up and down at the same frequency as respiration. This influence of respiration on heart rate has been known for more than one century and is called respiratory sinus arrhythmia (RSA). Properly defined, RSA is a rhythmical fluctuation in heart periods at the respiratory frequency that is characterized by a shortening and lengthening of heart periods in a phase relationship with inspiration and expiration, respectively [4]. RSA is being used increasingly as a measure of vagal control of the heart. As a result, the high frequency peak, which often occurs at the same frequency as the respiration peak, corresponds to the RSA and it is purely parasympathetic in origin [5].

From experience, one might contest that the frequency of respiration is not limited to within the narrow band of 0. 15 Hz to 0.4 Hz. The normal respiration rate can be as low as only a few breaths per minute at rest and as high as up to 40 breaths per minute during intense exercise [2]. This stresses the fact that, when doing research on heart rate variability to determine parasympathetic activity, the frequency of respiration must be known. More specifically, the power spectrum of the respiration waveform should be computed. In most of the literature, the area under the frequency band between 0.15 Hz to 0.4 Hz is considered parasympathetic in origin. However, it has been proven that in cases of intense physical activity, the upper limit in this band can reach as high as 0.75 Hz [6] .

Unlike parasympathetic activity, the sympathetic activity is not easily separated from the power spectrum of heart rate variability [3]. It has been hypothesized that the low frequency peak (0.06 Hz to 0. 15 Hz) is a mixture of both parasympathetic activity and sympathetic activity. A better concept that is used to isolate the sympathetic activity is that of "sympatho-vagal balance" which recognizes both reciprocal and non-reciprocal parasympathetic and sympathetic influences on heart rate by computing the low frequency to high frequency ratio [7]. An increase in the low frequency to high frequency ratio indicates an increase of sympathetic activity, a decrease in parasympathetic activity, or a reciprocal change in both.

1.5 Scope of Thesis

The ultimate goal of this research work is to use time-frequency analysis of heart rate variability to investigate the physical and mental exertion attributed to exercise. The aim of time-frequency analysis is to understand and develop tools that can describe rapid changes in a time varying spectrum. Expansion of the concept of spectral analysis of heart rate variability into time-frequency analysis gives us the ability to quantitatively assess the changes in the parasympathetic activity and sympathovagal balance as a function of time.

In this research, the analysis was performed on the 45 minute tilt data collected on Gulf War Veterans at the East Orange Veterans Affairs Medical Center. Programs developed in LabView were used to perform the time-frequency analysis on the tilt data while data acquisition was done using another software called SnapMaster. The research provides knowledge on how the parasympathetic and sympathetic activity of the veteran changes under stress. Analysis of the subjects was performed before stress when they lay in the supine position and during stress when they were in the tilt position. An effort was made to find out the changes occurring in the autonomic nervous system during tilt. The power spectrum of each subject in the interval starting from five minutes supine position and ending five minutes into the tilt position was observed using time-frequency analysis. This interval was analyzed to study the change in the autonomic nervous system of the gulf war veteran immediately after the veteran was tilted to 70 degrees.

CHAPTER 2

TIME FREQUENCY ANALYSIS

2.1 Introduction

Standard spectral analysis by Fourier transform or by constructing autoregressive models have been extensively applied in the attempt to evaluate quantitatively the fluctuations in beat-to-beat (R-R) intervals and respiration under steady state conditions [3]. Analysis over a long time window, usually 5-10 min, does not show information about the time-varying structure of the spectra. Instantaneous changes of the signal content, typical for cardiovascular signals, is thus smeared out or appears as a wideband noise. Therefore, it is a common practice that a reasonably "stationary" part of the signal is identified and analyzed. However, the spectral estimation is dependent on the chosen observation window, and consequently the interpretability of the results is limited [8].

Time analysis is among the standard methodologies used to study the signal x (t) as a function of time. Its main emphasis is on quantifying the energy, $|x(t)|^2 \Delta t$, which is the energy density in a small amount of time Δt, contained in that signal x (t) [22]. However if we want to gain more understanding of the components that constitute our signal, it is customary to investigate an alternative way of looking at the signal, "frequency analysis". Therefore, if we expand the signal as

we can think of $X(f)$ as the signal in the frequency-domain and $|X(f)|^2 \Delta f$ as the fractional energy in the frequency interval Δf at frequency f. Note that by inverting equation 2.1, we can define the signal in the frequency-domain [22].

$$X(f) = \int_{-\infty}^{\infty} x(t)\, e^{-j2\pi ft} dt \qquad (2.2)$$

where $X(f)$ is referred to as the Fourier Transform (FT) of $x(t)$.

Thus, the Fourier Transform and its inverse establish a one-to-one relation between time and frequency domain. Although the FT allows the passage from one domain to the other, it does not allow a combination of the two domains. In particular, most time information is not easily accessible in the frequency domain. While the spectrum X (f) shows the overall strength with which any frequency f is contained in the signal x (t), it does not generally provide easy to interpret information about the *time localization* of spectral components [44]. In Figure 2.1, we illustrate two cases, where each contains three sine waves of equal duration time of 4 seconds and frequencies of 5 Hz, 20 Hz and 35 Hz. The only difference among case (a) and (b) is that different frequencies occur at different times. The power spectrum, as shown in figure 2.2, is the same for the two signals. It shows that frequencies 5 Hz, 20 Hz and 35 Hz were present for both cases but does not show the specific duration of time they existed. To fully describe such a situation we have to give the frequencies for each particular time.

2.2 Joint Time-Frequency Analysis

Recently, joint time-frequency signal representation has received considerable attention as a powerful tool for analyzing a variety of signals and systems [8]. In particular, if the

frequency content is time varying as in signals of biological origin, then this approach is quite attractive. Although either the time domain description or its Fourier transform carries complete information about the signal, none of them reveals explicitly the frequency spectrum at a particular time or the time at which a particular frequency component occurs.

Time-frequency signal representations characterize signals over a joint time-frequency plane. They thus combine time-domain and frequency-domain analyses to yield a potentially more revealing picture of the temporal localization of a signal spectrum. Time-frequency distributions (TFDS) of signals map a one-dimensional function of time, x (t), into a two-dimensional function of time and frequency, $\rho(t, f)$. Most TFDs are "time-varying representations" which are similar conceptually to a musical score with time running along one axis and frequency along the other axis. The values of the TFD surface above the time-frequency plane give an indication as to which spectral components are present at each particular time [44]. The major drawback of separate time and frequency analysis is that they tell us the frequencies that existed for the total duration of the signal and not the duration when the different frequency components existed. However use of time-frequency analysis shows that one can fully describe the existence of a specific frequency at each instant of time.

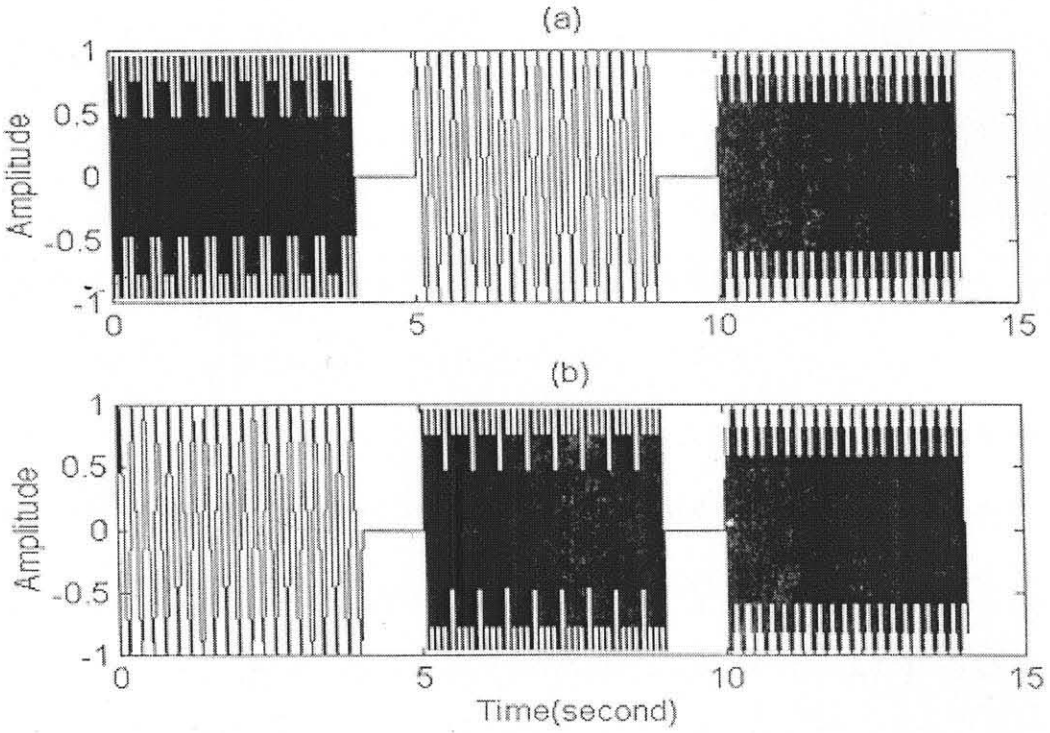

Figure 2.1 Two finite duration signals containing the same frequencies (5 Hz ,20 Hz and 35 Hz) occurring at different times

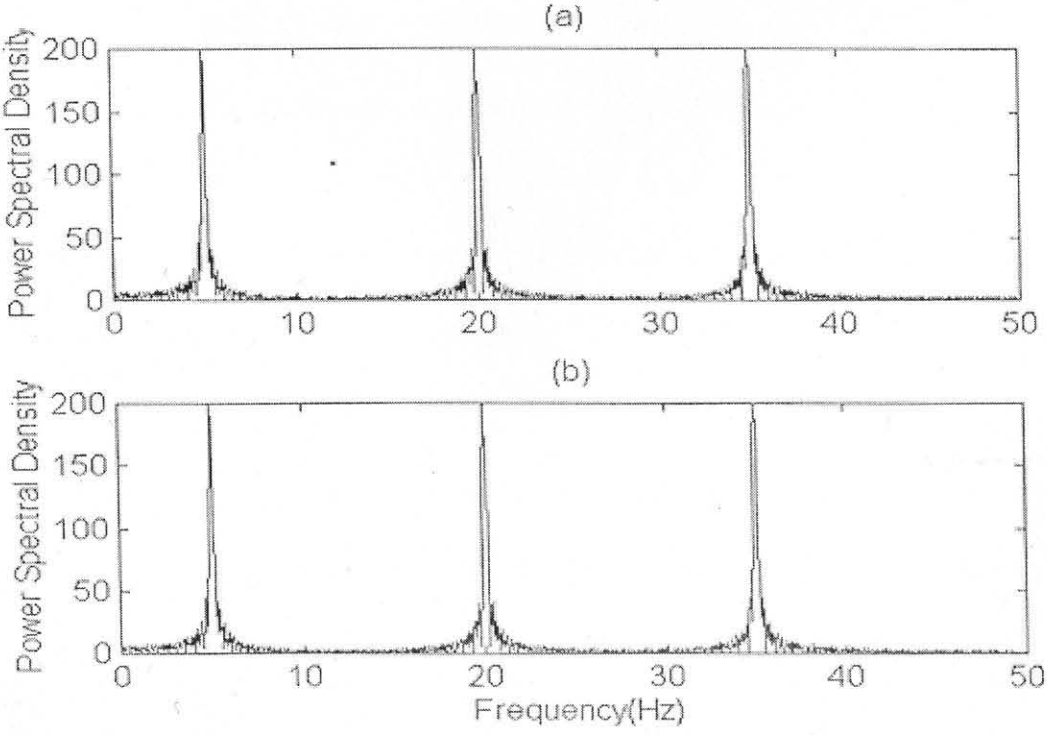

Figure 2.2 The power spectra for the 2 finite duration signals above the spectrum

2.2.1 Analytic Signal

For time frequency analysis it is usually convenient to work with the complex counterpart of a real signal. The main reason for using an analytic signal is that if the real signal is used then there is both a positive and a negative part to the spectrum which gives rise to cross terms between them. By eliminating the negative frequencies we eliminate the cross terms between it and the positive frequencies.

An analytic signal z (t) is a complex-valued signal whose spectrum is single-sided ($Z(f) \neq 0$ for $f > 0$). Because of this property of its spectrum, the imaginary part of the analytic signal is the Hilbert transform of the real part. Thus, to generate an analytic signal from a given signal, one should take the Hilbert transform of the signal, which would become the imaginary part of analytic signal.

2.2.2 General Class of Time-Frequency Distributions

Most popular time-frequency representations can be expressed in terms of the general bilinear time-frequency distribution representations proposed by Dr. Leon Cohen. This allows one to generate all time frequency distributions via a simple procedure. The mathematical formulation for the general class is [22]:

$$\rho_z(t, f) = \iiint_{-\infty} e^{j2\pi\nu(u-t)}\, g(\nu, \tau)\, z(u + \tau/2) z^*(u - \tau/2)\, e^{-j2\pi f}\, d\nu du d\tau \qquad (2.8)$$

The $g(\nu, \tau)$ is an arbitrary function called the kernel and it determines the characteristics of the time frequency distribution. Note that z is an analytic signal and z^* is the complex

conjugate of z. One of the most desirable properties of the kernel is the marginals property.

Time and Frequency Marginals:

For a given time if we added up the bits of energy at different frequencies we will get the total energy $|z(t)|^2$ at that instant of time. Also if for a given frequency we add all the timepieces we should get the total energy at that frequency $|Z(f)^2|$. That is if $z(t)$, $\rho_z(t, f)$ are signal and distribution of signal respectively then;

$$\int \rho_z(t, f)\, df = z(t) = z^*(t) = |z(t)^2| \tag{2.9}$$

Similarly;

$$\int \rho_z(t, f)\, dt = Z(f) = Z^*(f) = |Z(f)^2| \tag{2.10}$$

Let us integrate the left-hand side of equation w.r.t frequency (2.10)

From equation (2.8)

$$\int_{\infty} \rho_z(t, f)\, df = \int_{\infty} \iiint_{\infty} e^{j2\pi\nu(u-t)} g(\nu, \tau)\, z(u + \tau/2) z^*(u - \tau/2)\, e^{-j2\pi f}\, d\nu du d\tau df \tag{2.11}$$

Using the definition of the Fourier transform we can write;

$$\int_{\infty} e^{-j2\pi ft}\, df = \delta(\tau) \tag{2.12}$$

Hence

$$\int_{\infty} \rho_z(t, f)\, df = \iiint_{\infty} e^{j2\pi\nu(u-t)} g^*(\nu, \tau)\, z^*(u + \tau/2) z(u - \tau/2)\, d\nu du d\tau \tag{2.13}$$

$$\int_{\infty} \rho_z(t, f)\, df = \iint_{\infty} e^{j2\pi\nu(u-t)} g(\nu, 0) |z(u)|^2\, d\nu du \tag{2.14}$$

The only way equation (2.14) can be made equal to $|z(t)|^2$ is to take

$$\int_{\infty} e^{j2\pi\nu(u-t)} g(\nu, 0) d\nu = \delta(t-u) \tag{2.15}$$

which forces

$$g(\nu,0) = 1 \tag{2.16}$$

Similarly, we can show the condition on the kernel to satisfy the frequency marginal is

$$g(0,\tau) = 1 \tag{2.17}$$

The term marginal is borrowed from the common usage in probability theory. The historical origin of the term marginal can be best described with an example. Let us consider a grid where the horizontal axis is the frequency and the vertical axis is time of the population. In each box you put the energy at a particular time and frequency. Suppose we add up all the rows and write the number all the way to the left. These numbers indicate the total energy at a particular time. Similarly if you add all the columns and write the numbers on the bottom of the page then that will be the total energy at a particular frequency. You have written the number at the margin, hence the word "marginal".

2.2.3 Linear Time-Frequency Distribution

All linear time-frequency distributions (TFDS) satisfy the superposition or linearity principle which states that if $x(t)$ is a linear combination of some signal components, then the TFD of $x(t)$ is the same linear combination of the TFDs of each of the signal components [44].

$$x(t) = c_1 x_1(t) + c_2 x_2(t) \Rightarrow \rho_x(t, f) = c_1 \rho_{x1}(t, f) + c_2 \rho_{x2}(t, f) \tag{2.18}$$

Where $\rho_x(t, f)$, $\rho_{x1}(t, f)$, $\rho_{x2}(t, f)$ are time-frequency distributions of $x(t)$, $x_1(t)$, $x_2(t)$ respectively and c_1, c_2 are constant coefficients.

Linearity is a desirable property in any application involving multicomponent signals because there already exists powerful analysis techniques for signals with such a property. One linear TFD of basic importance is the short-time Fourier transform.

2.2.4 Short Time Fourier Transform

The short time Fourier transform was the first tool devised for analyzing a signal in the time-frequency domain [47]. This is done by extracting a small piece of the signal and taking its Fourier transform, and by continuing this process we show the existing frequency components at each instant of time. We can present this idea mathematically by first designing a window function, $h(\tau - t)$ which will emphasize the times around the fixed time of interest t. We then multiply the signal with the window function s(t) and take its Fourier transform:

$$S_t(f) = {}^{t+\Delta}\int_{t-\Delta} s(\tau)\, h(\tau-t) e^{-j2\pi ft}\, d\tau \qquad (2.19)$$

As this process is continued for each particular time we obtain a different spectrum. The totality of these spectra makes a time-frequency distribution. The energy density of the signal at the fixed time t is

$$\rho_{sp}(t, f) = \left| {}^{t+\Delta}\int_{t-\Delta} s(\tau)\, h(\tau-t) e^{-j2\pi ft}\, d\tau \right|^2 \qquad (2.20)$$

where $\rho_{sp}(t, f)$ is called the spectrogram. The spectrogram can be also written in terms of the Fourier transforms of the signal and window function.

$$\rho_{sp}(t, f) = \left| \int_{t-\Delta}^{t+\Delta} S(f') H(f-f') e^{-j2\pi ft} df' \right|^2 \quad (2.21)$$

where H(f), S(f)are Fourier transforms of the signal and window function respectively. Note equation (2.21) can be used to study the behavior of the signal around the fixed frequency of interest f. The spectrogram should not be thought of as a different distribution because it is a member of a general class of distribution [21].

The advantage of the short-time Fourier transform is that it has an easily understandable interpretation and is positive every where. This is a desirable property when we want to interpret the spectrogram as the signal energy distribution in the time-frequency plane.

One of the shortcomings of the short-time Fourier transform is the trade off between time and frequency resolution. Consider two extreme choices of the analysis window h (t). The first case is that of perfect time resolution, that is, if the analysis window h (t) is a Dirac impulse,

$$h(t) = \rho(t) \Rightarrow \rho_{STFT}\, \rho(t, f) = s(t) e^{-2j\pi ft} \quad (2.22)$$

where $s(t)$, $\rho_{STFT}(t, f)$ are the signal and short time Fourier transform of the signal respectively. In this case, the short time Fourier transform essentially reduces to the signal (t), preserving all time variations of the signal but not providing any frequency resolution. The second case is that of perfect frequency resolution obtained with the all constant window h (t) =1, then;

$$H(f) = \rho(f) \Rightarrow \rho_{STFT}(t, f) = S(f) \quad (2.23)$$

where H (f) , S(f) are Fourier transform of window and signal respectively. Here the short time Fourier transform reduces to the Fourier transform and does not provide any

time resolution. Therefore, because of the uncertainty principle, both h (t) and H (f) can not be made arbitrarily narrow.

Another shortcoming of the spectrogram is that it does not satisfy time and frequency marginal properties at the same instant. If we write the signal s (t) and window h (t) in terms of their amplitudes and their phase;

$$S(t) = A(t)\, e^{jv(t)} \text{ and } h(t) = A_h(t)\, e^{jvh(t)} \tag{2.24}$$

And similarly for their Fourier transforms

$$S(f) = B(f)\, e^{j\varphi(f)} \text{ and } H(f) = B(f)\, e^{j\varphi(f)} \tag{2.25}$$

Then the marginals are;

$$\int \rho_{STFT}(t, f)\, df = \int A^2(t')\, A_h^2(t' - t)\, dt' \tag{2.26}$$

$$\int \rho_{STFT}(t, f)\, df = \int B^2(f')\, B_h^2(f' - f)\, df' \tag{2.27}$$

These do not equal the instantaneous energy or energy density spectrum, namely $A^2(t)$ and $B^2(f)$ [21]. But they do approach them as we narrow the window in the respective domains. However window h (t) and H (f) can not be narrowed concurrently.

The short time Fourier transform is a linear signal decomposition, and there are no cross terms between signal components. However, the spectrogram is also a bilinear signal energy distribution due to the magnitude squaring operation. Thus, the spectrogram has cross terms that are not noticeable because they are inherently filtered out by a lowpass filter defined by the ambiguity function of the window [47].

2.2.5 Quadratic Time-Frequency Distribution

Although linearity of the TFD is a desirable property, the quadratic (bilinear) structure of a TFD is an intuitively reasonable assumption when we want to translate a TFD as a time-frequency energy distribution, since energy is a quadratic signal representation. All quadratic TFD satisfies the quadratic superposition principle, which is defined as [44]

$$x(t) = c_1x_1(t)+c_2x_2(t) \Rightarrow \rho_x(t, f) = |c_1|^2\rho_{x1}(t, f) + |c_2|^2\rho_{x2}(t, f)+c_1c_2\rho_{x1\,x2}(t, f)+c_2c_1\rho_{x2x1}(t, f) \quad (2.28)$$

where $\rho_x(t, f)$, $\rho_{x1}(t, f)$ and $\rho_{x2}(t, f)$ are the auto-time frequency distributions, and $\rho_{x1\,x2}(t, f)$ and $\rho_{x2\,x1}(t, f)$ are the cross time-frequency distributions of $x(t)$, $x_1(t)$, $x_2(t)$ respectively. c_1 , c_2 are constant coefficients. Thus, for an n-component signal $x(t)$ the TFD $\rho_x(t, f)$ will comprise n signal terms and = n (n-1)/2 cross terms [44], a fact that makes the visual analysis of the TFD of multicomponent signals difficult.

Among all the bilinear TFD with energetic interpretation, The Wigner distribution (WD) is the most widely studied and applied since it satisfies a large number of desirable mathematical properties.

2.3 Wigner Distribution

The Wigner Distribution (WD) has been employed as an alternative to overcome the shortcoming of the STFT. The WD was first introduced in the context of quantum mechanics [13] and revived for signal analysis by Ville [14]. It possesses very high resolution in both time and frequency, and it has many other nice properties as well. It has been successfully implemented for the analysis of several biological signals: circadian

rhythms of cardiac beats [15], ECG signal [16], blood flow velocity wave-forms [17], ultrasonic Doppler signals [18], auditory neuron activity [19], and acoustic signals [20]. The applicability of the WD for the analysis of blood pressure, respiratory, and beat-to beat fluctuations were also assessed by Novak, 1993 [8]. It was shown that the discrete Wigner distribution follows well the instantaneous changes of spectral content of cardiovascular and respiratory signals, which characterize the dynamics of autonomic nervous system responses. Two major drawbacks of the WD are that it is not necessarily nonnegative, and its bilinearity produces cross terms (or interference) between two signal components located at different regions in the time-frequency plane. This may lead to serious misinterpretations regarding the signal spectral contents. Many attempted to rectify these shortcomings by incorporating a smoothing window function in both the time and frequency domains, thus defining the smoothed pseudo Wigner Distribution. This provided better resolution in time and frequency and reduced the interference between the signal components.

Among all the bilinear TFD, the Wigner distribution (WD) is the most studied and applied [23]. The Wigner distribution can be obtained from the general class equation (2.8) by taking the kernel g (v, τ) = 1:

$$\rho_w(t, f) = \int_{-\infty}^{\infty} z(t - \tau/2)\, z^*(t+\tau/2) e^{-2j\pi f t}\, d\tau \qquad (2.29)$$

where ρ_w (t, f), z(t) and z* *(t)* are the Wigner distribution, an analytic signal and the complex conjugate of the analytic signal respectively. From equation (2.29) we see that for each particular time we are adding up pieces made from the product of the signal at a

past time multiplied by the signal at an equal future time. The Wigner distribution satisfies many properties, which are described as follows:

The WD is a real valued function that is;

$$\rho_w (t, f) = \rho_w^* (t , f) \tag{2.30}$$

Since the kernel of the WD is one for any value of v and r, then the complex conjugate of the kernel is always one. That is;

$$g (v, \tau) = g^* (-v, -\tau) = 1 \tag{2.31}$$

The WD satisfies the time and frequency shift properties as long as the kernel of the WD [g (v, τ) = 1] is not a function of time and frequency that is;

$$s (t) = z(t - t_0) \Rightarrow \rho_s (t, f) = \rho_z (t - t_0 , f) \tag{2.32}$$

$$s (t) = z(t)\, e^{j2\pi f_0 t} \Rightarrow \rho_s (t, f) = \rho_z (t , f - f_0) \tag{2.33}$$

where z (t), s(t), ρ_z (t, f) and ρ_s (t, f) are the signal, the shifted signal, the distribution of signal and the distribution of the shifted signal respectively. To prove this property one should take the kernel of the WD independent of time and frequency and set it equal to one, that is:

$$g(v, \tau) = 1 \text{ where } v \notin R_{\text{time}} \text{ and } \tau \notin R_{\text{frequency}} \tag{2.34}$$

Let $\rho_z (t , f)$, $\rho_s (t, f)$ represent the WD of the signal z(t) and the shifted signal s(t),then

$$\rho_s(t, f) = \int_{-\infty}^{\infty} z[\, t - \tau/2 - t_0]\, z^* [\, t + \tau/2 - t_0]\, e^{-2j\pi f t}\, d\tau \tag{2.35}$$

and

$$\rho_s(t, f) = \int_{-\infty}^{\infty} z[\, t - \tau/2\,]\, z^* [\, t + \tau/2]\, e^{-2j\pi f t}\, d\tau = \rho_z (t - t_0 , f) \tag{2.36}$$

To prove the frequency shifting one can use a similar argument.

The WD is uniquely related to the signal up to a constant phase factor [21]. To understand this idea, take the inverse Fourier transform of equation 2.29 with respect to f,

$$z[\, t - \tau/2]\, z^*\, [\, t + \tau/2] = \rho_w(t, f)\, e^{2j\pi ft}\, df \qquad (2.37)$$

Then, let:

$$t + \tau/2 \rightarrow t' \; ; \; t - \tau/2 \rightarrow t \text{ and } \tau \rightarrow t - t'$$

Which gives;

$$z(t)z^*(t') = \int \rho_w(t, f)\, [(t + t')/2\, , f)]\, e^{2j\pi f(t-t')}\, df \qquad (2.38)$$

Taking a particular value for $t' = 0$ and dividing both sides by $z^*(t')$, we obtain;

$$z(t) = 1/[z^*(0)] \int \rho_w(t/2, f)\, e^{2j\pi ft}\, df \qquad (2.39)$$

One can therefore recover the original signal from the Wigner distribution for a given resolution. The preceding relation can be used to determine whether a signal exists which will generate a given $\rho_w(t, f)$.

The Wigner distribution also satisfies the marginals properties. To prove these, one can use the constraint of the kernel for marginals properties that is;

$$g(v, 0) = 1 \text{ and } g(0, \tau) = 1 \qquad (2.40)$$

By inspection, the kernel of the Wigner distribution $g(v, \tau)$,satisfies both marginals. Thus, the Wigner distribution satisfies the total energy. Note the converse is not true [21]. For a finite duration signal the Wigner distribution is zero before the signal starts and after the signal ends [21]. If we have a band limited signal, the Wigner distribution will be zero for all frequencies that are not included in that band. These properties are

called the support properties of the Wigner distribution. In general the Wigner distribution is not zero when the signal is zero [47].

Consider the multicomponent signal z(t):

$$z(t) = z_1(t) + z_2(t) \tag{2.41}$$

The Wigner distribution is:

$$\rho_w(t, f) = \rho_{w11}(t, f) + \rho_{w22}(t, f) + \rho_{w12}(t, f) + \rho_{w21}(t, f) \tag{2.42}$$

where $\rho_w(t, f)$, $\rho_{w11}(t, f)$ and $\rho_{w22}(t, f)$are the auto Wigner distributions of $z(t)$, $z_1(t)$ and $z_2(t)$ respectively. The terms $\rho_{w12}(t, f)$ and $\rho_{w21}(t, f)$ are called the cross Wigner distributions. Therefore the Wigner distribution of the sum of the two signals is not the sum of their respective Wigner distributions. In general the Wigner distribution puts cross terms in between any two frequencies and any two times [21]. Figure 2.3 presents the Wigner distribution of a signal, which is the sum of two sine waves of one-second duration with frequencies of 100 and 400 hertz. Note the cross term in the middle of the

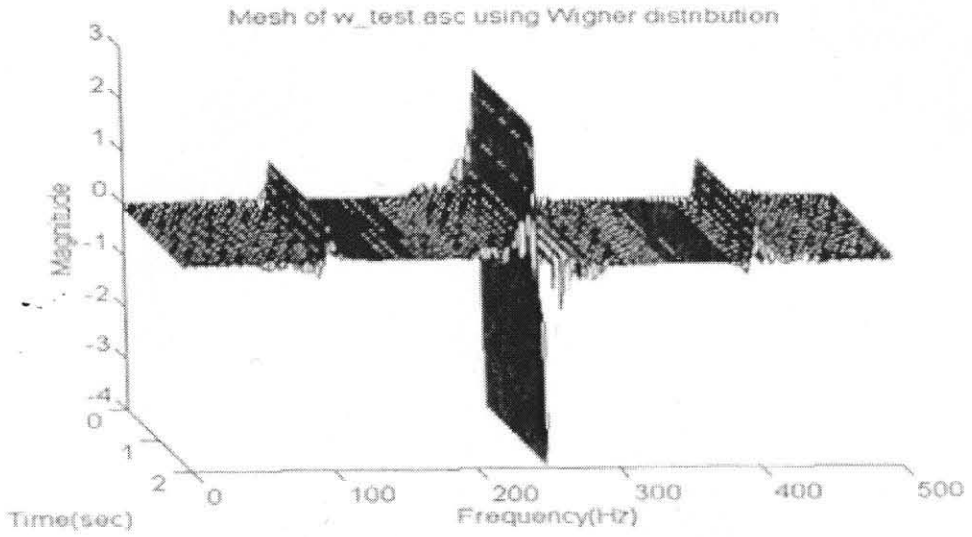

Figure 2.3 The Wigner distribution of the sum of two finite duration sine waves

two frequencies is 250 hertz. Another draw back of the Wigner distribution is that it always has negative regions throughout the time-frequency plane, except in the case of the Gaussian signal where the amplitude is modulated [22].

2.3.1 Windowed Wigner Distribution

In practice one is forced to calculate the Wigner distribution using equation (2.43):

$$\rho_w = \int_{t-\Delta}^{t+\Delta} h(\tau)\, z[t-\tau/2]\, z^*[t+\tau/2]\, e^{-j2\pi ft}\, d\tau \qquad (2.43)$$

where h(t) is a window function. This is due to the finite nature of the data. The resulting distribution has the effect of smoothing the Wigner distribution over frequency and is called the Pseudo Wigner distribution (PWD) [46]. The PWD sometimes results in a better-looking distribution in that certain cross terms are suppressed. One can clean the cross terms by smoothing the Pseudo Wigner distribution over time, which is called the Smoothed Pseudo Wigner distribution (SPWD). Smoothing the Pseudo Wigner distribution is performed as follows;

$$\rho_{ws}(t, f) = \iint_{window\,(L)} L(t - t', f - f').\ \rho_w(t', f')\, dt'\, df' \qquad (2.44)$$

where L , ρ_{ws} (t, f) and ρ_w (t, f) are smoothing function, the Smoothed Pseudo Wigner distribution and the Pseudo Wigner distribution respectively. The advantages of the Smoothed Pseudo Wigner distribution are that for certain types of smoothing, a positive distribution is obtained and the cross terms are suppressed. However smoothing destroys some of the desirable properties of the Wigner distribution: if L is taken to be independent of the signal, then the only way to obtain a positive distribution is by sacrificing the marginals properties [22].

2.4 Analysis using HRView: A Power Spectrum Tool

HRView developed by Boston Medical Technologies, Boston, MA, is a powerful software tool to compute and analyze the Power Spectrum of HRV. The *HRView* application suite now available in the market includes four major applications. These are:

1. HRVCAL, used for equipment calibration.
2. HRVACQ, used for acquiring HRV data.

3. HRVEDIT, used for editing HRV data after acquisition.
4. HRVANLYS, used for analyzing the acquired and edited HRV data.

In this research only the fourth application of HRView (HRVANLYS) was used since the data acquisition was performed using another tool called the SnapMaster explained in detail in section 3.1. Spectral analysis of HRV data requires the times at which R waves occurred. The output from the HRView gives the following information:

- Total power spectral density in the specified band
- Peak power spectral density in the specified band.
- Frequency at which the peak power spectral density occurs in the specified band

The standard FFT spectrum is a fast method of generating spectra. Power spectrum can be performed using either the Blackman Tukey or FFT spectral type. Various windows like Hanning, Blackman or Triangle can be chosen. In this research we have used FFT spectral type with Hanning window to be consistent with the research work done in the past. FFT spectra are computed with Hanning window to prevent aliasing. The following are the parameters in the HRView, which are relevant to be discussed in this context.

Time-Series Frequency

After the ECG is recorded an approximate time series which is a plot of the heart rate Vs time is presented on the screen. The *TS Frequency* in Hertz is the frequency at which this time series is generated. Since acquisition was not done using HRView this parameter takes the default 3 Hz value set by HRView.

Run Duration—this displays the total duration of the data run under analysis. In this study this value varies from 45 minutes to 50 minutes

Nyquist Freq—Theoretical maximum frequency that can be analyzed $= \left(\frac{1}{2(TS\ Frequency)} \right)$.

 # Pts FFT—sets the number of points in the time series used to develop each spectrum. This in turn determines the window length which displays the power spectrum. Custom setting has been used to set this parameter to 1121 points in order to view the five minutes interval.

If there are not enough actual time series data to fill out the window then each time series will be padded to its right with the mean value of the actual time series data shown on the screen. This will have implications on the associated analyses; primarily, the power spectral density will decrease in proportion to the amount of the padding. For example, if 70% of the data in the window is actual, and 30% is padded, the associated power spectral density will be 30% lower than would be expected if the entire window were composed of actual data.

CHAPTER 3

DATA ACQUISITION, ANALYSIS AND RESULTS

3.1 Data Acquisition

The ECG was acquired with a Quinton Q4000 Stress Test Monitor (Quinton Instrument Co., Seattle, WA), with electrodes placed in the three bipolar limb lead configuration. Output from the Q4000 was ECG leads I, II and III, plus a sync pulse, with amplitude of $3V_{p\text{-}p}$. The sync pulse is a short duration square wave pulse that is synchronized with the QRS wave of the ECG. The analog output voltage from the Quinton was the input to the DAS –16 card that was used to convert the Analog signal to Digital Signal. The DAS-16 was configured to accept three channels of data, each having an amplitude range of –5 volts to +5 volts. The output of the Quinton Q4000 was isolated from the DAS –16 card by an isolation amplifier to protect the subject from 120 volts electric shock. The ECG was sampled at 200 samples per second and is stored in binary format. Because there is no filtering between the Quinton and the Data acquisition board, the ECG was sampled at 200 samples per second to avoid aliasing due to 60 Hz. The signal was acquired using Snap Master data acquisition software.

3.1.1 Analog-to-Digital Conversion

A discrete time signal is defined by specifying the value of an analog signal only at discrete times, called sampling instant [45]. Once the sampled values are quantized and encoded, a digital signal results. A digital signal is formed from a continuous-time, analog signal by a process called analog-to-digital (A/D) conversion. A block diagram of an analog-to-digital converter is shown in Figure 3.1

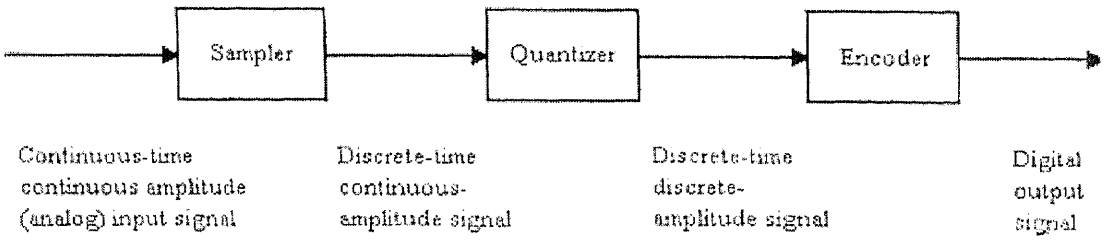

Figure 3.1 Block diagram of an analog-to-digital converter (from R. Ziemer, W. Tranter, and R. Fannin, *Signals and Systems: Continuous and Discrete, 1989)*

The first component is a sampler that extracts sample values from a continuous time continuous amplitude (analog) input signal at specified sampling instants. The output of the sampler is a discrete time signal with continuous amplitude because the sampled values assume the same continuous range of values assumed by the input signal. The second component in an A/D converter is a quantizer, which quantizes the continuous amplitude range of samples into a finite number of amplitude values. The last

component is an encoder, which maps each quantized sample value onto a digital word. For a binary representation, the number of quantizing levels q and the digital word length n are related by

$$q = 2^n \tag{3.1}$$

In order to be able to reconstruct the original signal from the sampled signal, there are three important points that must be followed. The first point involves the sampling rate, and is covered by the sampling theorem which states that a band limited signal, having no frequency components above f_h hertz, is completely specified by samples that are taken at a uniform rate with a frequency greater than or equal to $2f_h$ hertz. In other words, the time between samples is no greater than $1/2f_h$ seconds. The frequency $2f_h$ is known as the Nyquist frequency. To understand why the sampling frequency must be greater than twice the highest frequency in the signal, the spectrum of the input signal and the spectrum of the sampled signal are displayed in Figure 3.2. Figure 3.2(a) shows that the spectrum of the input signal is double sided, consisting of power at both positive and negative frequencies. Figure 3.2 (b) shows the spectrum of the properly sampled signal containing the spectrum of the original signal repeating at integer multiples of the sampling frequency. Figure 3.2 (c) shows the effect of sampling at too low of a sampling rate. This effect is known as aliasing, and makes it impossible to recover the original signal.

The second important point to be made about the reconstructing of the original wave from the sampled wave, is that a low pass filter must be used to pass only those frequencies contained in the original spectrum.

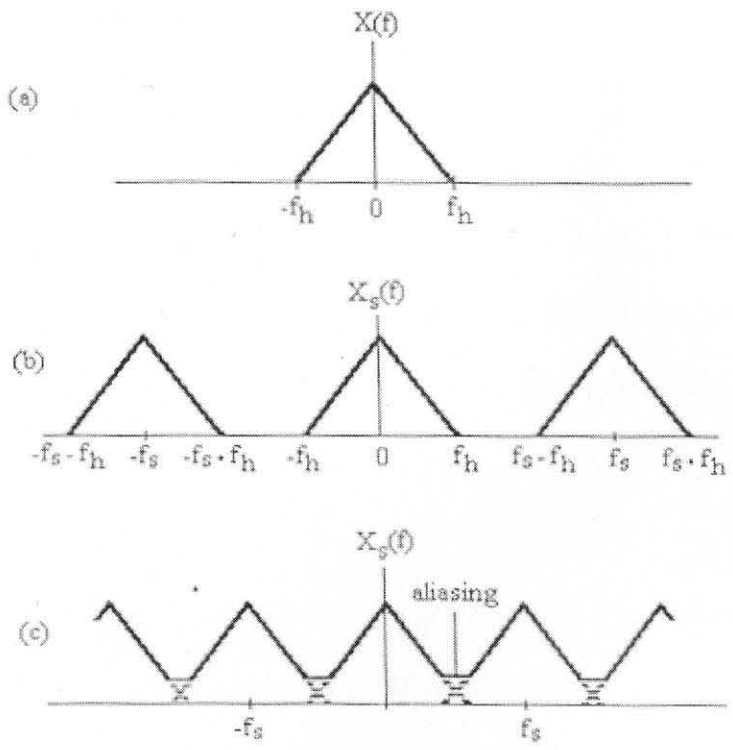

Figure 3.2 Spectrum of (a) the original signal (b) sampled signal and (c) improperly sampled signal (from R. Ziemer, W. Tranter, and R. Fannin, *Signals and Systems: Continuous and Discrete, 1989)*

To reduce the quantization error it is important to have enough quantization levels and to make sure the amplitude range of the signal uses all the quantization levels.

3.2 Data Analysis

3.2.1 Data Conversion

The ECG signal was collected using the Snap Master software and stored in binary format. This binary format was then converted to the ASCII format using the Snap Master software. Once this was done the ECG signal was scanned and cleaned for bad beats, undetected beats and for premature ventricular beats. This was done using S+, a highly enhanced statistical package. In order to scan the data into S+, the data was converted from Dos (operating system) to the Unix (operating system), to make it compatible to Unix (Solaris) platform on which S+ works. Once the scanning is done into S+ software program "do.ecg" programmed in S+, is run on the data file which picks the R- waves from the data file. Interactive graphs open up once the program is run and you can see the selected R waves. In order to clean the files of missed beats (R-waves) another program in S+, "fix.ecg" was run on the data file. This then produces interactive graphs on a sun workstation, which employs a protocol called the X-windows on the Solaris operating system. This lets you edit the data file and choose the proper R-beats. On the graph you have various options to edit the data file, like inserting and deleting the R- waves. Once this is done the data file is then edited to get it in the proper format that labview code can read. The format required consisted of two columns:

1. IBI in seconds from the last R-wave and tab delimited
2. Time in seconds of the R- wave.

This is the input to the HRView on which the power spectrum analysis is performed. Once the data was put into this format the data files were transferred from the

Unix machine to the PC on which the labview code runs. The Time Frequency code requires the first column to be in number of samples per second. An Excel worksheet was used to format and get the data in the required format. The code used to perform this is attached in the Appendix. Programs written in Perl, a Unix based language was used to remove the unwanted zeros, which appeared at the end of the file. (Attached in the appendix). Although the IBI represents the heart period at discrete points, the IBI signal is not suitable for FFT analysis because the discrete points, located at each R-wave, are not evenly spaced. In order to produce equidistant IBI samples suitable for analysis, the IBI signal must be interpolated [5]. The interpolation method used was that of a backward step function. This method assumes that no new information about the direction of the time series is available until the occurrence of the next heartbeat. Therefore, the amplitude of all the interpolated values between a beat at time T_{m-1} and the beat at T_m were set equal to the time difference between T_m and T_{m-1}. The interpolated interbeat interval (IIBI) is then sampled to produce an IIBI with evenly spaced samples. The final step to obtain the HRV signal used in our analysis is to decimate the IIBI signal by a factor of ten (the ECG is sampled at 200 Hz). When the signal is decimated by a factor of ten, every tenth point of the original signal is kept, and the nine points in between are not used. This can be done because the IIBI signal contains no frequency components above 6 Hz. Once this decimation is done the analysis is done by FFT using the LabView code. The results from these data file are stored in postscript format.

Stationarity

A stationary time series is characterized by the fact that the statistical portion of the series does not depend on the time but rather depends on the difference between time points. In particular, the series will have :

- Constant mean .
- Correlation between differences at two different time points depends only on how far apart they are.

The series is not stationary if,

1.The mean level is not constant over time.

2.The extent of deviations is changing over time.

3.3 Subjects and Experimental Protocols

3.3.1 Protocol

A total of 27 subjects participated in the study designed by Dr. Lamanca. The age of the subjects ranges from 25 to 50 years. Each subject was instructed not to consume any food or drinks containing caffeine after the midnight before the test and made to sign on an "Informed Consent" form. Also they were instructed not to consume any food 3 hours prior to the test. The subjects were classified as healthy veterans and veterans with gulf war syndrome. About 15 subjects were suffering from the Gulf War Syndrome. 12 subjects were considered healthy veterans. The symptoms of The gulf war syndrome are unexplained tiredness. The classification was done on the basis of the heart-related diseases and health history. The health history was easy to obtain, since a record of the

veterans health was available with the Armed forces. No person having a history of heart diseases was tested.

The protocol consisted of the subject being tilted to 70 degrees for 45 minutes. Initially when the subject arrived, the breathing and blood pressure responses were measured, as the subject lay supine for about 20 minutes. The patient was secured to the table with straps across the legs and lower chest. Electrodes were put around the chest and neck area to record heart rate. A Finapres was used to measure the blood pressure. After this the table was inclined to an angle of 70-degree and the subject remained at this angle for 45 minutes. During this interval data related to ECG and respiration was collected. After this time interval the subject was lowered to a supine position for 5 minutes.

Table 3.1 General Information about each subject

Subject	Sex(M/F)	Age(Years)	Height(Cm)	Weight(Kg)
V001	M	38	163.8	72.3
V002	M	40	188	90.5
V004	M	30	179.1	75
V006	M	27	175.1	87.3
V007	M	29	167.6	74
V010	F	27	148.6	52.7
V012	M	28	175.26	72.27
V013	F	32	162.56	80
V019	M	28	181	85.15
V025	M	31	167.64	98.7
V030	F	47	170	65.25
V032	M	34	185.42	79.2
V039	M	27	165.5	79
V041	M	50	180.3	84.5
V042	M	31	175.89	96.75
V045	M	29	173.8	87
V047	M	28	172	63.34

Table 3.1 (continued)

Subject	Sex(M/F)	Age(Years)	Height(Cm)	Weight(Kg)
V051	F	36	134.6	83.2
V052	M	25	175.26	81.45
V053	M	26	179	103
V055	M	28	176	77.4
V057	M	32	169	95
V060	M	30	170	125
V062	M	28	187	95
V064	M	28	180	72.45
V067	F	31	172.7	73.5
V082	M	49	172.7	66.6

3.4 Results

The tilt data was investigated using the LabView code, Wigner (See Appendix A). This Labview code performs time frequency analysis using the Wigner distribution which can be derived from the general class equation (2.8) by taking g (v, τ) = 1:

$$\rho_w(t, f) = \int_{-\infty}^{\infty} z(t - \tau/2)\, z^*(t+\tau/2) e^{-2j\pi ft}\, d\tau \qquad (3.2)$$

where ρ_w (t, f), z(t) and z* *(t)* are the Wigner distribution, analytic signal and the complex conjugate of the analytic signal respectively. From equation (3.2) we see that for each particular time we are adding up pieces made from the product of the signal at a past time multiplied by the signal at an equal future time.

HRView is a tool to compute the Power Spectrum of ECG and hence is frequency domain based. The Wigner distribution computes the spectral characteristics using time as well as the frequency as its domain. We expect the techniques to give similar results as the analysis is done on the same data although the domain is different. Thus a comparison of two techniques was resorted to.

Data of 22 veterans was analyzed using the LabView code which performs the Time Frequency Analysis and the HRView tool which performs the power spectrum analysis. The graphs shown in figures 3.3 and 3.4 are plotted by the LabView code which performs TF Analysis, using the result from the time interval starting from the last five minutes of the supine position and ending after the first five minutes of the tilt position. These graphs were drawn using the data collected on the veteran in the 45 minutes tilt

test. The peaks in each of these figures occurs generally in the time interval 295 to 310 seconds of the graph at which time the subject is tilted.

Figure 3.3 shows a sample graph of the activity in the high frequency region with respect to time. Figures 3.3 and 3.4 show a peak occurring at the instance of tilt (between 295 seconds and 305 seconds). Initially this peak was thought to be noise occurring due to motion artifact. To evaluate this further, the data was plotted using S+ and checked to see

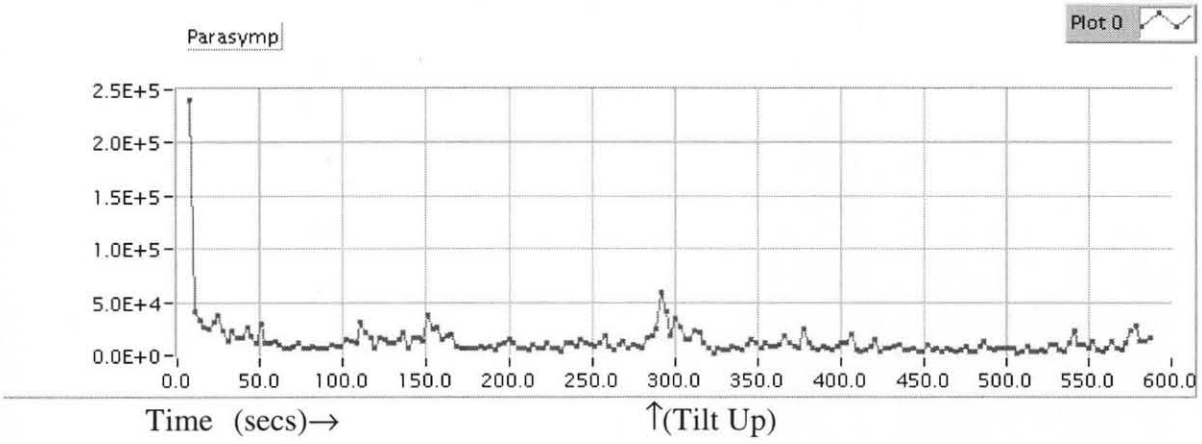

Figure 3.3 Sample graph (Subject X) of Activity in the HF wrt time

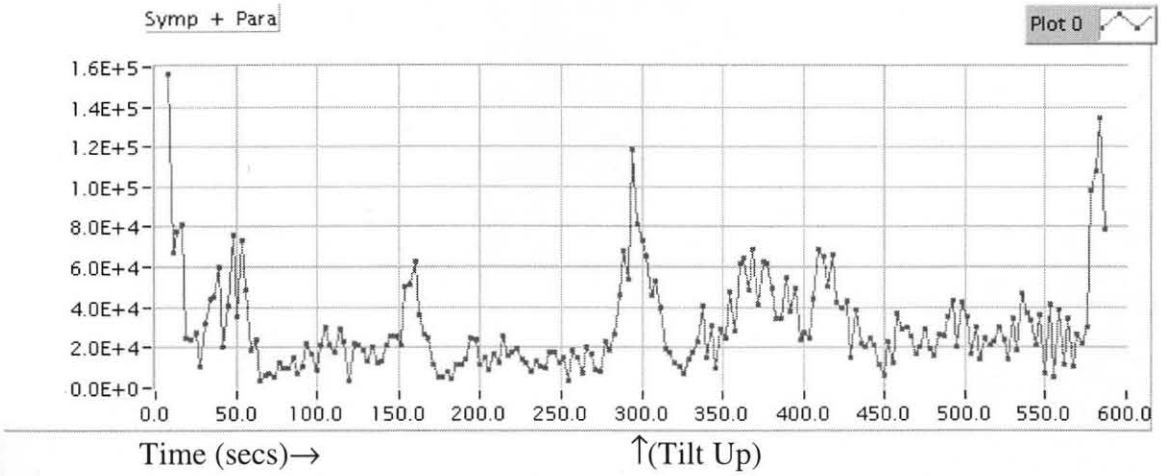

Figure 3.4 Sample graph (X) of Activity in the low frequency region wrt time

if the R-waves were properly represented. It was found that the R-waves were represented properly in the data.

The average power values at high frequency for each subject were computed when the subject lay in the supine position (from 10 seconds to 275 seconds) and when the subject was in the tilted position (from 310 to 580 seconds). Table 3.2 shows the average values computed for gulf war veterans.

Table 3.2. Average values of high frequency region (parasympathetic component) of each subject

Subjects	Age	Sex	Height	Weight	GWS	High Frequency (HF) Activity (Parasympathetic)		
	Years		Cm	Kgs		Before tilt (Supine)	After tilt (At 70 degree tilt)	% Change
V002	40	M	188	91		51404.4	20659.7	-59.81%
V004	30	M	179	75		44344.9	28276.2	-36.24%
V006	27	M	175	87		33824.8	17524.5	-48.19%
V007	29	M	168	74		114999.9	65612.4	-42.95%
V010	27	F	149	53		11194.4	5421.1	-51.57%
V012	28	M	175	72		94015.6	78234.5	-16.79%
V019	28	M	181	85	S	135265.8	63187.3	-53.29%
V025	31	M	168	99	S	49573.8	26285.1	-46.98%
V030	47	F	170	65	S	43519.7	23921.3	-45.03%
V032	34	M	185	79		96482.3	37665.9	-60.96%
V041	50	M	180	85		113877.6	59116.0	-48.09%
V045	29	M	174	87	S	36744.4	21295.9	-42.04%
V047	28	M	172	63	S	44157.8	32353.9	-26.73%
V051	36	F	135	83	S	30788.9	14361.2	-53.36%
V052	25	M	175	81		83643.5	30676.6	-63.32%
V053	26	M	179	103	S	62809.6	34549.7	-44.99%
V055	28	M	176	77		160756.5	53452.1	-66.75%
V057	32	M	169	95	S	24832.0	15319.5	-38.31%
V060	30	M	170	125	S	6384.8	2953.0	-53.75%
V064	28	M	180	72	S	148040.7	96647.8	-34.72%
V067	31	F	173	74	S	36423.7	21183.4	-41.84%
V082	49	M	173	67		48851.7	34909.7	-28.54%

Our aim is now to compare different population sets from the above table. A t test is a statistical method to draw inferences about population means between the two groups, from this type of data sets. A paired test is used when there is a natural pairing of observations in the samples, such as when a sample group is tested twice before and after an experiment in this case the experiment being the tilt. T Test assuming unequal variance was performed when the data was distinct, i.e. when the subjects were different (healthy and sick). Conclusion was based on the following:

The null hypothesis, H_o: $\mu_d = D_0 = 0$ (where $\mu_d = \mu_1 - \mu_2$, μ_1= mean of values before tilt and μ_2 = mean of values after tilt.).

The alternate hypothesis was: H_a: $\mu_d > D_0$ Or $\mu_d < D_0$ Or $\mu_d \neq D_0$.

For specified value of confidence (α) and degree of freedom df = n-1

1. reject Ho if $t > t_\alpha$
2. reject Ho if $t < -t_\alpha$
3. reject Ho if $|t| > t_{0.5\alpha}$
4. cannot reject Ho if P(T<=t) > 0.05.

where t = tStat and t_α =t critical.

A t-test assuming unequal variance was performed on the average values in the high frequency activity region between healthy veterans and veterans with the gulf war syndrome before tilt.

The t-test statistics are shown below:

T TEST 1 Statistical analysis of HF activity (Parasympathetic component) between healthy veterans and veterans with gulf war syndrome before tilt

T Stat	-0.401728018
P(T<=t)	0.692889523
T Critical (95% CL)	1.739606432

We can conclude with 95% CL that the mean of healthy veterans before tilt may be equal to the activity before tilt of veteran with gulf war syndrome.

A t-test assuming unequal variance was performed in the high frequency activity region between healthy and veterans suffering from the gulf war syndrome after tilt. The t-test statistics are shown below:

T TEST 2 Statistical analysis of HF activity (Parasympathetic component) after tilt between healthy Veterans and Veterans with gulf war syndrome.

t Stat	1.140457474
P(T<=t)	0.280673299
t Critical (95% CL)	1.812461505

We can conclude with 95% CL that the mean of healthy veterans after tilt may be equal to the activity during tilt of veterans with the gulf war syndrome.

Figure 3.4 shows a sample graph of the change in autonomic activity in the low frequency region with respect to time. The average value of the low frequency activity of each subject was computed when the subject was in the supine position (from 10 seconds to 275 seconds) and also when the subject was in tilted position (from 310 seconds to 580

seconds). Table 3.3 shows the average value for this region of healthy as well as subjects with the gulf war syndrome.

Table 3.3 Average values of the activity in the low frequency region (Sympathetic + Parasympathetic component) for each subject

Subjects	Age	Sex	Height	Weight	GWS	Low Frequency activity (Symp +Parasymp)		
	Years		Cm	Kgs		Before tilt (Supine)	After tilt (70degree Tilt)	% Change
V002	40	M	188	91		12182.34	18662.50	53.19%
V004	30	M	179	75		22259.21	26377.69	18.50%
V006	27	M	175	87		6445.82	11357.01	76.19%
V007	29	M	168	74		68289.04	79363.40	16.22%
V010	27	F	149	53		3726.80	5770.44	54.84%
V012	28	M	175	72		29740.12	41348.34	39.03%
V019	28	M	181	85	S	46429.75	70587.33	52.03%
V025	31	M	168	99	S	19645.07	26184.74	33.29%
V030	47	F	170	65	S	16949.98	22280.05	31.45%
V032	34	M	185	79		21745.69	38687.97	77.91%
V041	50	M	180	85		32416.82	51265.69	58.15%
V045	29	M	174	87	S	15544.97	27299.96	75.62%
V047	28	M	172	63	S	16773.88	21887.52	30.49%
V051	36	F	135	83	S	9936.25	13551.63	36.39%
V052	25	M	175	81		23919.40	58443.21	144.33%
V053	26	M	179	103	S	16974.79	28259.75	66.48%
V055	28	M	176	77		17326.81	46544.44	168.63%
V057	32	M	169	95	S	8548.97	13340.55	56.05%
V060	30	M	170	125	S	1348.85	3003.92	122.70%
V064	28	M	180	72	S	42389.23	59021.19	39.24%
V067	31	F	173	74	S	7995.34	14393.90	80.03%
V082	49	M	173	67		11251.43	16082.91	42.94%

A paired t-test was performed to statistically compare the data before and after tilt in the above table.

The t-test statistics are shown below:

T TEST 3 Statistical analysis of LF activity (Symp + Parasymp component) before tilt and after tilt for each subject.

t Stat	-5.732384003
P(T<=t)	5.43917E-06
t Critical (95% CL)	1.720743512

Based on the above evidence we can accept the alternate hypothesis and prove that the values after tilt are greater than values before tilt with 95% confidence. This implies that there is higher sympathetic activity after tilt.

A t-test assuming unequal variance was performed to compare the low frequency activity between healthy veterans and veterans with the gulf war syndrome before tilt. The t-test statistics are shown below:

T TEST 4 Statistical analysis of LF activity (Symp + Parasymp component) before tilt between healthy veterans and veterans with gulf war syndrome.

t Stat	-1.439588921
P(T<=t)	0.090271785
t Critical (95%CL)	1.372184215

We can conclude with 95% CL that the low frequency activity before tilt in veterans suffering from the gulf war syndrome may be equal to the activity in healthy veterans.

A t-test assuming unequal variance was performed to compare the low frequency activity between healthy veterans and veterans with the gulf war syndrome after tilt. The t-test statistics are shown below:

T TEST 5 Statistical analysis of LF activity (Symp + Parasymp component) after tilt between healthy veterans and veterans with gulf war syndrome.

t Stat	-2.276957897
P(T<=t) one-tail	0.023011556
t Critical one-tail (95% CL)	1.372184215

We can conclude with 95% CL that the low frequency activity after tilt in veterans suffering from the gulf war syndrome is less than the activity in healthy veterans.

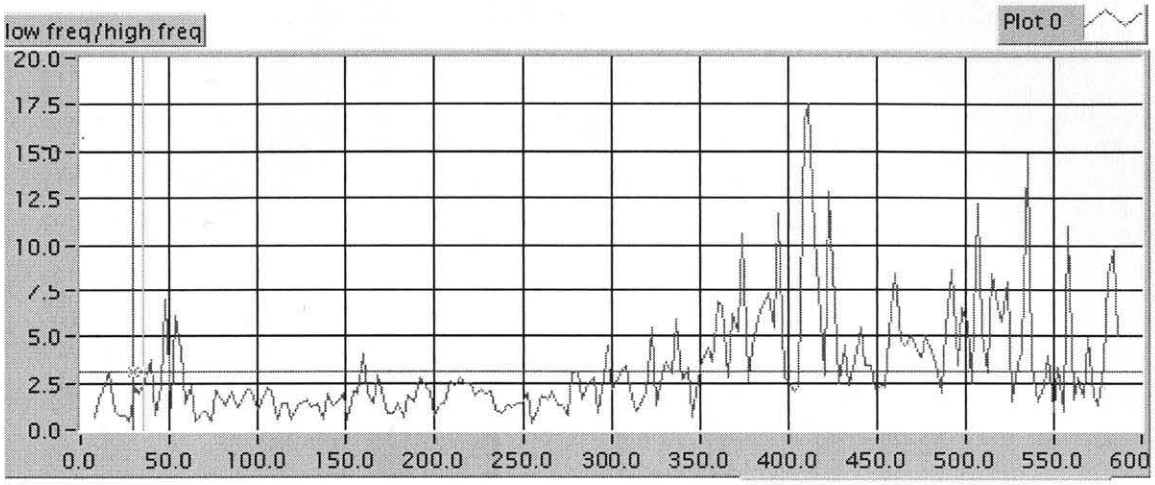

Figure 3.5 Ratio of low frequency to high frequency

Figure 3.5 shows a sample of the ratio of low frequency to high frequency. This graph gives us an indication of the change in the activity level in terms of ratio of low and high frequencies through the time span of the experiment Table 3.4 shows the average of ratios of low to high frequency of each subject before and during tilt.

Table 3.4 Average of ratios of low to high frequency for each subject

Subjects	Age	Sex	Height	Weight	GWS	Ratio low/high frequency		% Change
	Years		Cm	Kgs		Before tilt	After tilt	
V002	40	M	188	91		1.78	6.73	278.09%
V004	30	M	179	75		1.41	4.49	218.44%
V006	27	M	175	87		3.11	6.30	102.57%
V007	29	M	168	74		1.01	4.59	354.46%
V010	27	F	149	53		1.67	4.29	156.89%
V012	28	M	175	72		2.72	5.51	102.57%

Table 3.4 (continued)

Subjects	Age	Sex	Height	Weight	GWS	Ratio low/high frequency		% Change
	Years		Cm	Kgs		Before tilt	After tilt	
V019	28	M	181	85	S	1.68	4.50	167.86%
V025	31	M	168	99	S	1.54	4.64	201.30%
V030	47	F	170	65	S	1.68	1.68	0.00%
V032	34	M	185	79		2.25	5.51	144.89%
V041	50	M	180	85		2.47	5.54	124.29%
V045	29	M	174	87	S	1.64	2.84	73.17%
V047	28	M	172	63	S	2.21	4.48	102.71%
V051	36	F	135	83	S	1.67	5.57	233.53%
V052	25	M	175	81		1.71	3.43	100.58%
V053	26	M	179	103	S	2.25	4.79	112.89%
V055	28	M	176	77		3.78	7.62	101.59%
V057	32	M	169	95	S	2.14	4.17	94.86%
V060	30	M	170	125	S	2.32	4.21	81.47%
V064	28	M	180	72	S	2.82	6.09	115.96%
V067	31	F	173	74	S	3.02	5.49	81.79%
V082	49	M	173	67		3.64	6.96	91.21%

A paired t-test was performed to statistically compare the data before and after tilt. The t-test statistics are shown below:

T TEST 6 Statistical analysis of Graph Ratio (LF/HF) before tilt after tilt of each subject.

t Stat	-12.67177596
P(T<=t) one-tail	1.32472E-11
t Critical one-tail (95% CL)	1.720743512

We can prove that the values after tilt are greater than values before tilt with 95% confidence level. This indicates higher sympathetic activity after tilt.

A t-test assuming unequal variance was performed to compare the average of the graph ratios of low to high frequency activity between healthy veterans and the veterans suffering from the gulf war syndrome.

The two tailed t-test statistics are shown below:

T Test 7 Statistical analysis of Graph Ratio (LF/HF) before tilt between healthy veterans and veterans with gulf war syndrome.

t Stat	-0.744396318
P(T<=t)	0.467429878
t Critical (95% CL)	1.745884219

We can only conclude that the mean of healthy veterans before tilt may be equal to the activity before tilt of the veterans suffering from the gulf war syndrome.

A t-test assuming unequal variance was performed to compare the average graph ratios of low to high frequency activity between the healthy veterans and the veterans suffering from the gulf war syndrome during tilt.

The t-test statistics are shown below:

T Test 8 Statistical analysis of Graph Ratio (LF/HF) after tilt between healthy veterans and veterans with gulf war syndrome.

t Stat	-2.10978752
P(T<=t)	0.047674174
t Critical (95% CL)	1.724718004

We can conclude that the low frequency activity after tilt in veterans with the gulf war syndrome is less than activity in healthy veteran.

Table 3.5 lists the area under the peaks (from 295 seconds to 305 seconds) in the low frequency and in the high frequency region at the instant of tilt.

Table 3.5 Area under peaks in the low frequency and in the high frequency region at the instant of tilt.

Subjects	Age	Sex	Height	Weight	GWS	Area under Low Frequency peak	Area under High Frequency peak
	Years		Cm	Kgs			
V002	40	M	188	91		58126.49	24900.83
V004	30	M	179	75		109175.15	45118.26
V006	27	M	175	87		37787.89	9121.42
V007	29	M	168	74		203284.30	119210.82
V010	27	F	149	53		7611.73	5625.26
V012	28	M	175	72		120642.47	44417.14
V019	28	M	181	85	S	116048.41	63954.63
V025	31	M	168	99	S	34900.75	34587.37
V030	47	F	170	65	S	53724.09	30397.52
V032	34	M	185	79		46150512.0	5015256.50
V041	50	M	180	85		118174.81	45176.70
V045	29	M	174	87	S	79994.12	29412.29
V047	28	M	172	63	S	55232.29	20936.86
V051	36	F	135	83	S	31630.96	17862.18
V052	25	M	175	81		125452.83	63507.98
V053	26	M	179	103	S	88755.93	29661.82
V055	28	M	176	77		103263.81	28072.58
V057	32	M	169	95	S	53956.47	17114.32
V060	30	M	170	125	S	7081.48	2654.92
V064	28	M	180	72	S	214847.03	61441.63
V067	31	F	173	74	S	30436.65	9646.48
V082	49	M	173	67		69925.30	21565.79

A t-test assuming unequal variance was performed to compare the area under the peak, occurring at the instance of tilt, of the high frequency curve between the healthy veterans and veterans with gulf war syndrome.

The t-test statistics are shown below:

T Test 9 Statistical analysis between healthy veterans and veterans with gulf war syndrome of the area under the peak occurring at the instant of tilt, in the HF (Parasympathetic component) region.

t Stat	-0.077801128
P(T<=t)	0.938799745
t Critical (95% CL)	2.093024705

We can conclude with 95% CL that the mean of the two groups (healthy veterans and veterans with gulf war syndrome) may be equal.

A t-test assuming unequal variance was performed to compare the area under the peak, occurring at the instance of tilt, of the low frequency curve between the healthy veterans and the veterans suffering from gulf war veterans.

The t-test statistics are shown below:

T Test 10 Statistical analysis between healthy veterans and veterans with gulf war syndrome of the area under the peak occurring at the instant of tilt in the LF (Symp + Parasymp component) region.

t Stat	-0.018859868
P(T<=t)	0.985201478
t Critical (95%CL)	2.131450856

We can conclude with 95% CL that the mean of the two groups (healthy veterans and subjects suffering from the gulf war syndrome) may be equal.

3.4.1 Results Obtained using HRView

Table 3.6 High Frequency activity before tilt and after tilt using Power Spectrum Analysis (HRView)

Subjects	Age	Sex	Height	Weight	GWS	Before Tilt		
	Years		Cm	Kgs			After Tilt (70 degree Tilt)	% Change
V002	40	M	188	91		2.79E+00	6.90E-01	-75.2688
V004	30	M	179	75		3.72E+00	1.14E+00	-69.3548
V006	27	M	175	87		1.01E+00	1.37E+00	35.64356
V007	29	M	168	74		2.77E+01	7.41E+00	-73.2491
V010	27	F	149	53		1.57E+00	6.27E-01	-60.0637
V012	28	M	175	72		7.04E+00	2.51E+00	-64.3466
V019	28	M	181	85	S	7.37E+00	6.87E+00	-6.78426
V025	31	M	168	99	S	1.71E+00	1.15E+00	-32.7485
V030	47	F	170	65	S	1.35E+00	8.14E-01	-39.7037
V032	34	M	185	79		1.11E+01	8.99E+00	-19.009
V041	50	M	180	85		1.04E+01	3.26E+00	-68.6538
V045	29	M	174	87	S	2.72E+00	4.89E+00	79.77941
V047	28	M	172	63	S	1.00E+01	2.38E+00	-76.2
V051	36	F	135	83	S	3.75E+00	7.55E-01	-79.8667
V052	25	M	175	81		1.22E+00	2.64E+00	116.3934
V053	26	M	179	103	S	4.09E+01	1.47E+00	-96.4059
V055	28	M	176	77		2.29E+00	6.78E+00	196.0699
V057	32	M	169	95	S	9.38E+00	1.54E+00	-83.5821
V060	30	M	170	125	S	3.41E-01	4.99E-01	46.33431
V064	28	M	180	72	S	4.71E+00	1.26E+00	-73.2484
V067	31	F	173	74	S	1.59E+01	2.06E+00	-87.044
V082	49	M	173	67		2.45E+00	1.07E+00	-56.3265

A paired t-test was performed to statistically compare the high frequency activity before and after tilt.

The t-test statistics are shown below:

T TEST 11 Statistical analysis of HF activity (Parasympathetic component) of each subject before tilt and after tilt

t Stat	2.46639759
P(T<=t)	0.011169441
t Critical (95% CL)	2.079614205

Based on the above T test since the probability of T test is less than 0.05 we can accept the alternate hypothesis and infer that the values before tilt are greater than values after tilt with 95% confidence. This implies that the parasympathetic activity after tilt has reduced.

Table 3.7 Low Frequency activity before tilt and after tilt using Power Spectrum Analysis (HRView)

Subjects	Age	Sex	Height	Weight	GWS	Before tilt	After tilt	% Change
	Years		Cm	Kgs				
V002	40	M	188	91		2.58E+00	7.09E+00	63.61072
V004	30	M	179	75		2.50E+00	4.76E+00	47.47899
V006	27	M	175	87		1.46E+00	6.15E+00	76.26016
V007	29	M	168	74		9.44E+00	1.20E+01	21.33333
V010	27	F	149	53		2.54E+00	3.96E+00	35.85859
V012	28	M	175	72		2.61E+01	1.08E+01	-141.667
V019	28	M	181	85	S	9.92E+00	1.82E+01	45.49451
V025	31	M	168	99	S	2.90E+00	9.89E+00	70.67745
V030	47	F	170	65	S	2.31E+00	4.48E+00	48.4375
V032	34	M	185	79		9.32E+00	6.40E+01	85.4375
V041	50	M	180	85		6.18E+00	1.92E+01	67.8125
V045	29	M	174	87	S	4.41E+00	5.40E+00	18.33333
V047	28	M	172	63	S	2.78E+00	3.93E+00	29.26209
V051	36	F	135	83	S	3.46E+00	1.22E+01	71.63934
V052	25	M	175	81		1.35E+00	3.37E+00	59.94065
V053	26	M	179	103	S	2.01E+01	8.71E+00	-130.769
V055	28	M	176	77		4.92E+00	4.69E+01	89.50959
V057	32	M	169	95	S	4.97E+00	4.03E+00	-23.3251
V060	30	M	170	125	S	1.05E+00	3.34E+00	68.56287
V064	28	M	180	72	S	6.02E+00	8.38E+00	28.16229
V067	31	F	173	74	S	8.29E+00	2.07E+00	-300.483
V082	49	M	173	67		4.64E+00	6.56E+00	29.26829

A paired t-test was performed to statistically compare low frequency activity before and after tilt.

The t-test statistics are shown below:

T TEST 12 Statistical analysis of LF activity (Sympathetic+Parasymp. component) of each subject before tilt and after tilt.

t Stat	-1.799675921
P(T<=t)	0.043148753
t Critical (95% CL)	2.079614205

Based on the above evidence since the probability of T test is less than 0.05 we can accept the alternate hypothesis and infer that the values after tilt are greater than values before tilt with 95% confidence. This implies that there is higher sympathetic activity after tilt.

A t-test assuming unequal variance was performed on the average values in the high frequency activity region between healthy veterans and veterans with the gulf war syndrome before tilt.

The t-test statistics are shown below:

T TEST 13 Statistical analysis of HF activity (Parasympathetic component) between healthy veterans and veterans with gulf war syndrome before tilt

t Stat	-0.446151532
P(T<=t)	0.332071232
t Critical (95% CL)	1.739606432

We can conclude with 95% CL that the mean of healthy veterans before tilt may be equal to the activity before tilt of veteran with gulf war syndrome.

A t test assuming unequal variance was performed in the high frequency activity region between healthy and veterans suffering from the gulf war syndrome after tilt.

The t-test statistics are shown below:

T TEST 14 Statistical analysis of HF activity (Parasympathetic component) after tilt between healthy Veterans and Veterans with gulf war syndrome.

t Stat	0.652745
P(T<=t)	0.2619
t Critical (95% CL)	2.131451

We can conclude with 95% CL that the mean of healthy veterans after tilt may be equal to the activity during tilt of veterans with the gulf war syndrome.

The t-test statistics are shown below:

T TEST 15 Statistical analysis of LF activity (Symp + Parasymp component) before tilt between healthy veterans and veterans with gulf war syndrome.

t Stat	-0.09277
P(T<=t)	0.427315
t Critical (95%CL)	2.137218421

We can conclude with 95% CL that the low frequency activity before tilt in veterans suffering from the gulf war syndrome may be equal to the activity in healthy veterans.

A t-test assuming unequal variance was performed to compare the low frequency activity between healthy veterans and veterans with the gulf war syndrome after tilt.

The t-test statistics are shown below:

T TEST 16 Statistical analysis of LF activity (Symp + Parasymp component) after tilt between healthy veterans and veterans with gulf war syndrome.

t Stat	1.204702
P(T<=t) one-tail	0.126799
t Critical one-tail (95% CL)	2.200986

We can conclude with 95% CL that the low frequency activity before tilt in veterans suffering from the gulf war syndrome may be equal to the activity in healthy veterans.

3.5 Discussion

In order to find the changes occurring in the low frequency area due to tilt, a graph comparing the average low frequency activity before and after the tilt, for each subject was plotted. Figure 3.6 and figure 3.7 shows the graph of the average low frequency activity before and after the tilt for each subject (data obtained from table 3.1) found using TF Analysis and Power Spectral Analysis (done using HRView) respectively.

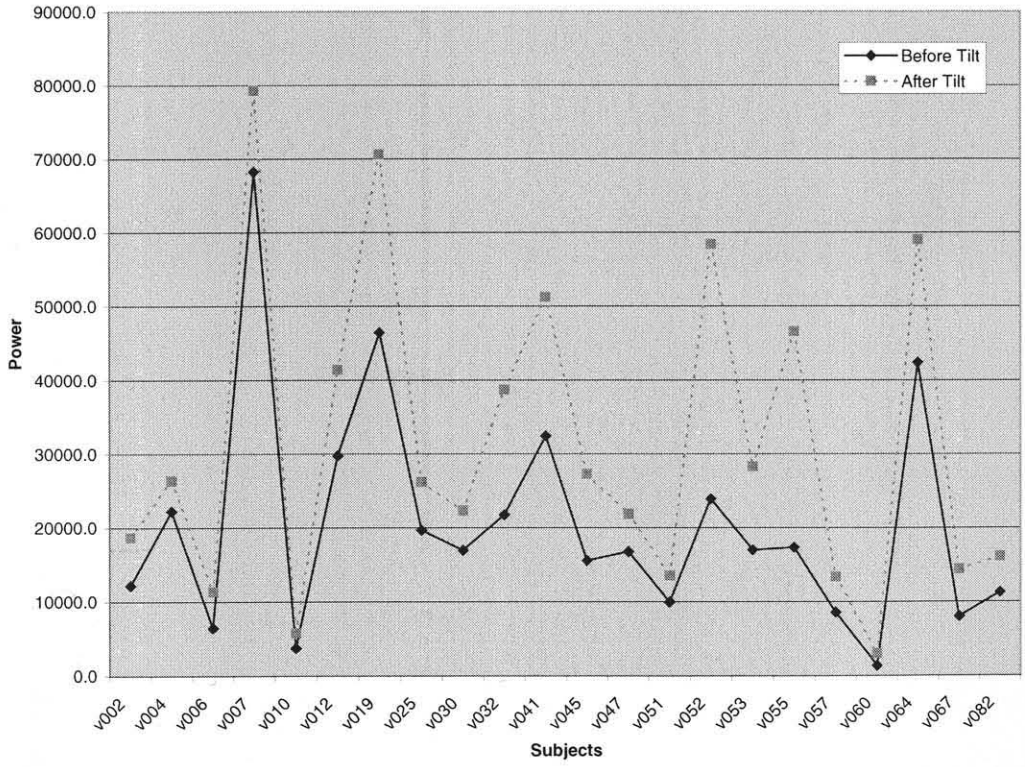

Figure 3.6 Average low frequency (Symp+Parasymp) activity of each subject using TF Analysis.

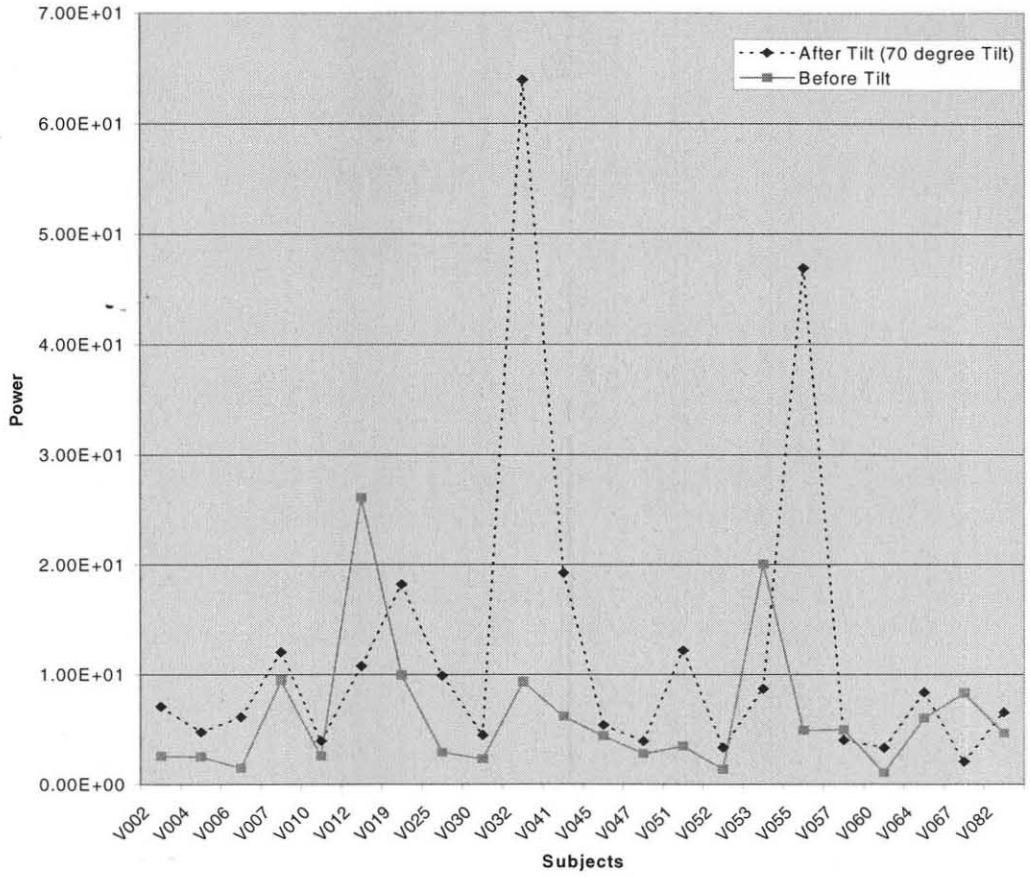

Figure 3.7 Average low frequency (Symp+Parasymp) activity of each subject using Power Spectrum Analysis (HRView)

HRView is a tool to compute the Power Spectrum of ECG and hence is frequency domain based. Wigner distribution computes the Spectral characteristics using time as well as the frequency as its domain. We expect the techniques to give similar results as the analysis is done on the same data although the domain is different. Thus a comparison of two techniques was resorted to.

From the paired t test analysis we can state with 95% CL that the activity in this region after tilting is higher than the activity in the supine position (t test 4 in section 3.4). This implies that the sympathetic activity is elevated after tilt. Figures 3.6 and 3.7 indicate that the LF activity after tilt is higher that the activity before tilt. This was found to be true when the analysis was done using TF method and also when it was done using HRView to calculate the Power Spectrum. Exceptions were found in Gulf War Veterans V012, V053, V057 and V067 when the analysis was done using HRView. In these subjects the low frequency activity after tilt was found to be lower than the low frequency activity before tilt.

A signal is non-stationary if the mean level is not constant and the extent of deviation is changing over time. Changes in the behavior of the ECG signal, like the amplitude and the variation of the signal, causes a change in its mean over a period of time. This makes the ECG signal non-stationary. It is possible that this non-stationarity is contributing to the abnormal results that were observed in some of the gulf war veterans. Breathing pattern affects the ECG signal (respiratory sinus arrhythmia). Since the gulf war veterans were not subjected to controlled breathing during the course of the test, there is possibility of non-stationarity being introduced because of the changes in the ECG behavior.

The other noticeable difference from the graph 3.6 and 3.7 is the difference in the amplitude of power. The reason for this is the difference in form of data that goes into Time frequency (IBI times the sampling frequency).

In order to find the changes occurring in the high frequency area due to tilt, a graph comparing the average high frequency activity before and after the tilt, for each subject was plotted. Figure 3.8 and figure 3.9 shows the graph of the average high frequency activity before and after the tilt for each subject (data obtained from table 3.2) found using TF Analysis and Power Spectral Analysis (done using HRView) respectively.

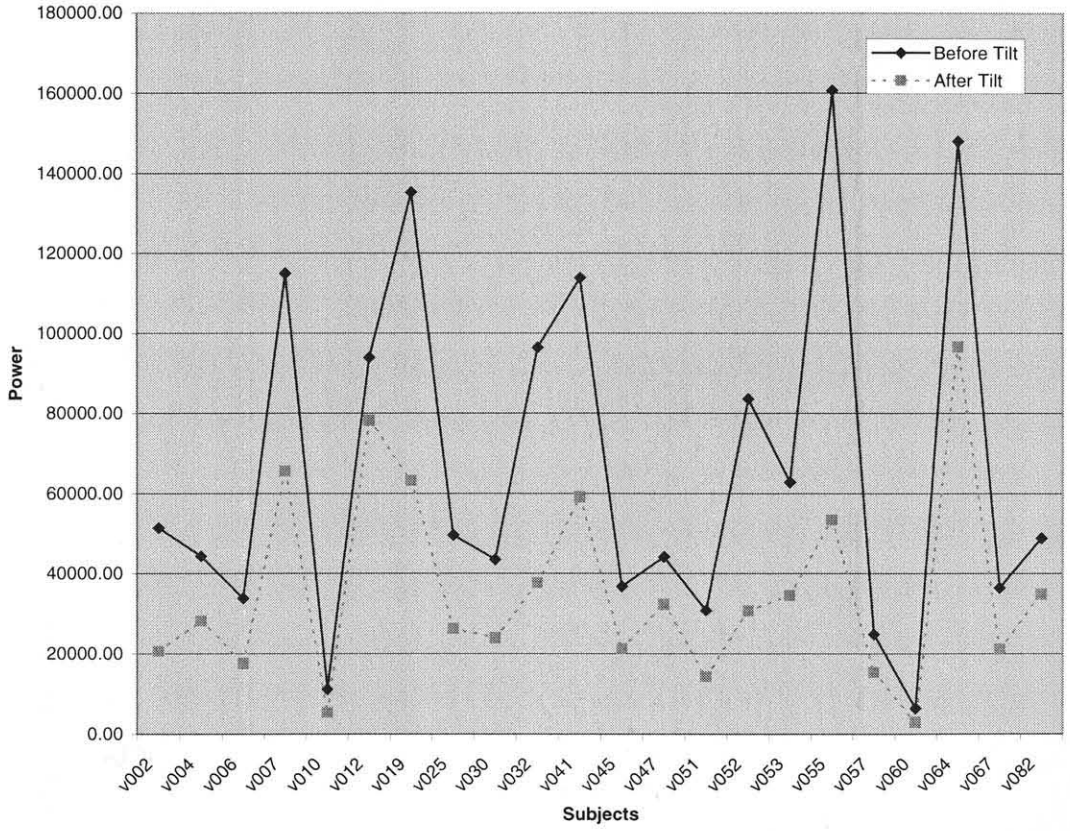

Figure 3.8 Average high frequency (Parasympathetic) activity before and after tilt of each subject using TF Analysis.

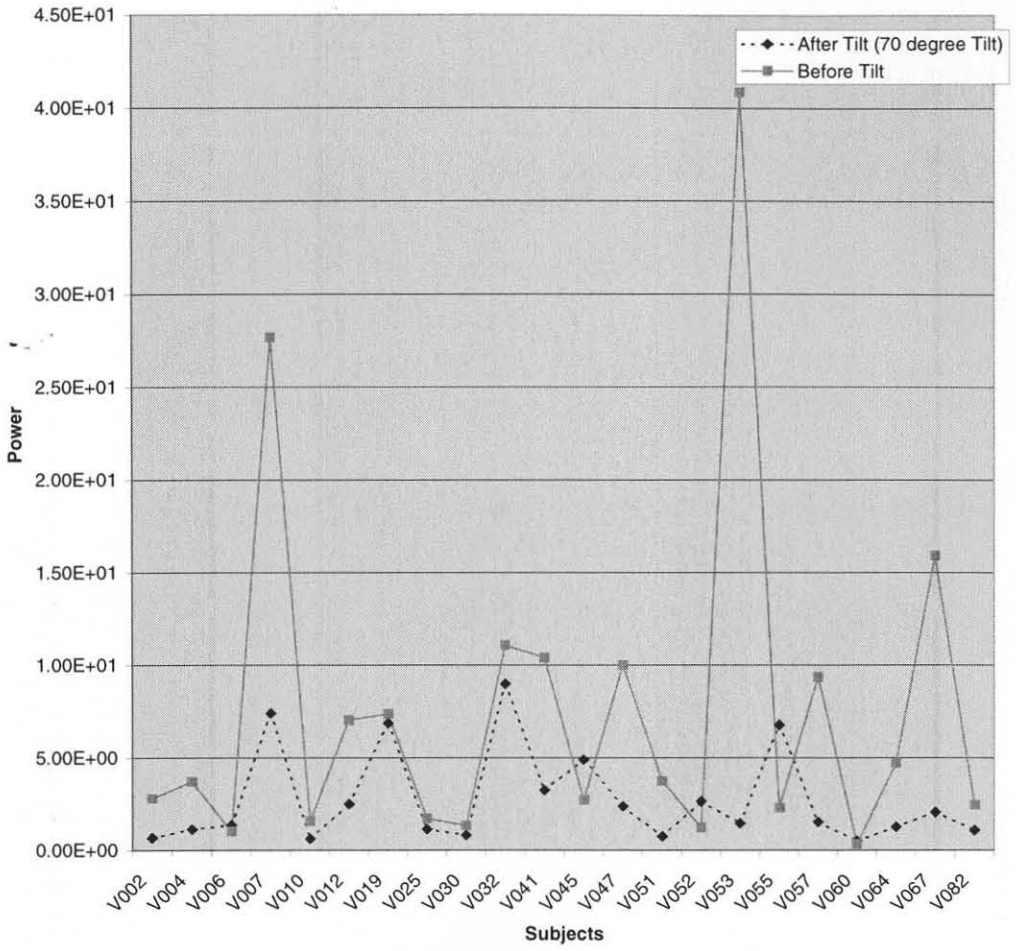

Figure 3.9 Average high frequency (Parasympathetic) activity before and after tilt of each subject using Power Spectrum Analysis.

Figures 3.8 and 3.9 indicate that the HF activity before tilt is higher than the activity after tilt. This was found to be true when the analysis was done using TF method and also when it was done using HRView to calculate the Power Spectrum. Exceptions were found in subjects V006, V045, V052, and V055 when the analysis was done using HRView. In these subjects the high frequency activity after tilt was found to be higher

than the high frequency activity before tilt. Again the abnormalities can be attributed to the nonstationarity of the ECG signal, as expalined before in this section.

A comparison of low frequency activity between healthy veterans and veterans with the gulf war syndrome before tilt with respect to age using TF Analysis and HRView is shown below.

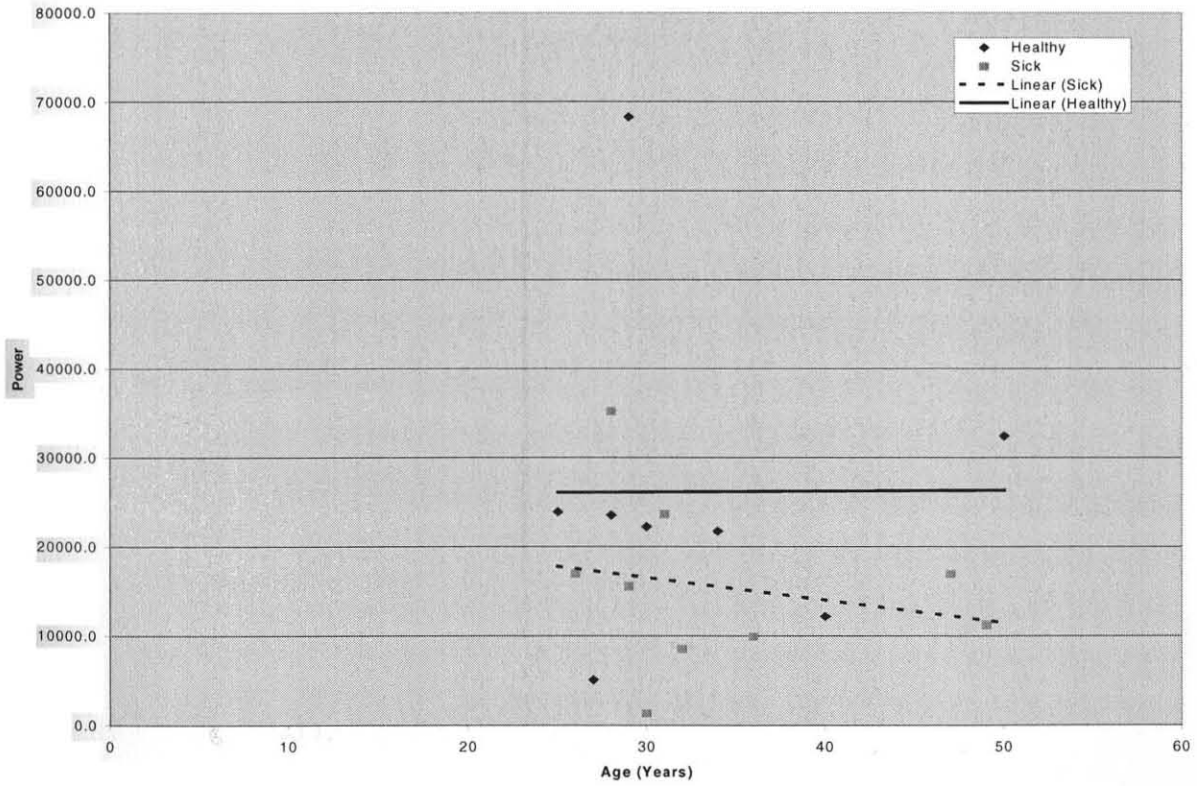

Figure 3.10 Comparison of low frequency activity between healthy veterans and veterans with the gulf war syndrome before tilt with respect to age using TF Analysis.

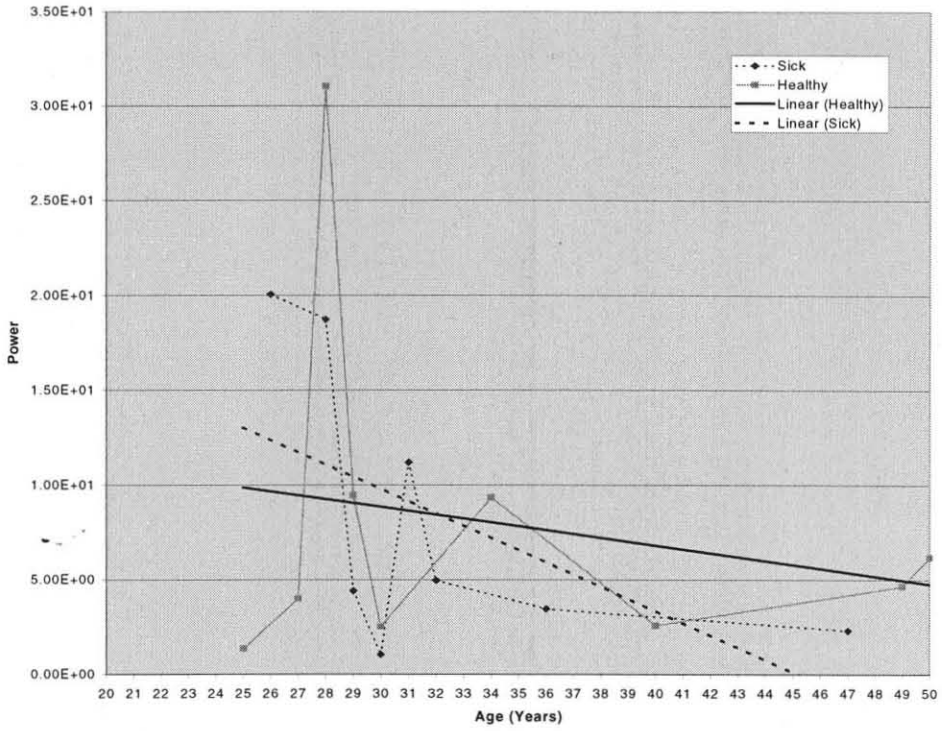

Figure 3.11 Comparison of low frequency activity between healthy veterans and veterans with the gulf war syndrome before tilt with respect to age using Power Spectrum

Figures 3.10 and 3.11 indicate that in subjects suffering from the gulf war syndrome it was observed that there is a drop in the low frequency (Symp+Parasymp) activity with age. This is clearly indicated by the trend line, which is a line of regression passing through all the points in the graph. The above inference is corroborated using the power spectrum analysis as shown in the graph below.

A comparison of low frequency activity between healthy veterans and veterans with the gulf war syndrome after tilt with respect to age was performed

Figure 3.12 and figure 3.13 shows the comparison of low frequency (Symp +Parasymp) activity between healthy veterans and veterans with gulf war syndrome after tilt with respect to age using TF Analysis and Power Spectrum Analysis respectively.

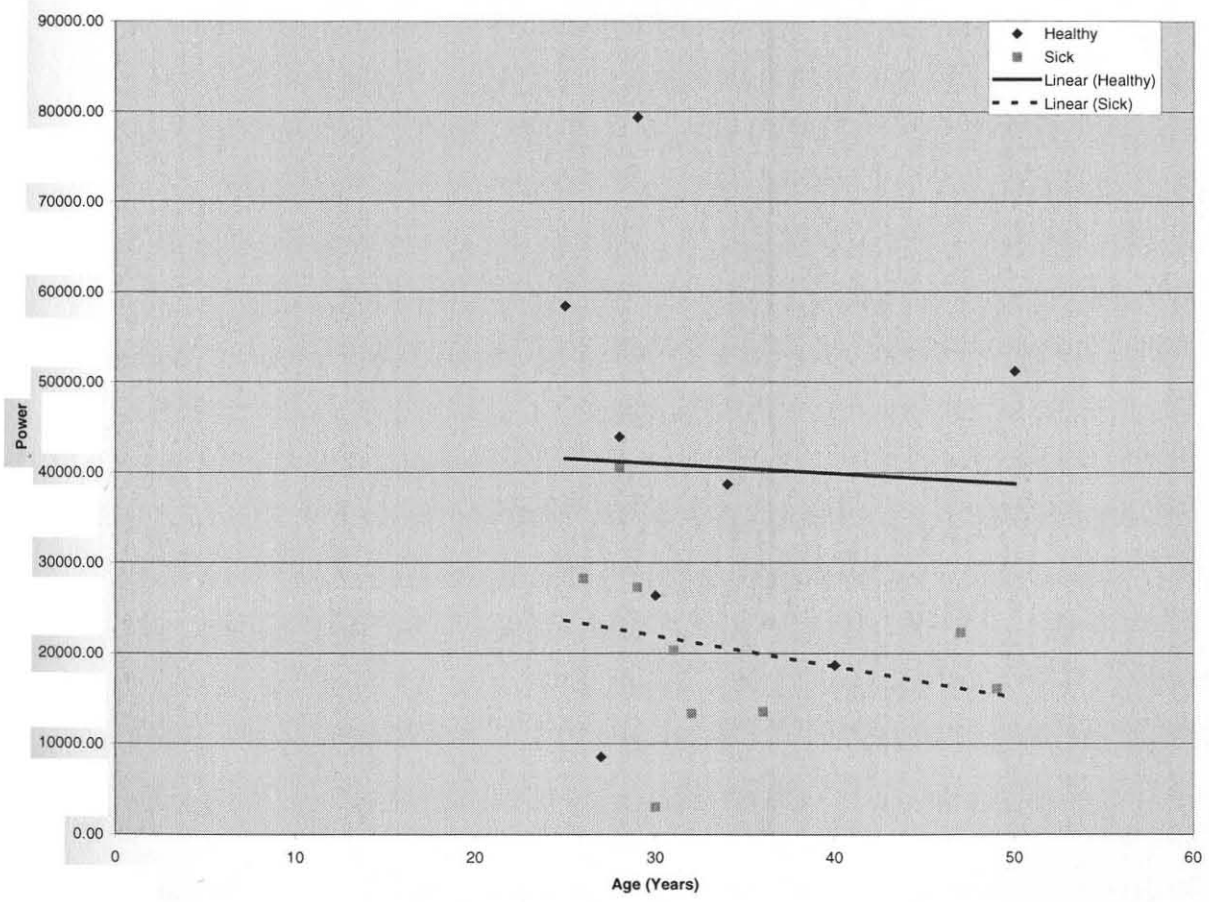

Figure 3.12 Comparison of low frequency activity between healthy veterans and veterans with the gulf war syndrome after tilt with respect to age using TF Analysis.

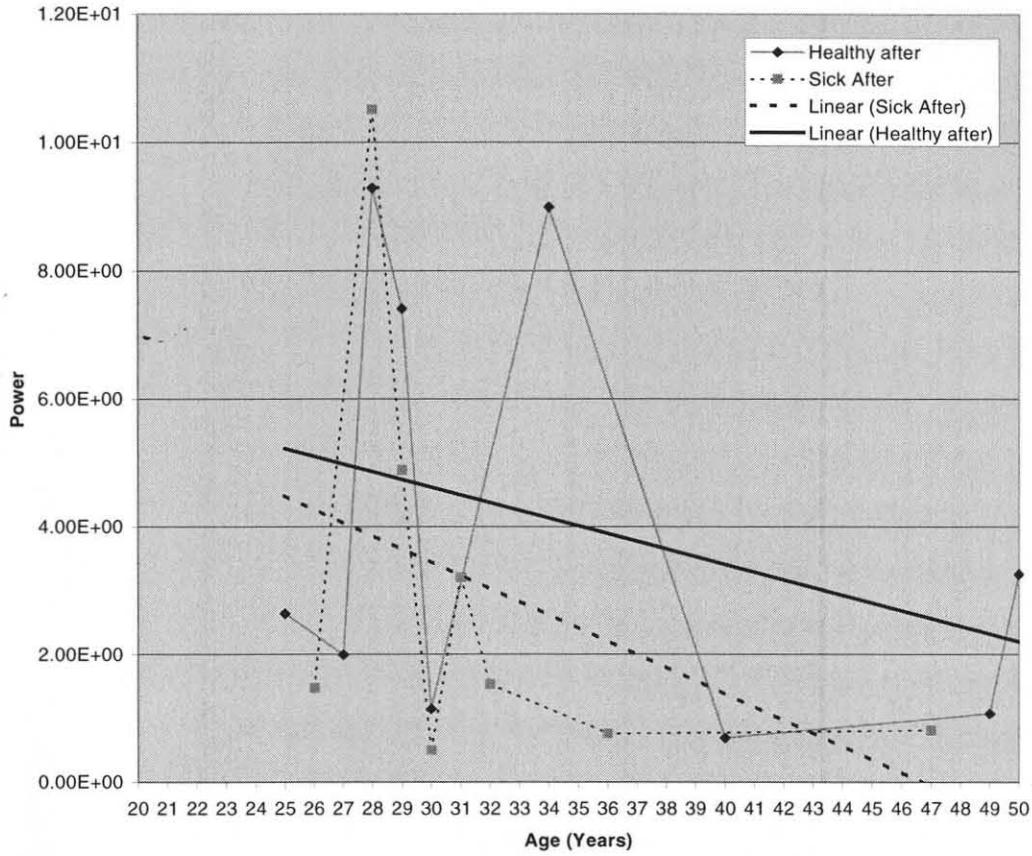

Figure 3.13 Comparison of low frequency (Symp+Parasymp) activity between healthy veterans and veterans with the gulf war syndrome after tilt with respect to age using Power Spectrum Analysis.

Figures 3.12 and 3.13 indicate that the low frequency activity reduces with age in healthy as well as subjects with gulf war veterans after tilt. In subjects suffering from the gulf war syndrome it is observed that there is a higher drop in the low frequency activity with age. This is clearly indicated by the trend line, which is a line of regression passing through all the points in the graph. Also it is evident from the t test performed in section 3.4 (t test 9) that the low frequency (Symp+Parasymp) activity in subjects with gulf war syndrome is lower than the healthy veterans for the same age

A comparison of high frequency activity between healthy veterans and veterans with the gulf war syndrome before tilt with respect to age was performed.

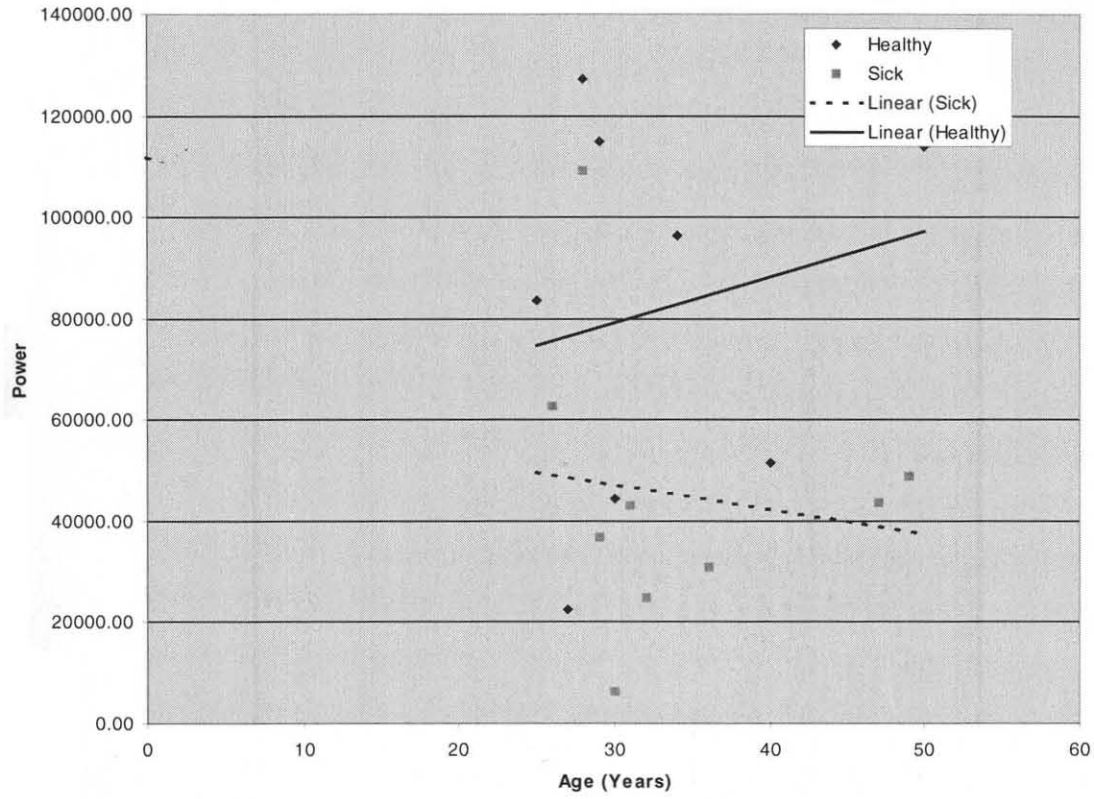

Figure 3.14 Comparison of high frequency (Parasymp) activity between healthy veterans and veterans with the gulf war syndrome before tilt with respect to age using TF Analysis.

Figure 3.14 indicates that the high frequency activity reduces with age in veterans with the gulf war syndrome as compared to healthy subjects before tilt. Also the trendline indicates that in healthy subjects the high frequency activity increases with age and in subjects with the gulf war syndrome it reduces with age.

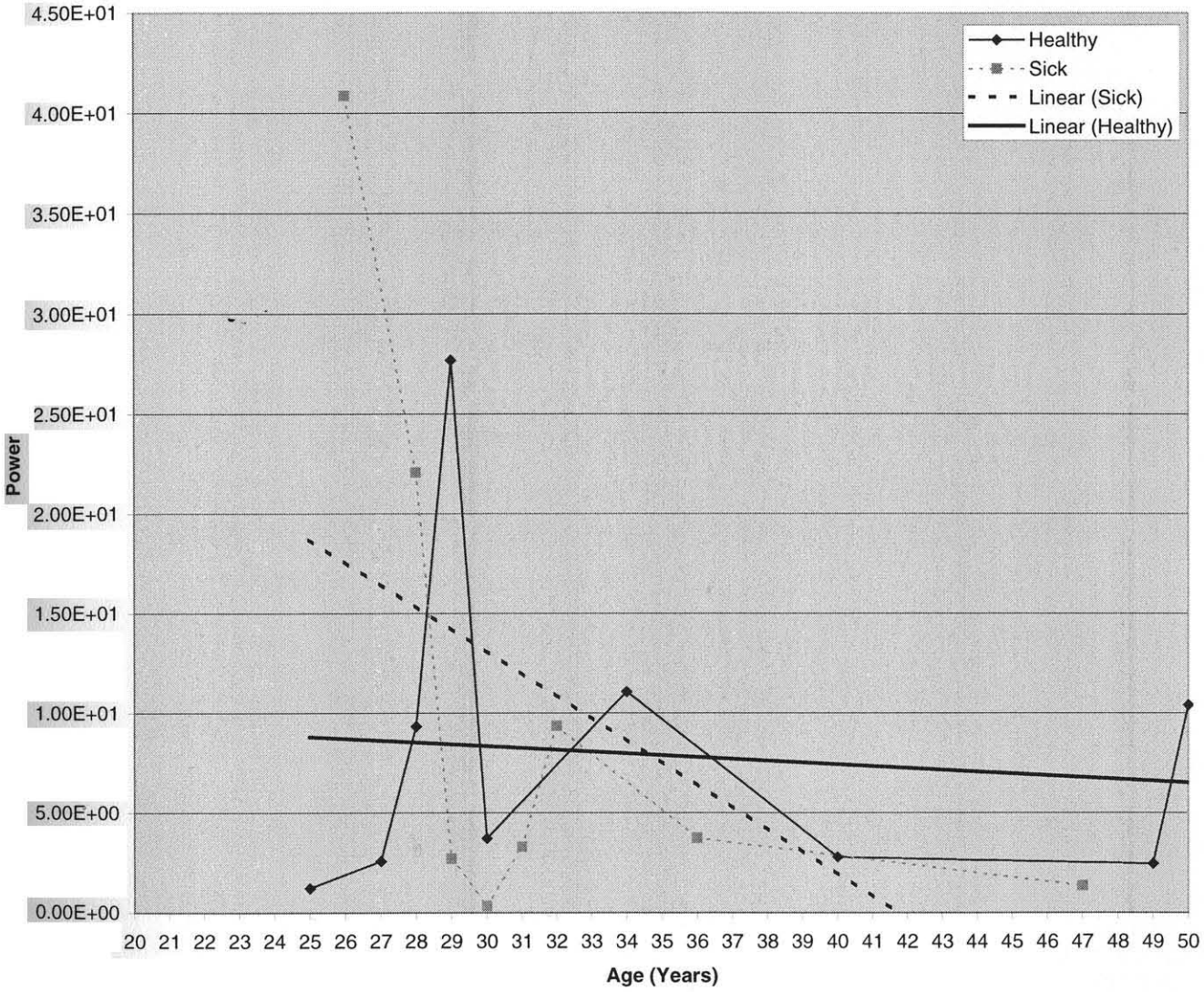

Figure 3.15 Comparison of high frequency (Parasymp) activity between healthy veterans and veterans with the gulf war syndrome before tilt with respect to age using Power Spectrum Analysis.

Unlike figure 3.14, the above figure indicates that the high frequency (Parasympathetic) activity in healthy subjects decreases with age which is as expected.

A comparison of high frequency activity between healthy veterans and veterans with the gulf war syndrome after tilt with respect to age was performed.

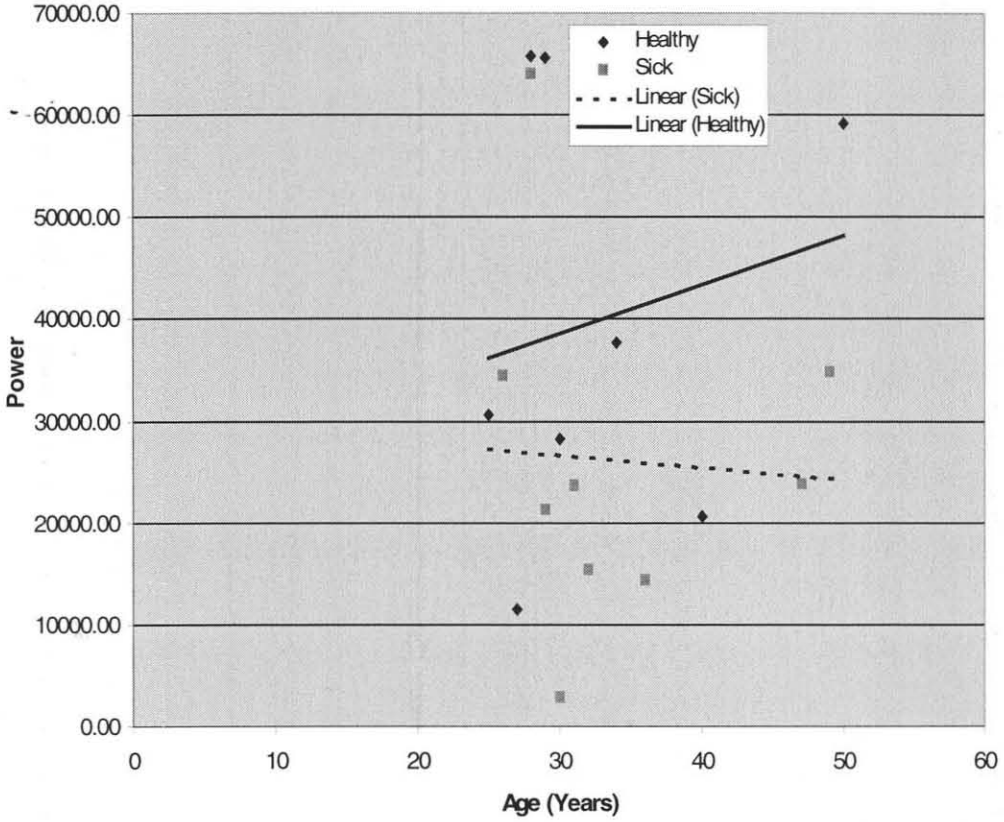

Figure 3.16 Comparison of high frequency (Parasymp) activity between healthy veterans and veterans with the gulf war syndrome after tilt with respect to age using TF Analysis.

Figure 3.16 indicates that the high frequency activity reduces with age in veterans with the gulf war syndrome as compared to healthy subjects after tilt. Also the trendline indicates that in healthy subjects the high frequency activity increases with age and in subjects with the gulf war syndrome it reduces with age.

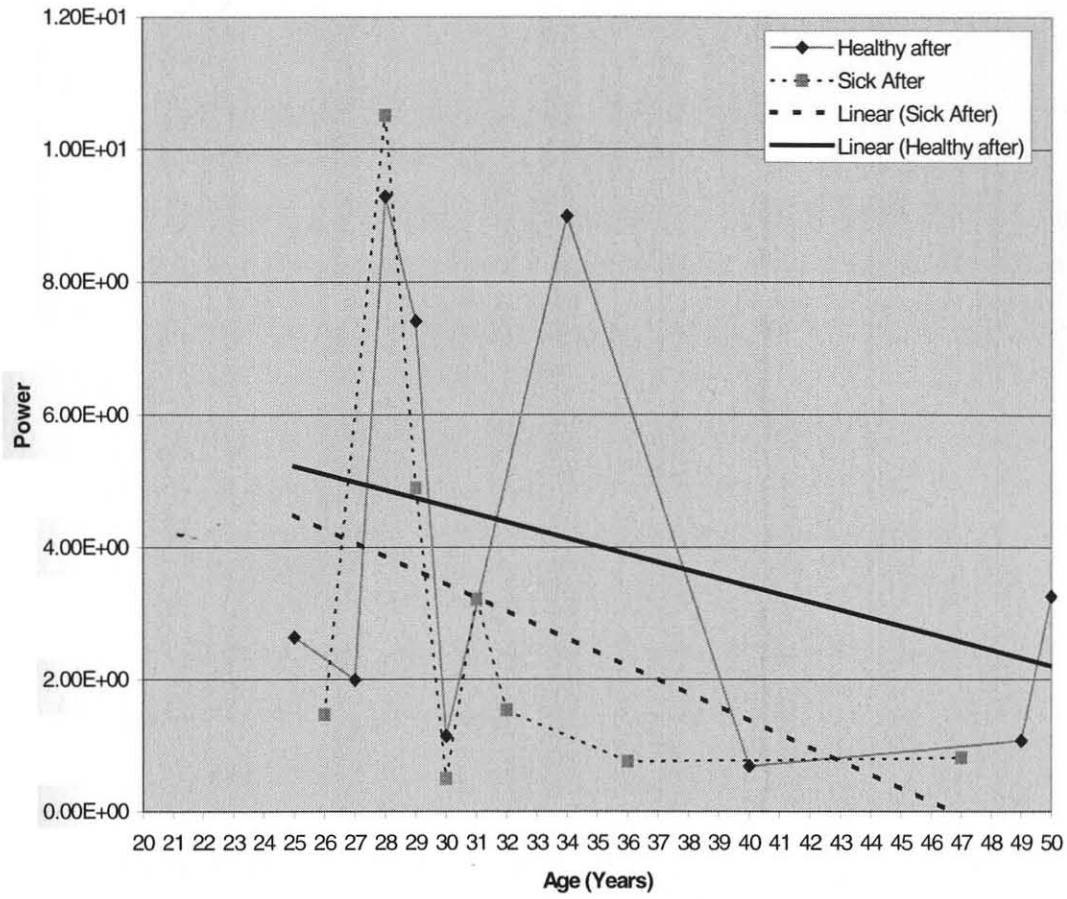

Figure 3.17 Comparison of high frequency (Parasymp) activity between healthy veterans and veterans with the gulf war syndrome after tilt with respect to age using Power spectrum Analysis

As shown above the trendline for subjects with gulf war syndrome is in agreement with that obtained using TF Analysis. But the trendline for healthy subjects obtained above is contrary to that obtained using TF Analysis.

3.6 Conclusion

The major drawback of power spectrum analysis is that they do not tell us the duration when the different frequency components existed. However use of time-frequency analysis shows that one can fully describe the existence of a specific frequency at each instant of time.

The statistical analysis done on the data regarding the area under the peaks at the instant of tilt for the veterans proved inconclusive. That is, there was no concrete distinction in the transition region between the supine and the tilt position for healthy veterans and the veterans suffering from the gulf war syndrome in the high as well as low frequency regions.

The following observations were obtained from the analysis:

The sympathetic activity after tilt is higher in all subjects as compared to the activity before tilt. (figure 3.6) using TF Analysis. Also the parasympathetic activity before tilt is higher in all subjects as compared to the activity after tilt. (figure 3.8). These results were as expected. The same results were inferred from the power spectrum analysis performed on the same data using HRView. A few exceptions were found when the analysis was done using HRView. It is possible that these exceptions occurred due to the non-stationarity of the ECG signal as explained in the earlier section.

The increase in sympathetic activity could be attributed to the response to stress due to gravity. This occurs because in tilt (70 degree postion) the heart has to put in more effort to maintain the blood flow to the upper regions of the body.

Figures 3.10. 3.12, 3.14, 3.16 indicate that for the same age group all subjects with the gulf war syndrome have the autonomic activity (i.e. parasympathetic and sympathetic activity) less than their healthy counterparts. Also for the same age group a higher drop in activity level of subjects with the gulf war syndrome is observed as compared to their healthy counterparts with increase in age. A similar result was obtained when the analysis was performed using the power spectrum analysis.

All the above indicators suggest that subjects with the gulf war syndrome show lower autonomic activity in general as compared to healthy subjects, thus indicating impairment in their autonomic nervous system. This could be attributed to the gulf war syndrome. Our findings suggest that heart rate variability may be one of the indicators to evaluate gulf war syndrome.

From the results obtained it is obvious that the two techniques agree on the changes occurring in the autonomic nervous system during the course of the study.

3.7 Future Work

It would be important to monitor recovery levels to attempt to explain the striking difference between the healthy veterans and the veterans suffering from the gulf war syndrome. For this the ECG should be monitored for a longer period even after the subject returns back to the supine position. This will help in assessing the time taken for the activity level of the autonomic nervous system to return to its normal state in healthy veterans as well as veterans suffering from the gulf war syndrome. This might also reveal the extent to which the gulf war syndrome affects the sympathetic as well as the parasympathetic nervous system. The period during which tilt occurs might offer data which reflect the changes in the autonomic activity. Analysis of data after the subject has stabilized might yield results, which are relatively free from aberrations due to motion artifacts. Comparison of various techniques like FFT, Blackman Tukey would enable analysis of power spectrum in different perspective.

A comparison of the healthy gulf war veterans with healthy non gulf war veterans would shed light on the possible as yet undetected effects of the gulf war on the veterans.

APPENDIX A

WIGNER LABVIEW CODE

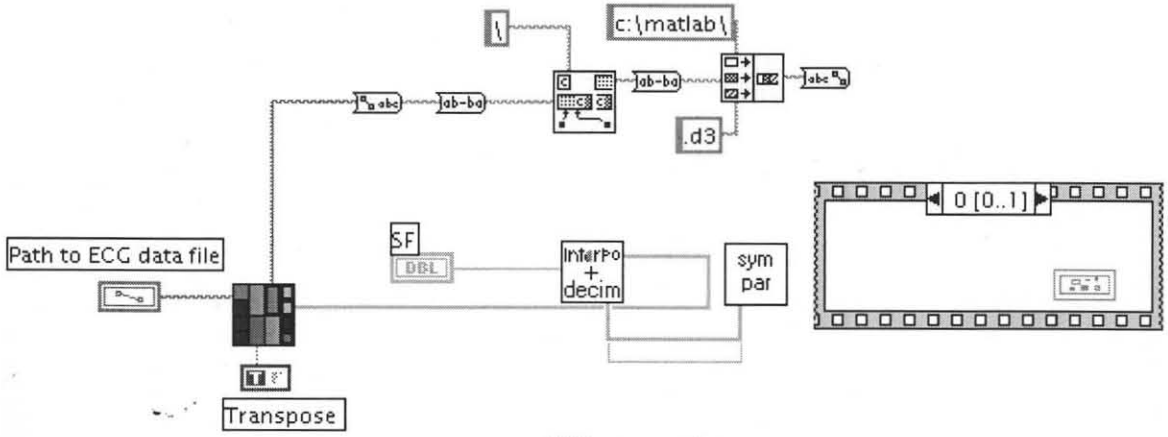

Wigner code

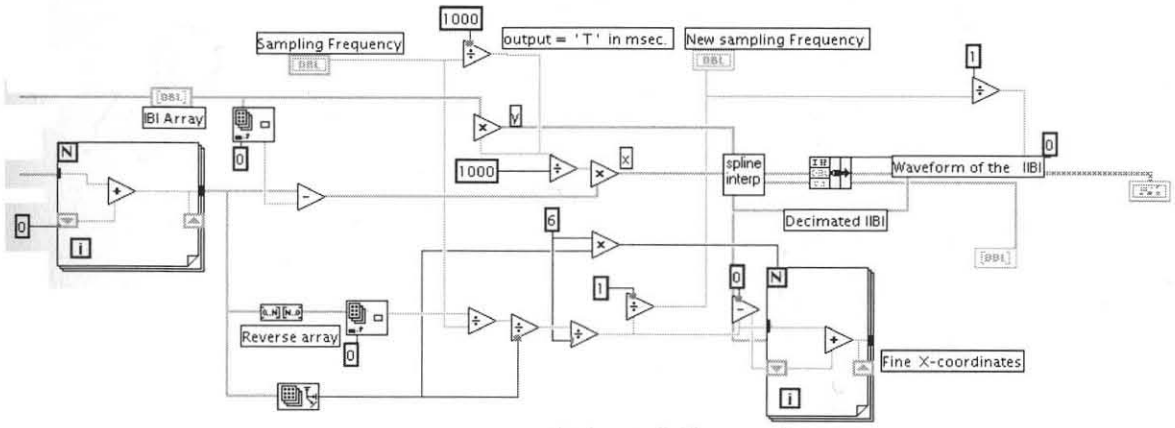

Interpolation code

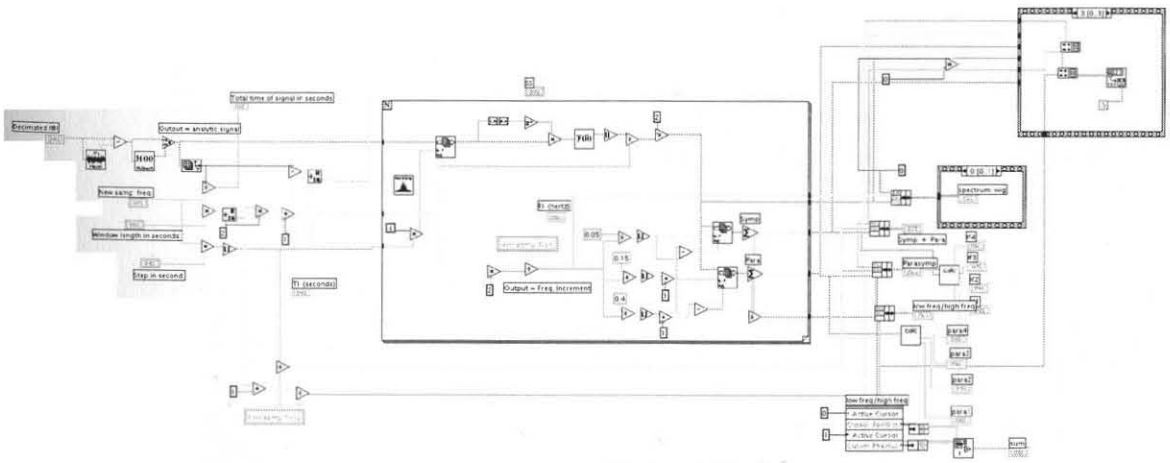

Output Code

APPENDIX B

RESULTS

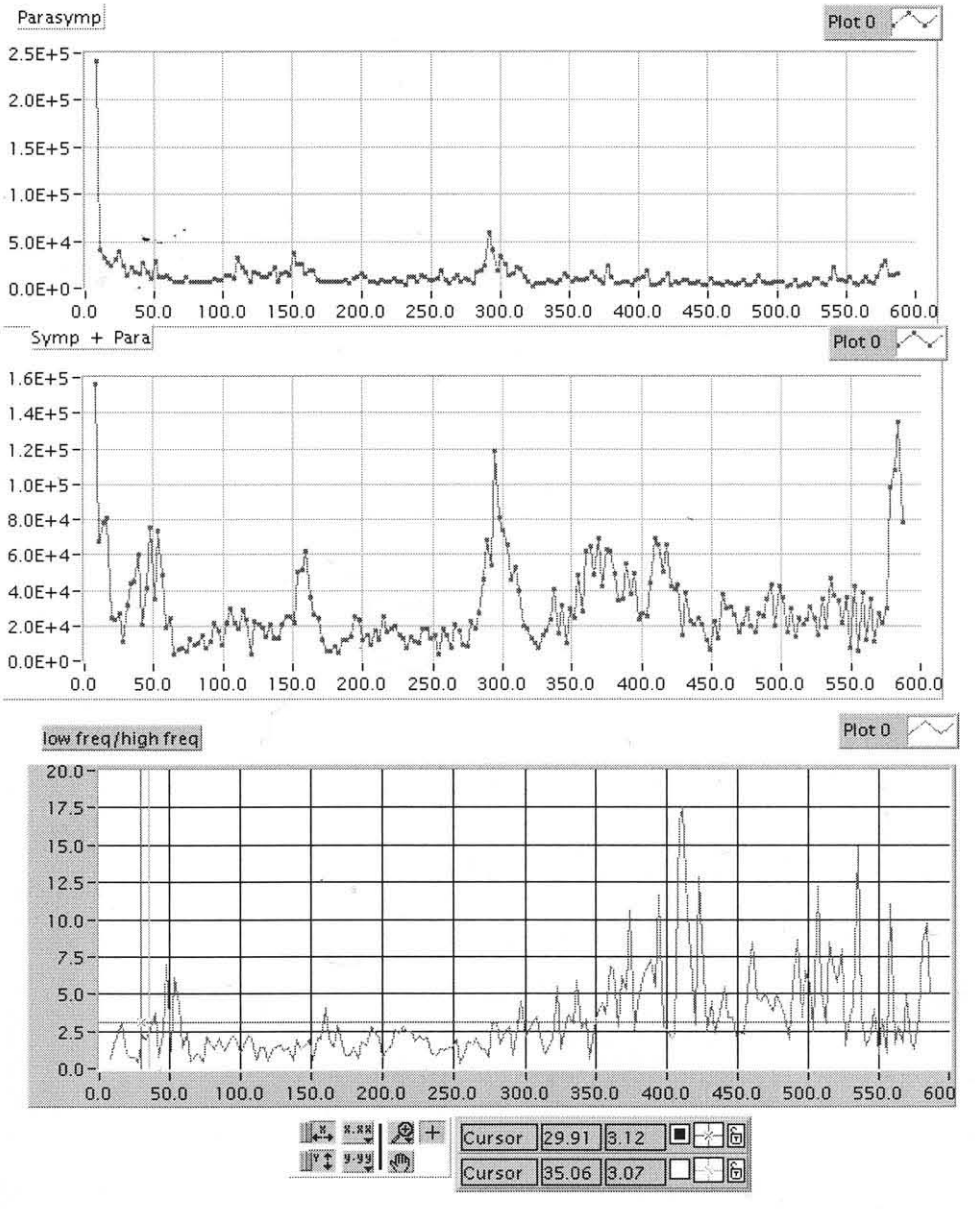
Parasymp
Plot 0
2.5E+5
2.0E+5
1.5E+5
1.0E+5
5.0E+4
0.0E+0
0.0 50.0 100.0 150.0 200.0 250.0 300.0 350.0 400.0 450.0 500.0 550.0 600.0
Symp + Para
Plot 0
1.6E+5
1.4E+5
1.2E+5
1.0E+5
8.0E+4
6.0E+4
4.0E+4
2.0E+4
0.0E+0
0.0 50.0 100.0 150.0 200.0 250.0 300.0 350.0 400.0 450.0 500.0 550.0 600.0
low freq/high freq
Plot 0
20.0
17.5
15.0
12.5
10.0
7.5
5.0
2.5
0.0
0.0 50.0 100.0 150.0 200.0 250.0 300.0 350.0 400.0 450.0 500.0 550.0 600
Cursor 29.91 3.12
Cursor 35.06 3.07

V002

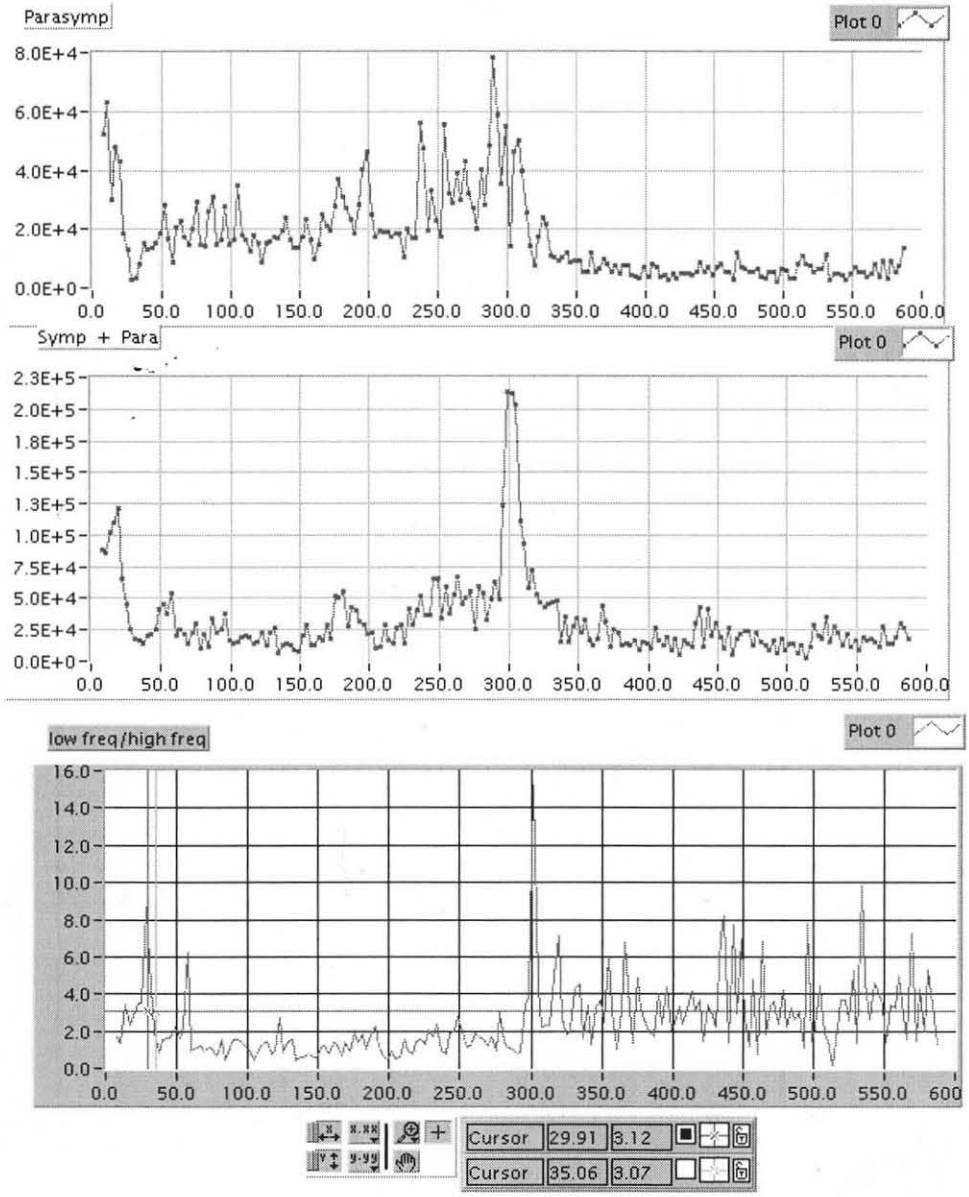
Parasymp
Plot 0
8.0E+4
6.0E+4
4.0E+4
2.0E+4
0.0E+0
0.0 50.0 100.0 150.0 200.0 250.0 300.0 350.0 400.0 450.0 500.0 550.0 600.0
Symp + Para
Plot 0
2.3E+5
2.0E+5
1.8E+5
1.5E+5
1.3E+5
1.0E+5
7.5E+4
5.0E+4
2.5E+4
0.0E+0
0.0 50.0 100.0 150.0 200.0 250.0 300.0 350.0 400.0 450.0 500.0 550.0 600.0
low freq/high freq
Plot 0
16.0
14.0
12.0
10.0
8.0
6.0
4.0
2.0
0.0
0.0 50.0 100.0 150.0 200.0 250.0 300.0 350.0 400.0 450.0 500.0 550.0 600
Cursor 29.91 3.12
Cursor 35.06 3.07

V004

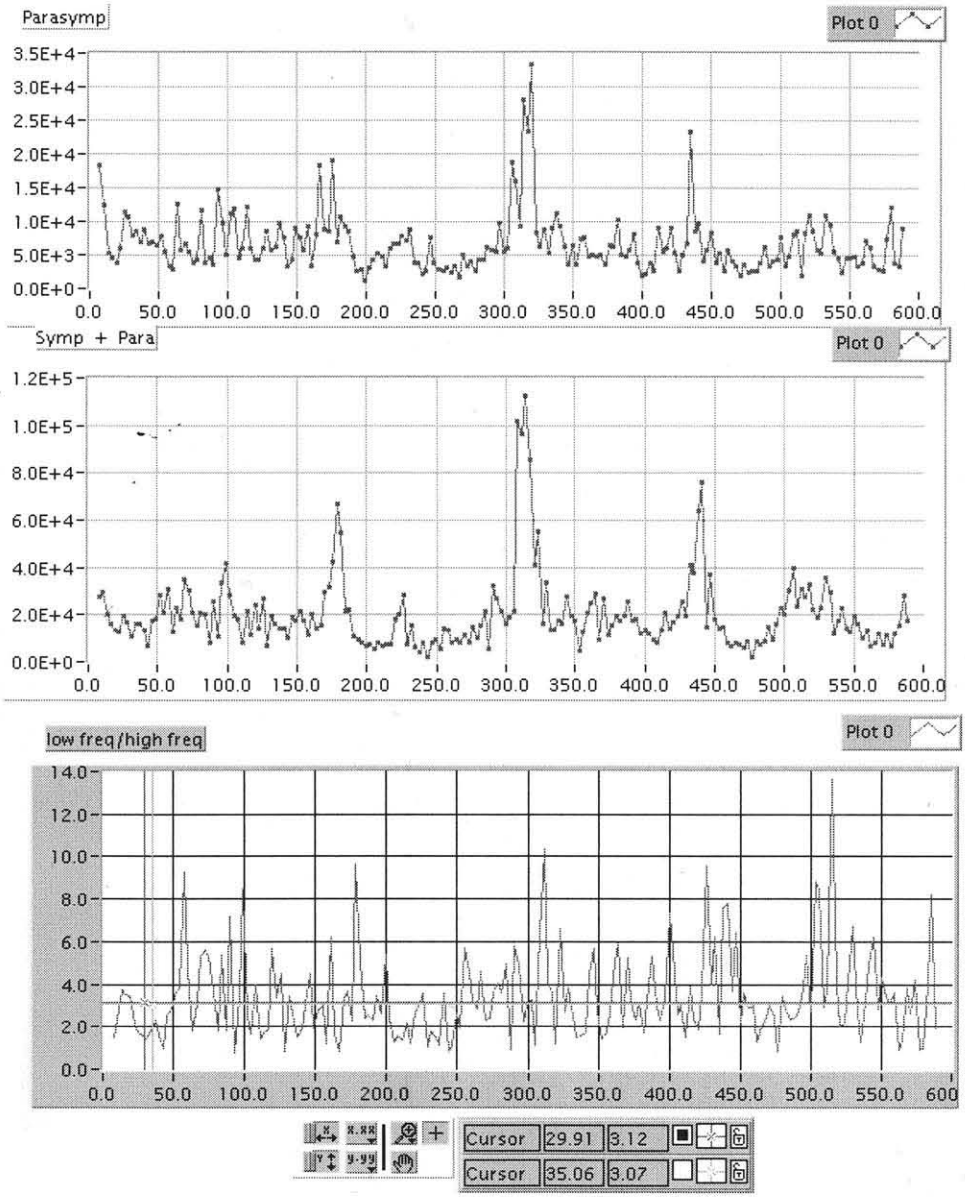
Parasymp
Plot 0
3.5E+4
3.0E+4
2.5E+4
2.0E+4
1.5E+4
1.0E+4
5.0E+3
0.0E+0
0.0 50.0 100.0 150.0 200.0 250.0 300.0 350.0 400.0 450.0 500.0 550.0 600.0
Symp + Para
Plot 0
1.2E+5
1.0E+5
8.0E+4
6.0E+4
4.0E+4
2.0E+4
0.0E+0
0.0 50.0 100.0 150.0 200.0 250.0 300.0 350.0 400.0 450.0 500.0 550.0 600.0
low freq/high freq
Plot 0
14.0
12.0
10.0
8.0
6.0
4.0
2.0
0.0
0.0 50.0 100.0 150.0 200.0 250.0 300.0 350.0 400.0 450.0 500.0 550.0 600
Cursor 29.91 3.12
Cursor 35.06 3.07

V006

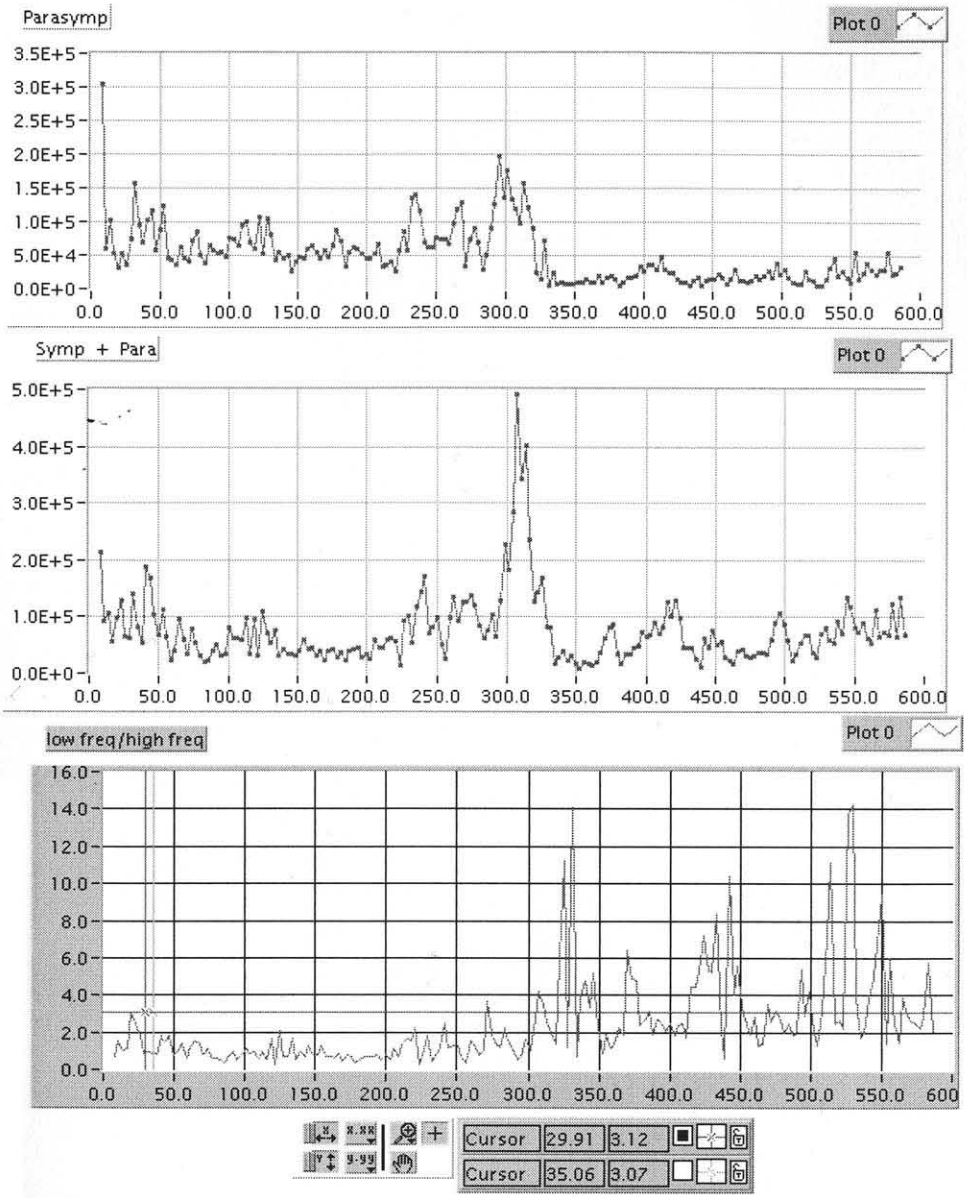
Parasymp
Plot 0
3.5E+5
3.0E+5
2.5E+5
2.0E+5
1.5E+5
1.0E+5
5.0E+4
0.0E+0
0.0 50.0 100.0 150.0 200.0 250.0 300.0 350.0 400.0 450.0 500.0 550.0 600.0
Symp + Para
Plot 0
5.0E+5
4.0E+5
3.0E+5
2.0E+5
1.0E+5
0.0E+0
0.0 50.0 100.0 150.0 200.0 250.0 300.0 350.0 400.0 450.0 500.0 550.0 600.0
low freq/high freq
Plot 0
16.0
14.0
12.0
10.0
8.0
6.0
4.0
2.0
0.0
0.0 50.0 100.0 150.0 200.0 250.0 300.0 350.0 400.0 450.0 500.0 550.0 600
Cursor 29.91 3.12
Cursor 35.06 3.07

V007

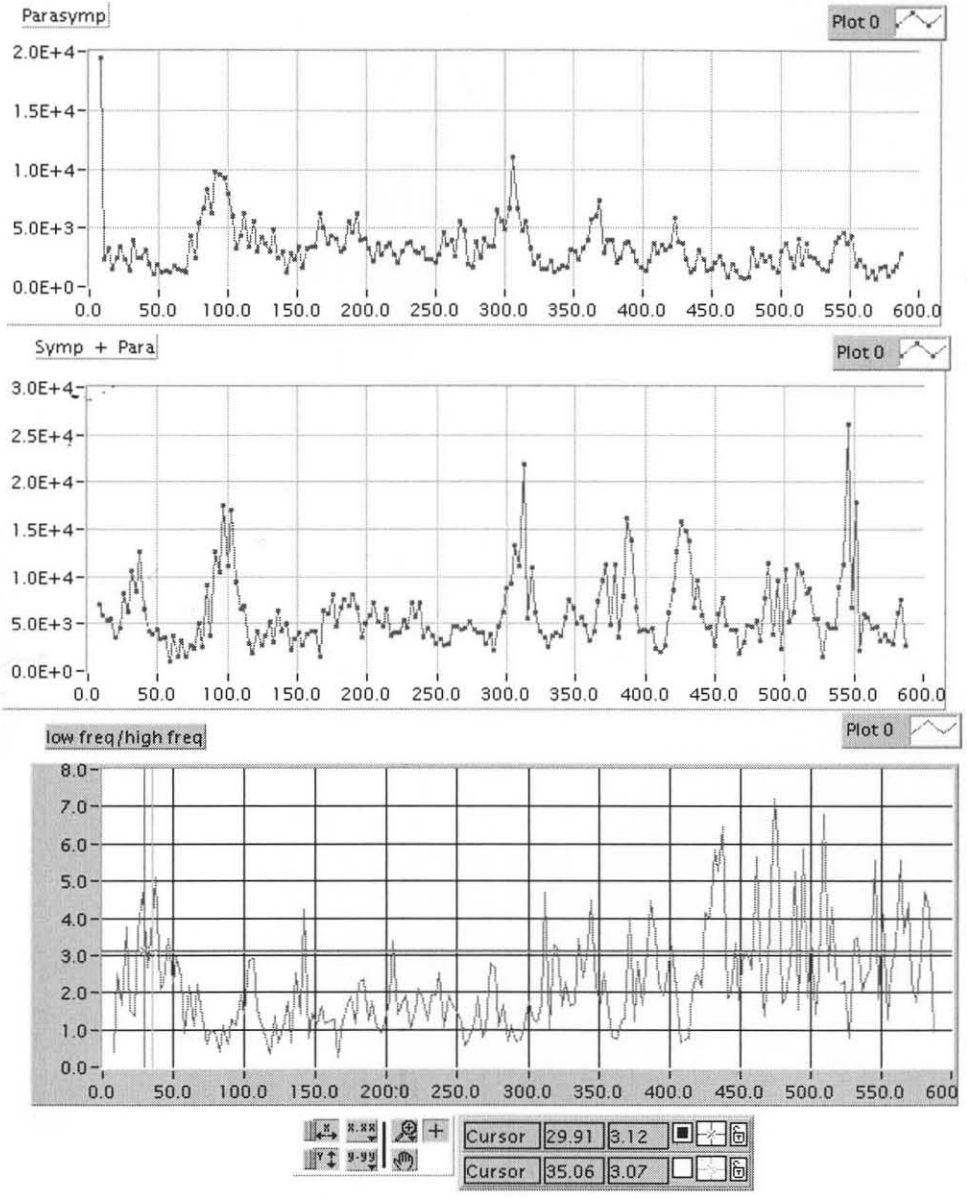
Parasymp
Plot 0
2.0E+4
1.5E+4
1.0E+4
5.0E+3
0.0E+0
0.0 50.0 100.0 150.0 200.0 250.0 300.0 350.0 400.0 450.0 500.0 550.0 600.0
Symp + Para
Plot 0
3.0E+4
2.5E+4
2.0E+4
1.5E+4
1.0E+4
5.0E+3
0.0E+0
0.0 50.0 100.0 150.0 200.0 250.0 300.0 350.0 400.0 450.0 500.0 550.0 600.0
low freq/high freq
Plot 0
8.0
7.0
6.0
5.0
4.0
3.0
2.0
1.0
0.0
0.0 50.0 100.0 150.0 200.0 250.0 300.0 350.0 400.0 450.0 500.0 550.0 600
Cursor 29.91 3.12
Cursor 35.06 3.07

V010

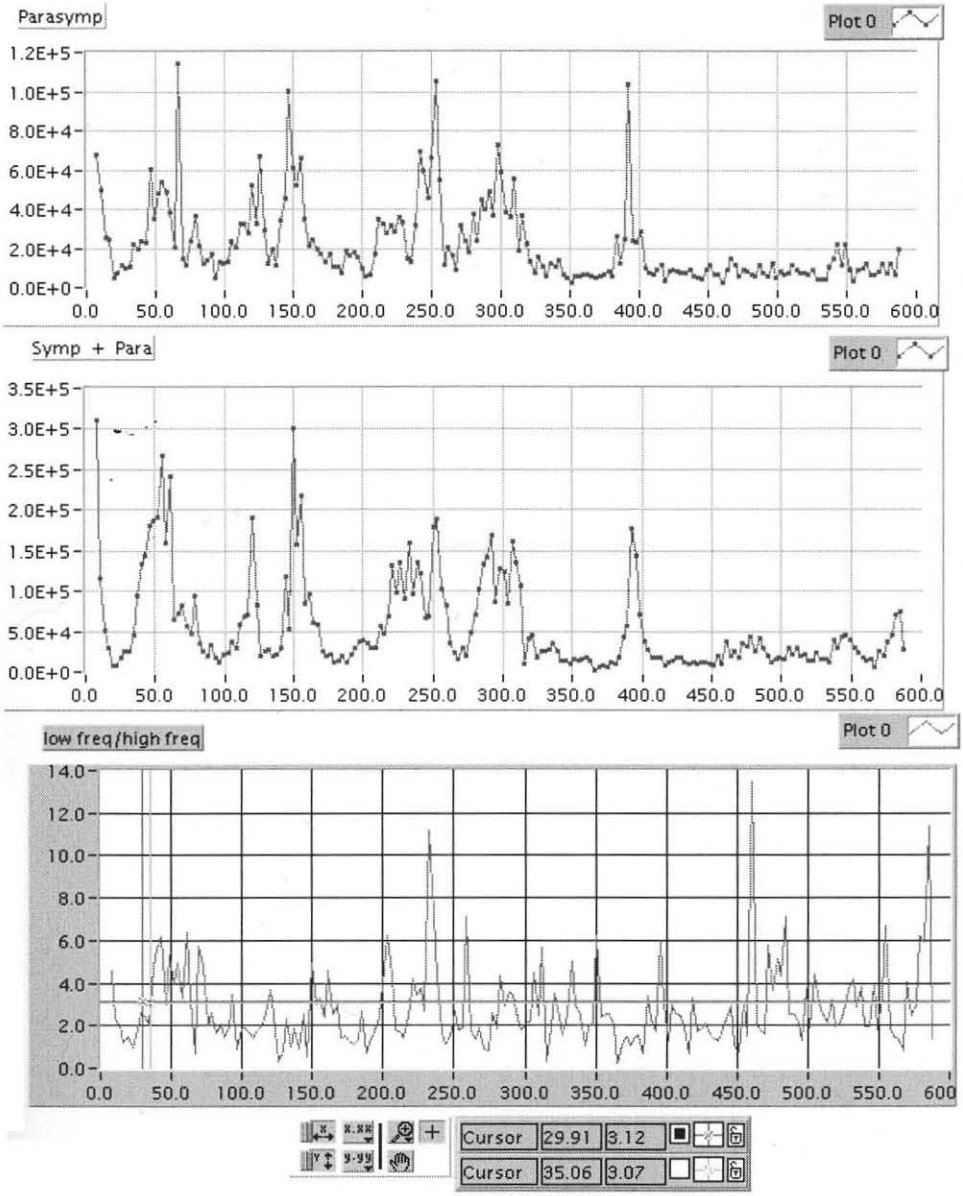
Parasymp
Plot 0
1.2E+5
1.0E+5
8.0E+4
6.0E+4
4.0E+4
2.0E+4
0.0E+0
0.0 50.0 100.0 150.0 200.0 250.0 300.0 350.0 400.0 450.0 500.0 550.0 600.0
Symp + Para
Plot 0
3.5E+5
3.0E+5
2.5E+5
2.0E+5
1.5E+5
1.0E+5
5.0E+4
0.0E+0
0.0 50.0 100.0 150.0 200.0 250.0 300.0 350.0 400.0 450.0 500.0 550.0 600.0
low freq/high freq
Plot 0
14.0
12.0
10.0
8.0
6.0
4.0
2.0
0.0
0.0 50.0 100.0 150.0 200.0 250.0 300.0 350.0 400.0 450.0 500.0 550.0 600
Cursor 29.91 3.12
Cursor 35.06 3.07

V012

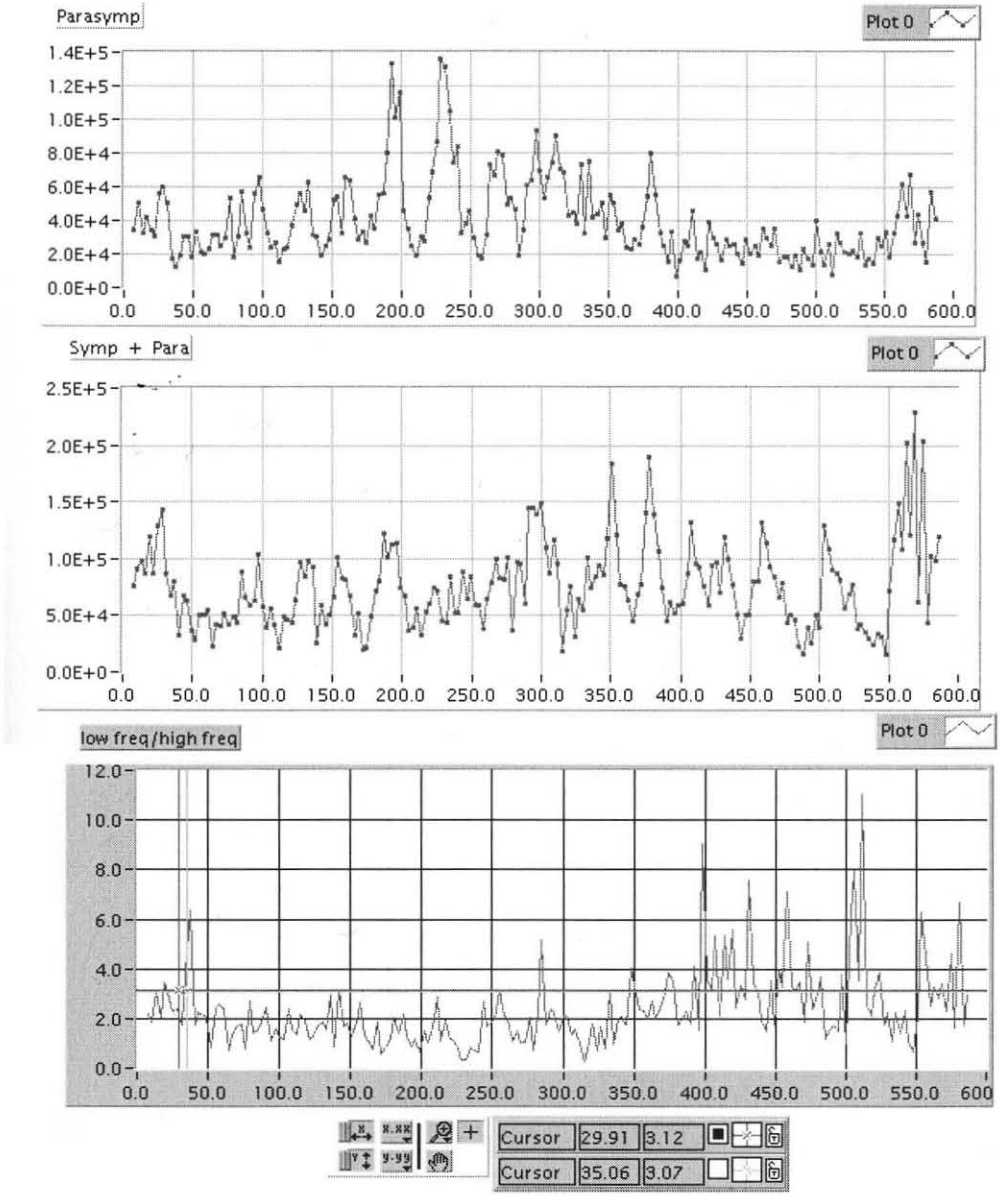
Parasymp
Plot 0
1.4E+5
1.2E+5
1.0E+5
8.0E+4
6.0E+4
4.0E+4
2.0E+4
0.0E+0
0.0 50.0 100.0 150.0 200.0 250.0 300.0 350.0 400.0 450.0 500.0 550.0 600.0
Symp + Para
Plot 0
2.5E+5
2.0E+5
1.5E+5
1.0E+5
5.0E+4
0.0E+0
0.0 50.0 100.0 150.0 200.0 250.0 300.0 350.0 400.0 450.0 500.0 550.0 600.0
low freq/high freq
Plot 0
12.0
10.0
8.0
6.0
4.0
2.0
0.0
0.0 50.0 100.0 150.0 200.0 250.0 300.0 350.0 400.0 450.0 500.0 550.0 600
Cursor 29.91 3.12
Cursor 35.06 3.07

V019

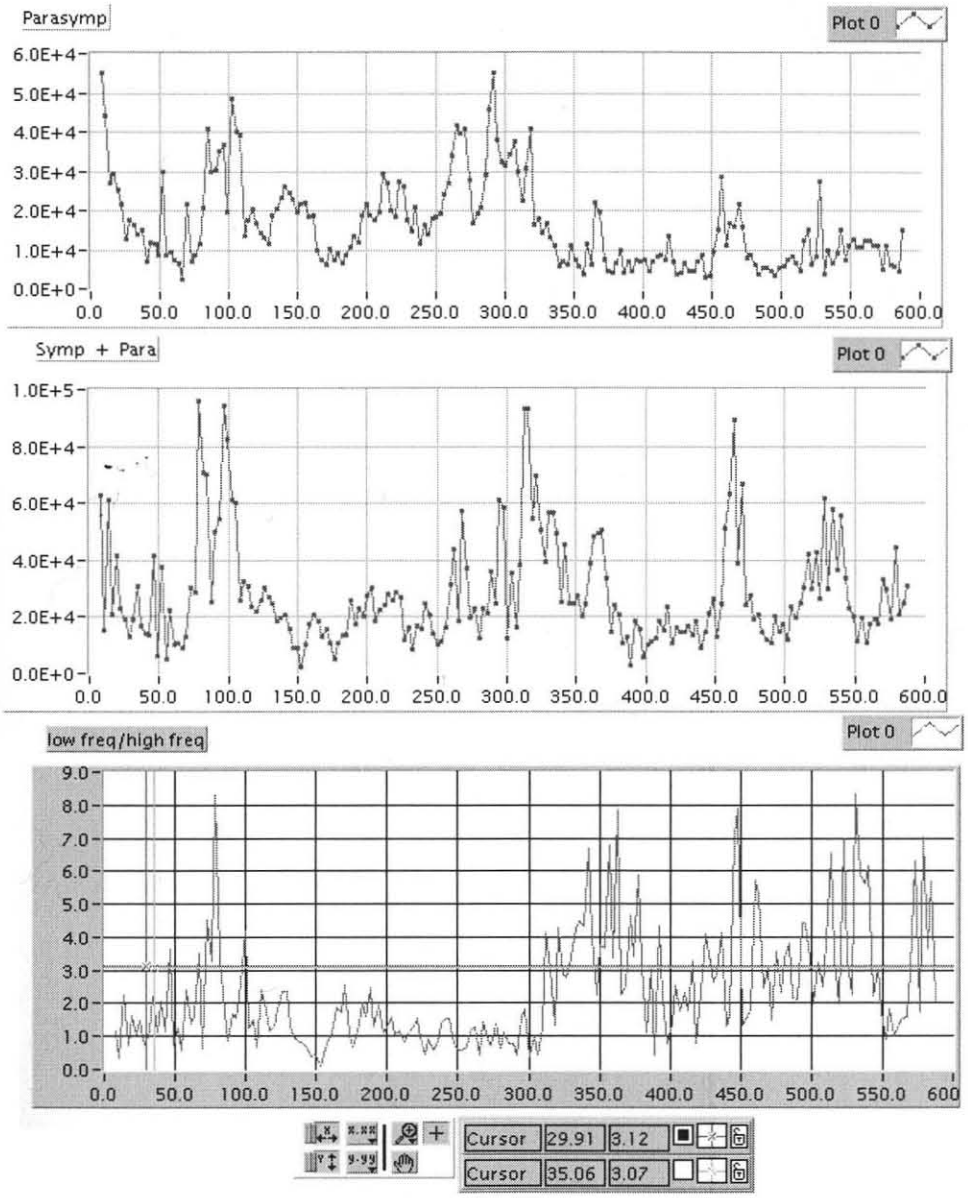
Parasymp
Plot 0
6.0E+4
5.0E+4
4.0E+4
3.0E+4
2.0E+4
1.0E+4
0.0E+0
0.0 50.0 100.0 150.0 200.0 250.0 300.0 350.0 400.0 450.0 500.0 550.0 600.0
Symp + Para
Plot 0
1.0E+5
8.0E+4
6.0E+4
4.0E+4
2.0E+4
0.0E+0
0.0 50.0 100.0 150.0 200.0 250.0 300.0 350.0 400.0 450.0 500.0 550.0 600.0
low freq/high freq
Plot 0
9.0
8.0
7.0
6.0
5.0
4.0
3.0
2.0
1.0
0.0
0.0 50.0 100.0 150.0 200.0 250.0 300.0 350.0 400.0 450.0 500.0 550.0 600
Cursor 29.91 3.12
Cursor 35.06 3.07

V025

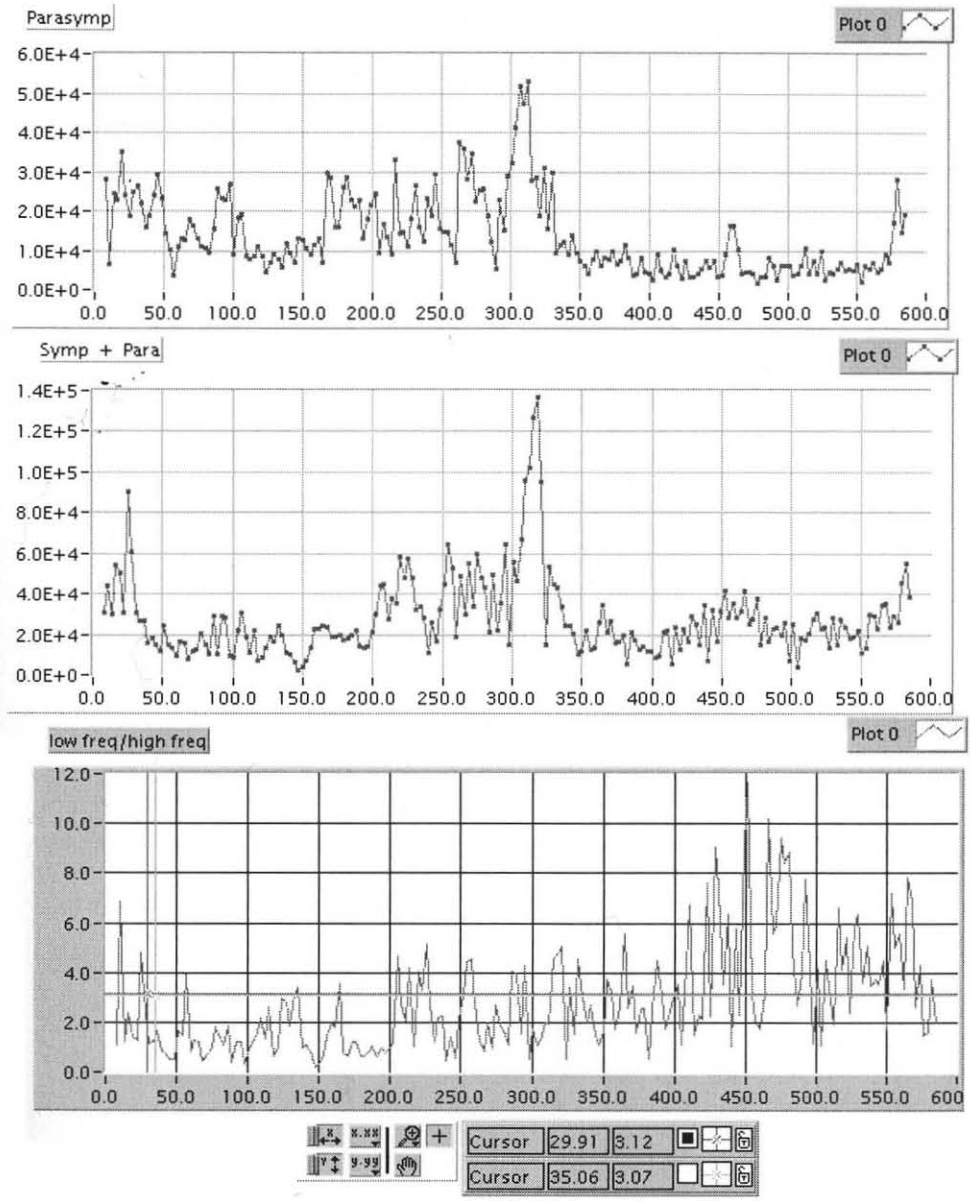
Parasymp
Plot 0
6.0E+4
5.0E+4
4.0E+4
3.0E+4
2.0E+4
1.0E+4
0.0E+0
0.0 50.0 100.0 150.0 200.0 250.0 300.0 350.0 400.0 450.0 500.0 550.0 600.0
Symp + Para
Plot 0
1.4E+5
1.2E+5
1.0E+5
8.0E+4
6.0E+4
4.0E+4
2.0E+4
0.0E+0
0.0 50.0 100.0 150.0 200.0 250.0 300.0 350.0 400.0 450.0 500.0 550.0 600.0
low freq/high freq
Plot 0
12.0
10.0
8.0
6.0
4.0
2.0
0.0
0.0 50.0 100.0 150.0 200.0 250.0 300.0 350.0 400.0 450.0 500.0 550.0 600
Cursor 29.91 3.12
Cursor 35.06 3.07

V030

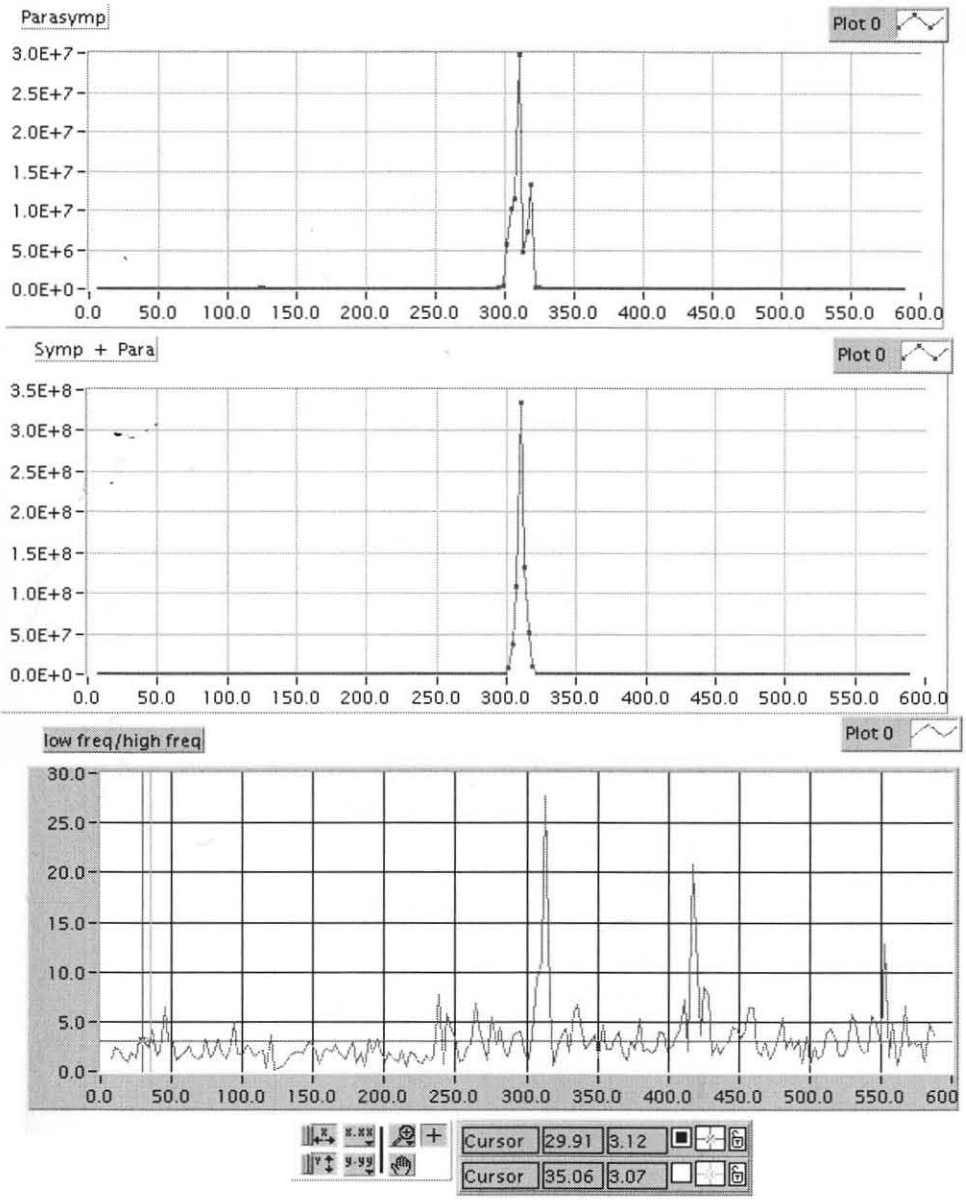
Parasymp
Plot 0
3.0E+7
2.5E+7
2.0E+7
1.5E+7
1.0E+7
5.0E+6
0.0E+0
0.0 50.0 100.0 150.0 200.0 250.0 300.0 350.0 400.0 450.0 500.0 550.0 600.0
Symp + Para
Plot 0
3.5E+8
3.0E+8
2.5E+8
2.0E+8
1.5E+8
1.0E+8
5.0E+7
0.0E+0
0.0 50.0 100.0 150.0 200.0 250.0 300.0 350.0 400.0 450.0 500.0 550.0 600.0
low freq/high freq
Plot 0
30.0
25.0
20.0
15.0
10.0
5.0
0.0
0.0 50.0 100.0 150.0 200.0 250.0 300.0 350.0 400.0 450.0 500.0 550.0 600
Cursor 29.91 3.12
Cursor 35.06 3.07

V032

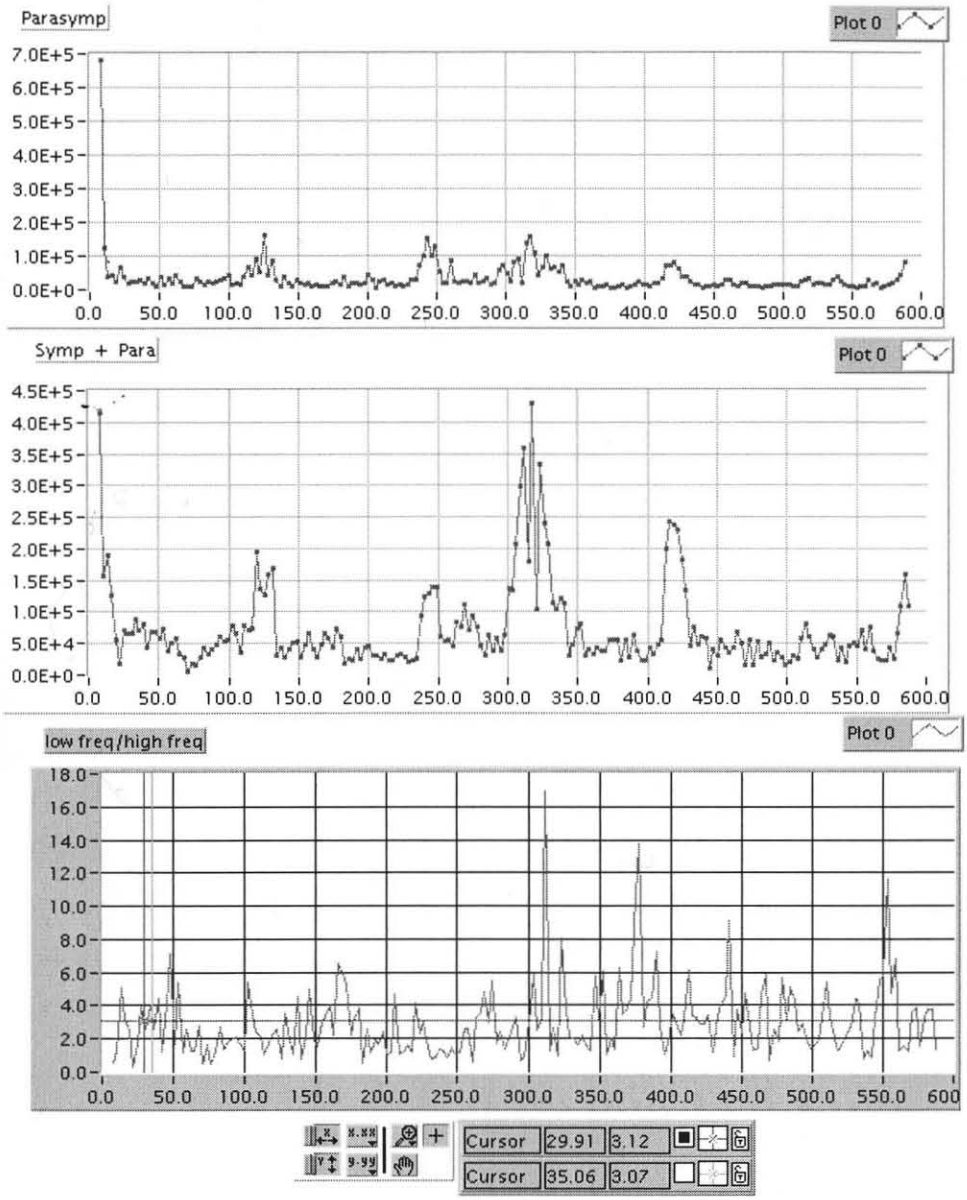
Parasymp
Plot 0
7.0E+5
6.0E+5
5.0E+5
4.0E+5
3.0E+5
2.0E+5
1.0E+5
0.0E+0
0.0 50.0 100.0 150.0 200.0 250.0 300.0 350.0 400.0 450.0 500.0 550.0 600.0
Symp + Para
Plot 0
4.5E+5
4.0E+5
3.5E+5
3.0E+5
2.5E+5
2.0E+5
1.5E+5
1.0E+5
5.0E+4
0.0E+0
0.0 50.0 100.0 150.0 200.0 250.0 300.0 350.0 400.0 450.0 500.0 550.0 600.0
low freq/high freq
Plot 0
18.0
16.0
14.0
12.0
10.0
8.0
6.0
4.0
2.0
0.0
0.0 50.0 100.0 150.0 200.0 250.0 300.0 350.0 400.0 450.0 500.0 550.0 600
Cursor 29.91 3.12
Cursor 35.06 3.07

V041

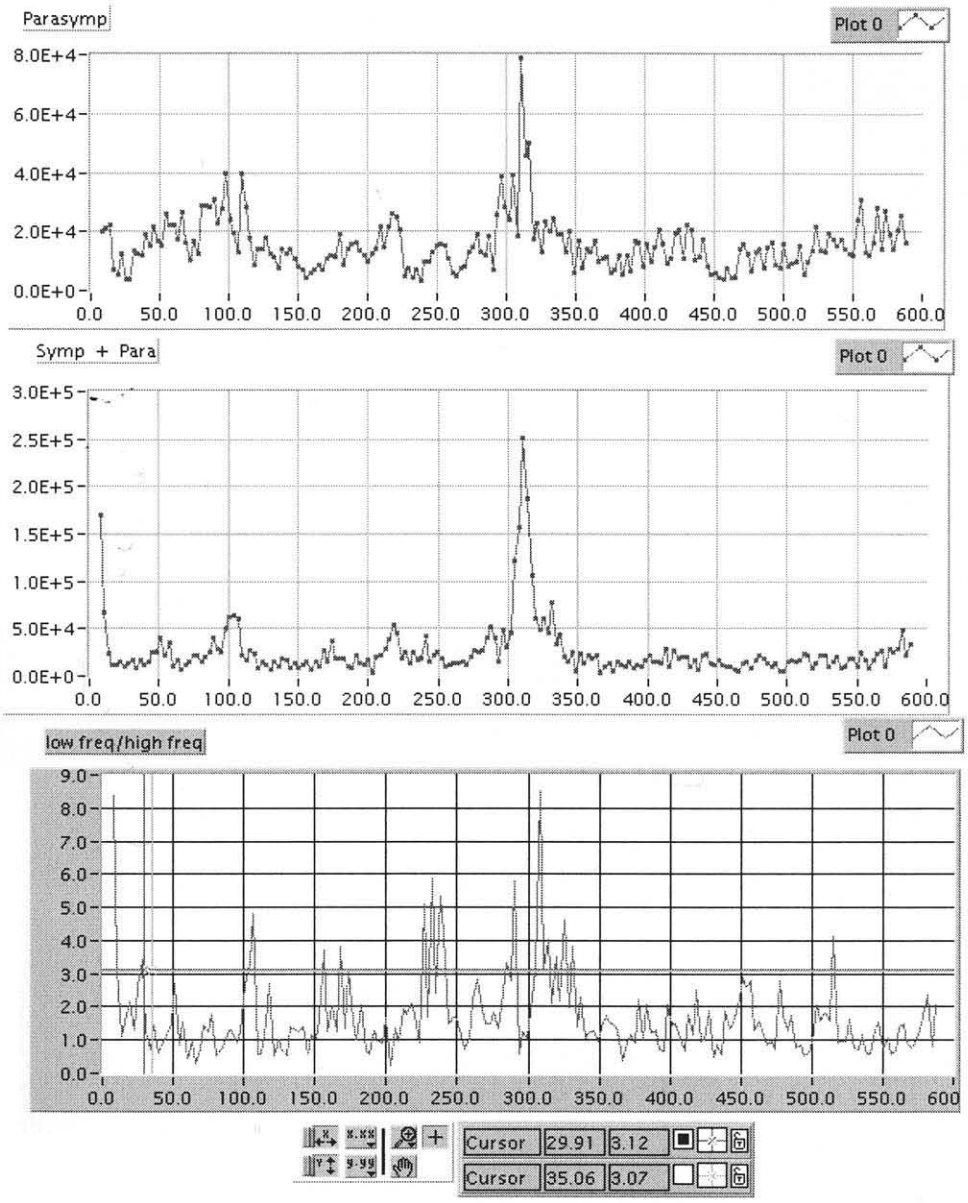
Parasymp
Plot 0
8.0E+4
6.0E+4
4.0E+4
2.0E+4
0.0E+0
0.0 50.0 100.0 150.0 200.0 250.0 300.0 350.0 400.0 450.0 500.0 550.0 600.0
Symp + Para
Plot 0
3.0E+5
2.5E+5
2.0E+5
1.5E+5
1.0E+5
5.0E+4
0.0E+0
0.0 50.0 100.0 150.0 200.0 250.0 300.0 350.0 400.0 450.0 500.0 550.0 600.0
low freq/high freq
Plot 0
9.0
8.0
7.0
6.0
5.0
4.0
3.0
2.0
1.0
0.0
0.0 50.0 100.0 150.0 200.0 250.0 300.0 350.0 400.0 450.0 500.0 550.0 600
Cursor 29.91 3.12
Cursor 35.06 3.07

V045

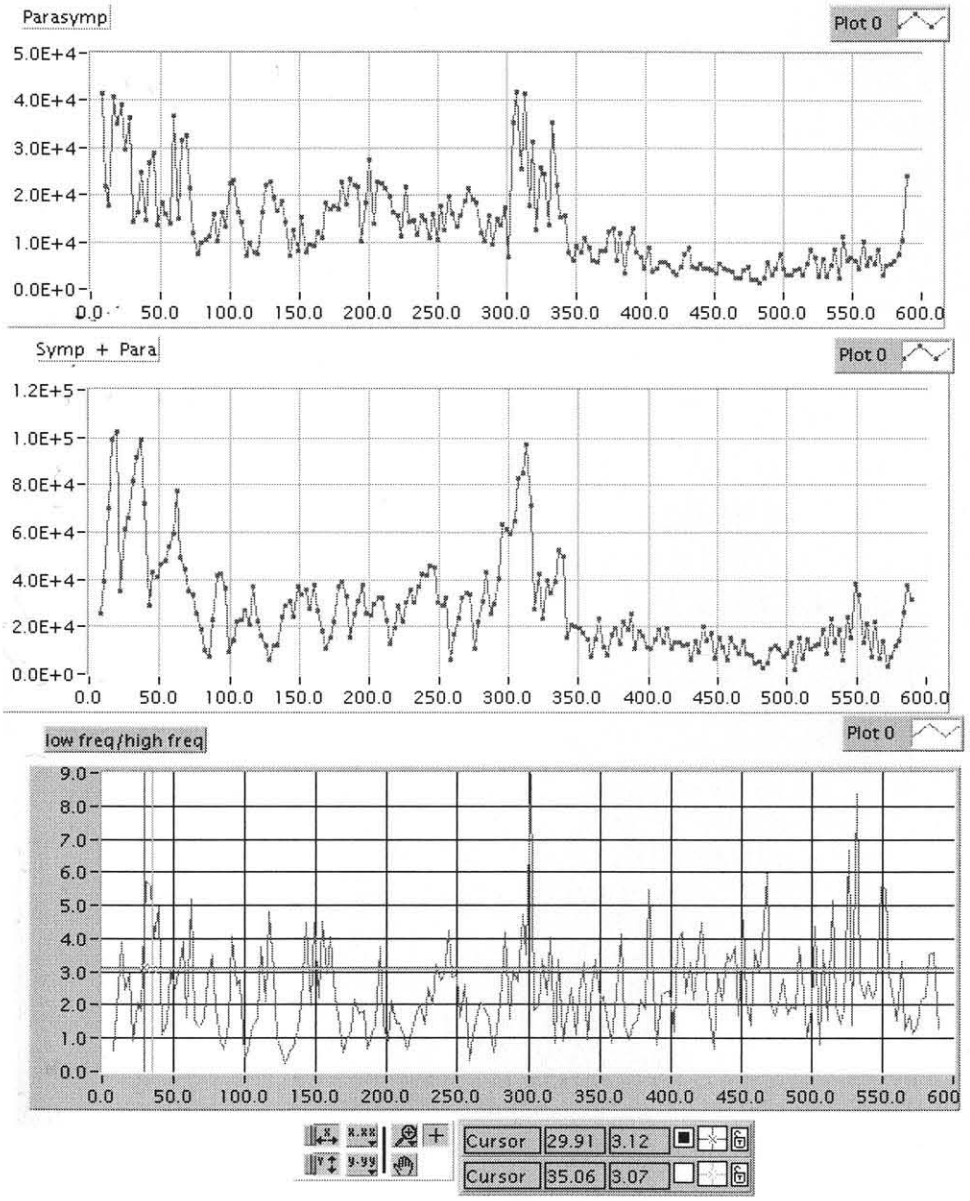
Parasymp
Plot 0
5.0E+4
4.0E+4
3.0E+4
2.0E+4
1.0E+4
0.0E+0
0.0 50.0 100.0 150.0 200.0 250.0 300.0 350.0 400.0 450.0 500.0 550.0 600.0
Symp + Para
Plot 0
1.2E+5
1.0E+5
8.0E+4
6.0E+4
4.0E+4
2.0E+4
0.0E+0
0.0 50.0 100.0 150.0 200.0 250.0 300.0 350.0 400.0 450.0 500.0 550.0 600.0
low freq/high freq
Plot 0
9.0
8.0
7.0
6.0
5.0
4.0
3.0
2.0
1.0
0.0
0.0 50.0 100.0 150.0 200.0 250.0 300.0 350.0 400.0 450.0 500.0 550.0 600
Cursor 29.91 3.12
Cursor 35.06 3.07

V047

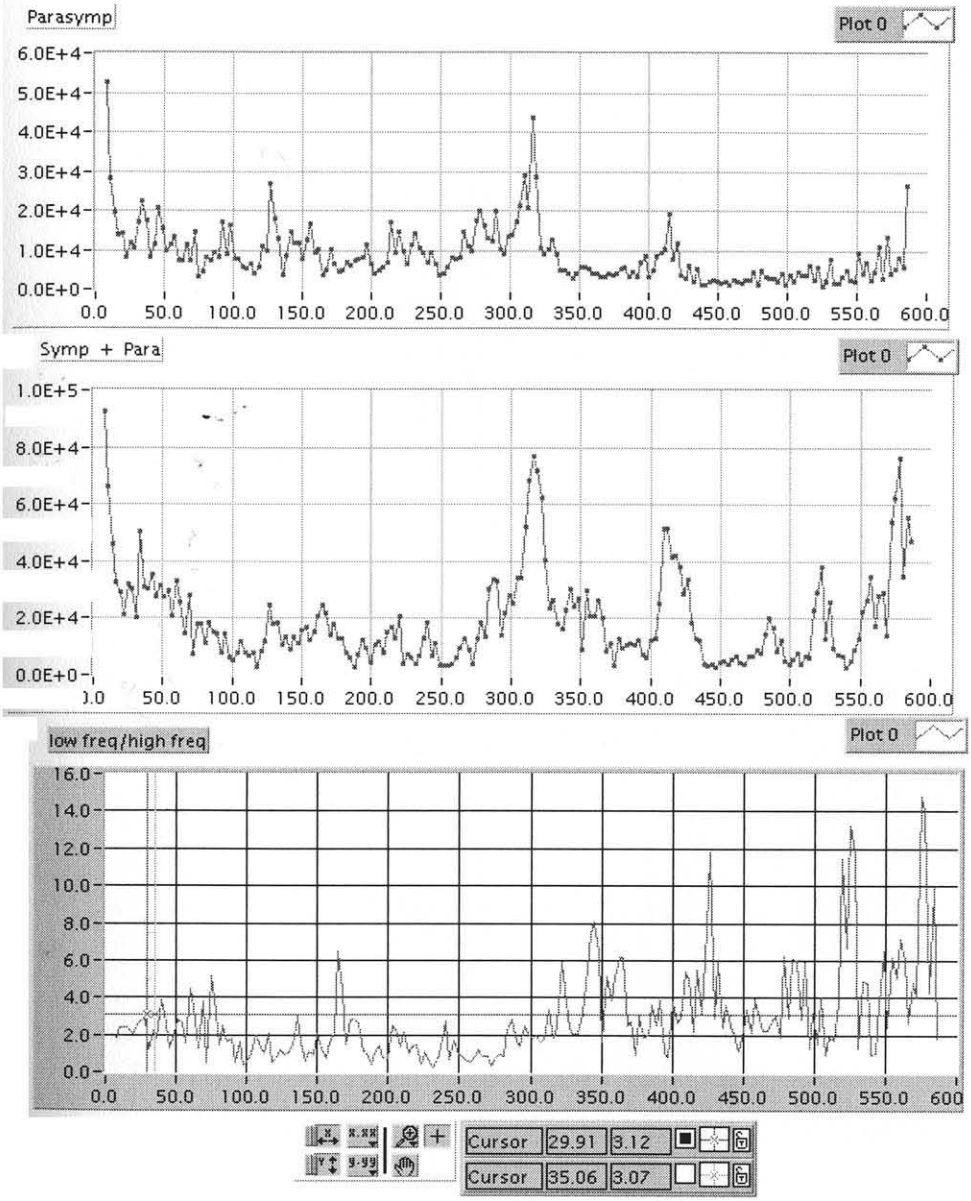
Parasymp
Plot 0
6.0E+4
5.0E+4
4.0E+4
3.0E+4
2.0E+4
1.0E+4
0.0E+0
0.0 50.0 100.0 150.0 200.0 250.0 300.0 350.0 400.0 450.0 500.0 550.0 600.0
Symp + Para
Plot 0
1.0E+5
8.0E+4
6.0E+4
4.0E+4
2.0E+4
0.0E+0
0.0 50.0 100.0 150.0 200.0 250.0 300.0 350.0 400.0 450.0 500.0 550.0 600.0
low freq/high freq
Plot 0
16.0
14.0
12.0
10.0
8.0
6.0
4.0
2.0
0.0
0.0 50.0 100.0 150.0 200.0 250.0 300.0 350.0 400.0 450.0 500.0 550.0 600
Cursor 29.91 3.12
Cursor 35.06 3.07

V051

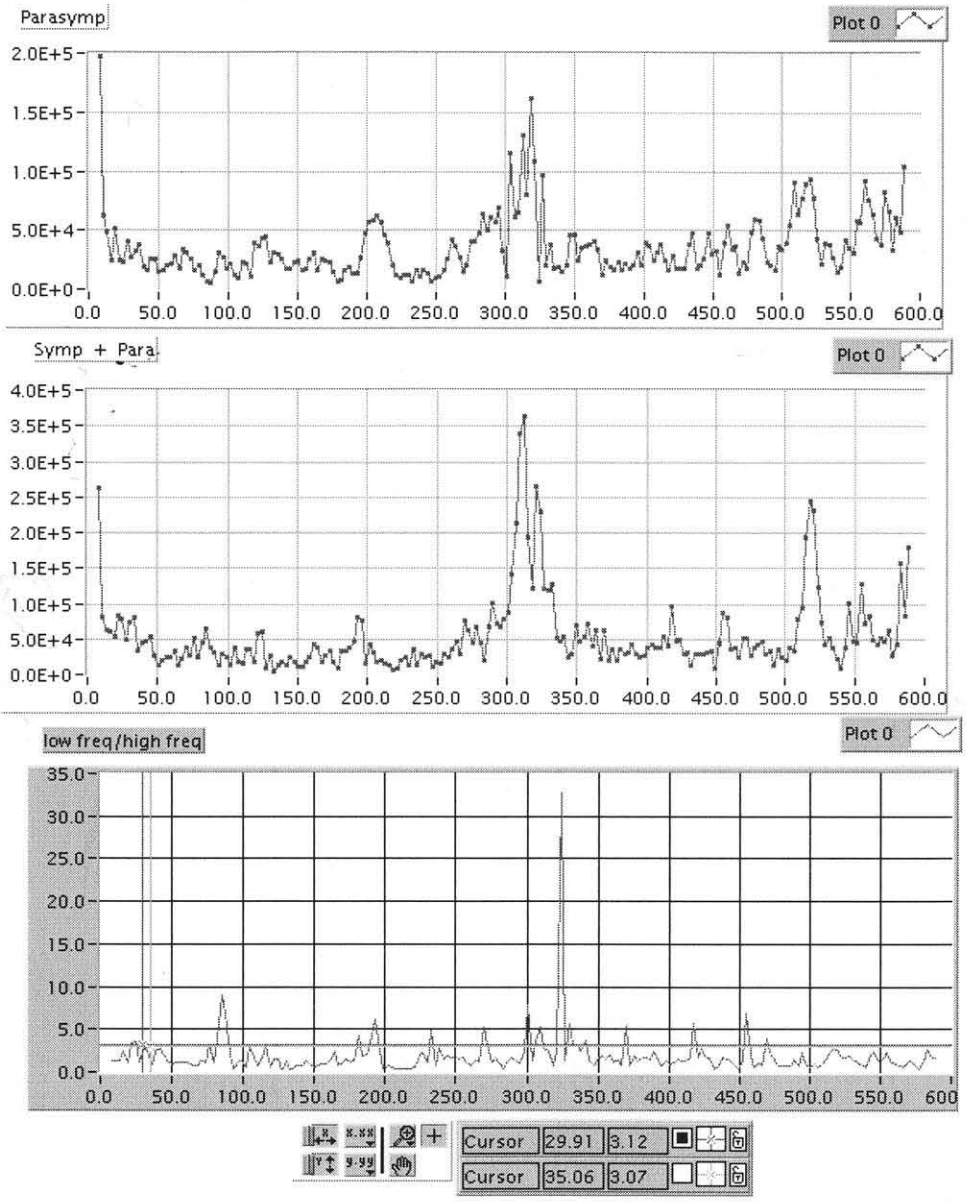
Parasymp
Plot 0
2.0E+5
1.5E+5
1.0E+5
5.0E+4
0.0E+0
0.0 50.0 100.0 150.0 200.0 250.0 300.0 350.0 400.0 450.0 500.0 550.0 600.0
Symp + Para
Plot 0
4.0E+5
3.5E+5
3.0E+5
2.5E+5
2.0E+5
1.5E+5
1.0E+5
5.0E+4
0.0E+0
0.0 50.0 100.0 150.0 200.0 250.0 300.0 350.0 400.0 450.0 500.0 550.0 600.0
low freq/high freq
Plot 0
35.0
30.0
25.0
20.0
15.0
10.0
5.0
0.0
0.0 50.0 100.0 150.0 200.0 250.0 300.0 350.0 400.0 450.0 500.0 550.0 600
Cursor 29.91 3.12
Cursor 35.06 3.07

V052

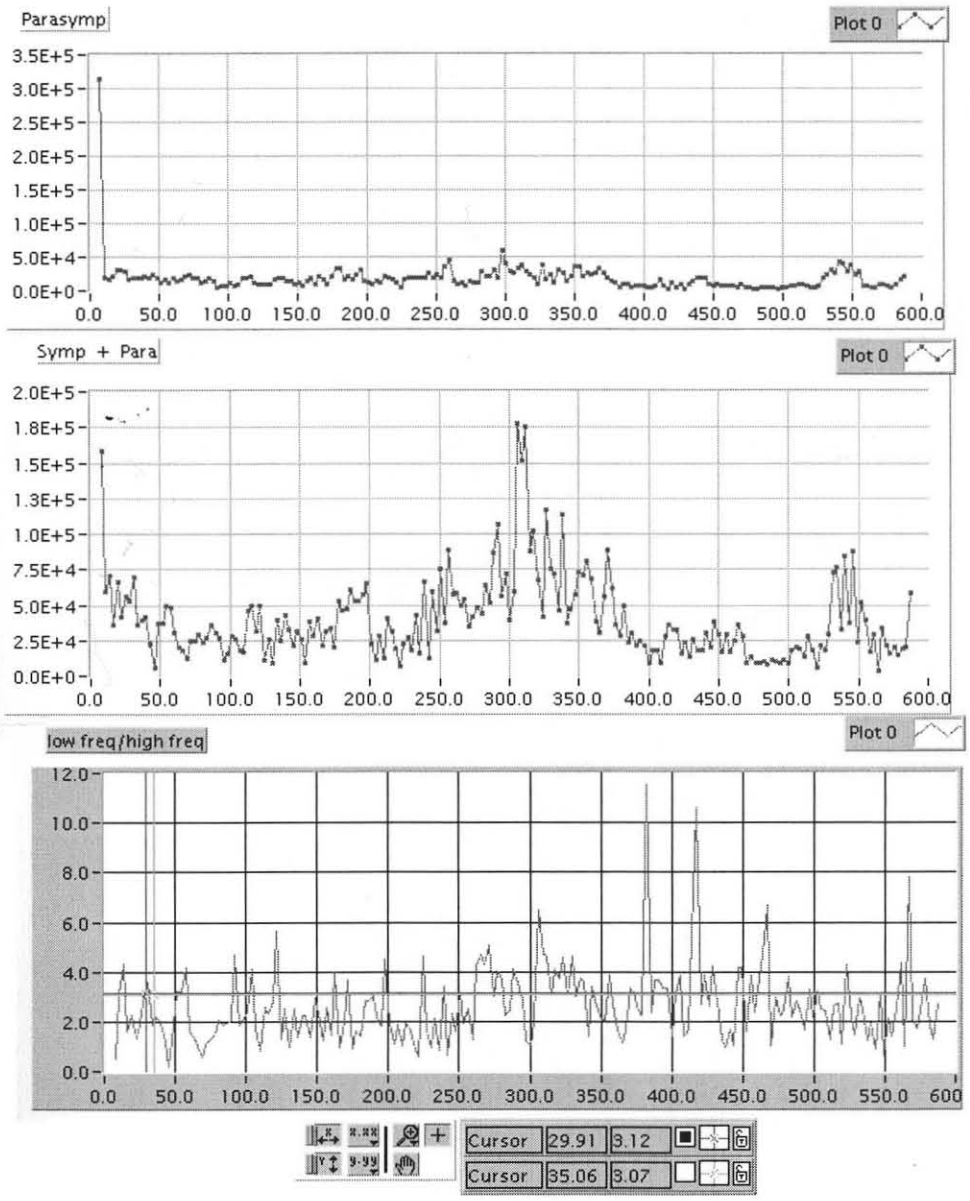
Parasymp
Plot 0
3.5E+5
3.0E+5
2.5E+5
2.0E+5
1.5E+5
1.0E+5
5.0E+4
0.0E+0
0.0 50.0 100.0 150.0 200.0 250.0 300.0 350.0 400.0 450.0 500.0 550.0 600.0
Symp + Para
Plot 0
2.0E+5
1.8E+5
1.5E+5
1.3E+5
1.0E+5
7.5E+4
5.0E+4
2.5E+4
0.0E+0
0.0 50.0 100.0 150.0 200.0 250.0 300.0 350.0 400.0 450.0 500.0 550.0 600.0
low freq/high freq
Plot 0
12.0
10.0
8.0
6.0
4.0
2.0
0.0
0.0 50.0 100.0 150.0 200.0 250.0 300.0 350.0 400.0 450.0 500.0 550.0 600
Cursor 29.91 3.12
Cursor 35.06 3.07

V053

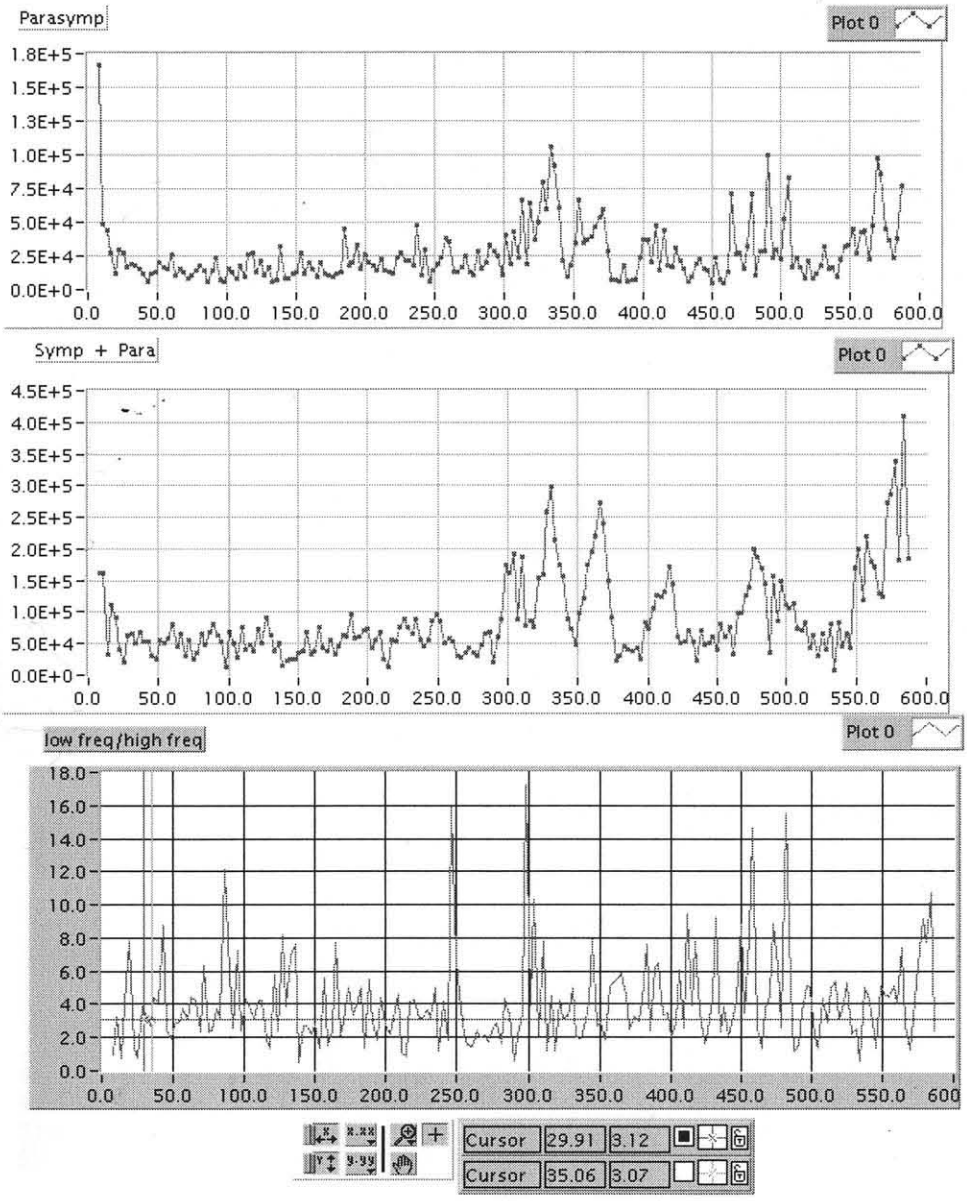
Parasymp
Plot 0
1.8E+5
1.5E+5
1.3E+5
1.0E+5
7.5E+4
5.0E+4
2.5E+4
0.0E+0
0.0 50.0 100.0 150.0 200.0 250.0 300.0 350.0 400.0 450.0 500.0 550.0 600.0
Symp + Para
Plot 0
4.5E+5
4.0E+5
3.5E+5
3.0E+5
2.5E+5
2.0E+5
1.5E+5
1.0E+5
5.0E+4
0.0E+0
0.0 50.0 100.0 150.0 200.0 250.0 300.0 350.0 400.0 450.0 500.0 550.0 600.0
low freq/high freq
Plot 0
18.0
16.0
14.0
12.0
10.0
8.0
6.0
4.0
2.0
0.0
0.0 50.0 100.0 150.0 200.0 250.0 300.0 350.0 400.0 450.0 500.0 550.0 600
Cursor 29.91 3.12
Cursor 35.06 3.07

V055

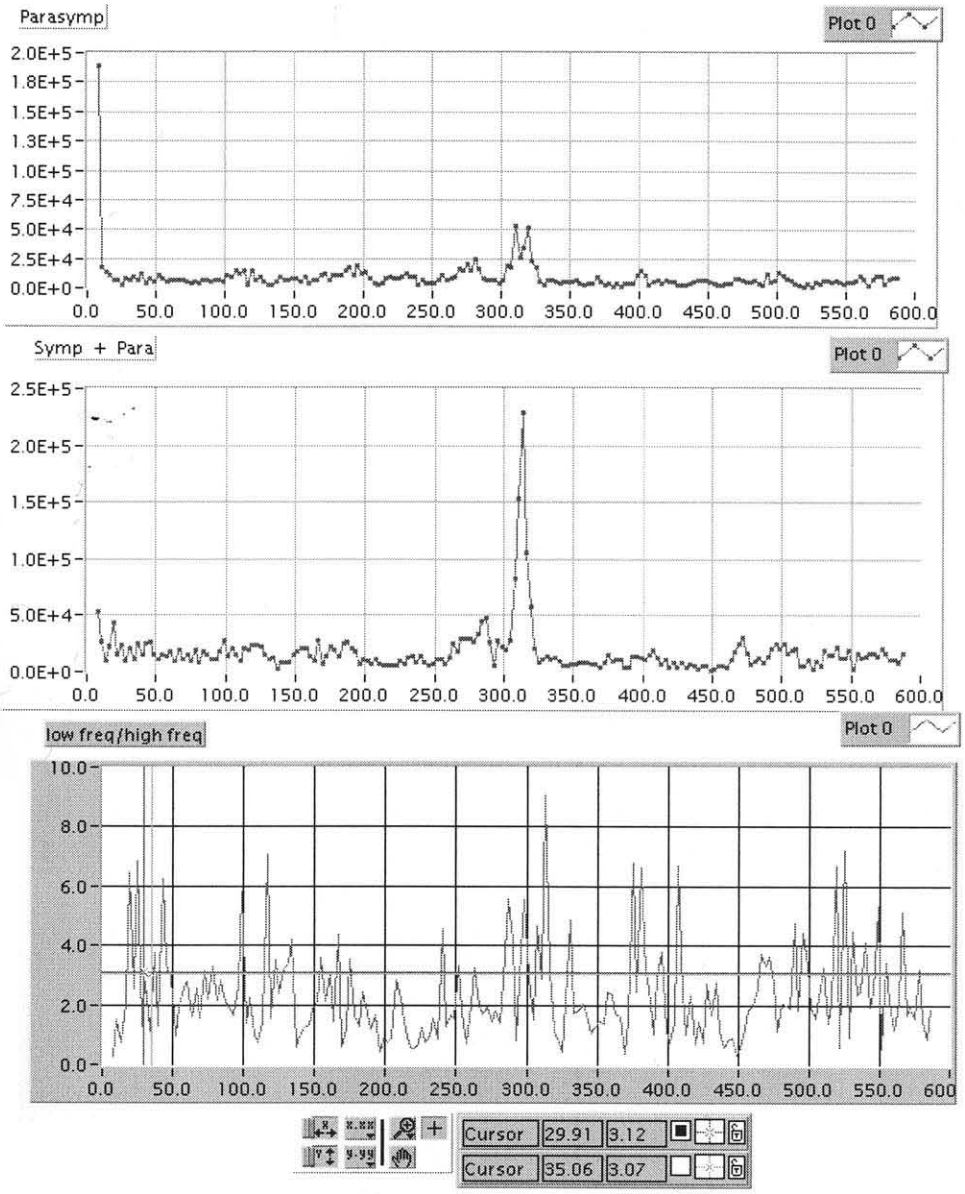
Parasymp
Plot 0
2.0E+5
1.8E+5
1.5E+5
1.3E+5
1.0E+5
7.5E+4
5.0E+4
2.5E+4
0.0E+0
0.0 50.0 100.0 150.0 200.0 250.0 300.0 350.0 400.0 450.0 500.0 550.0 600.0
Symp + Para
Plot 0
2.5E+5
2.0E+5
1.5E+5
1.0E+5
5.0E+4
0.0E+0
0.0 50.0 100.0 150.0 200.0 250.0 300.0 350.0 400.0 450.0 500.0 550.0 600.0
low freq/high freq
Plot 0
10.0
8.0
6.0
4.0
2.0
0.0
0.0 50.0 100.0 150.0 200.0 250.0 300.0 350.0 400.0 450.0 500.0 550.0 600
Cursor 29.91 3.12
Cursor 35.06 3.07

V057

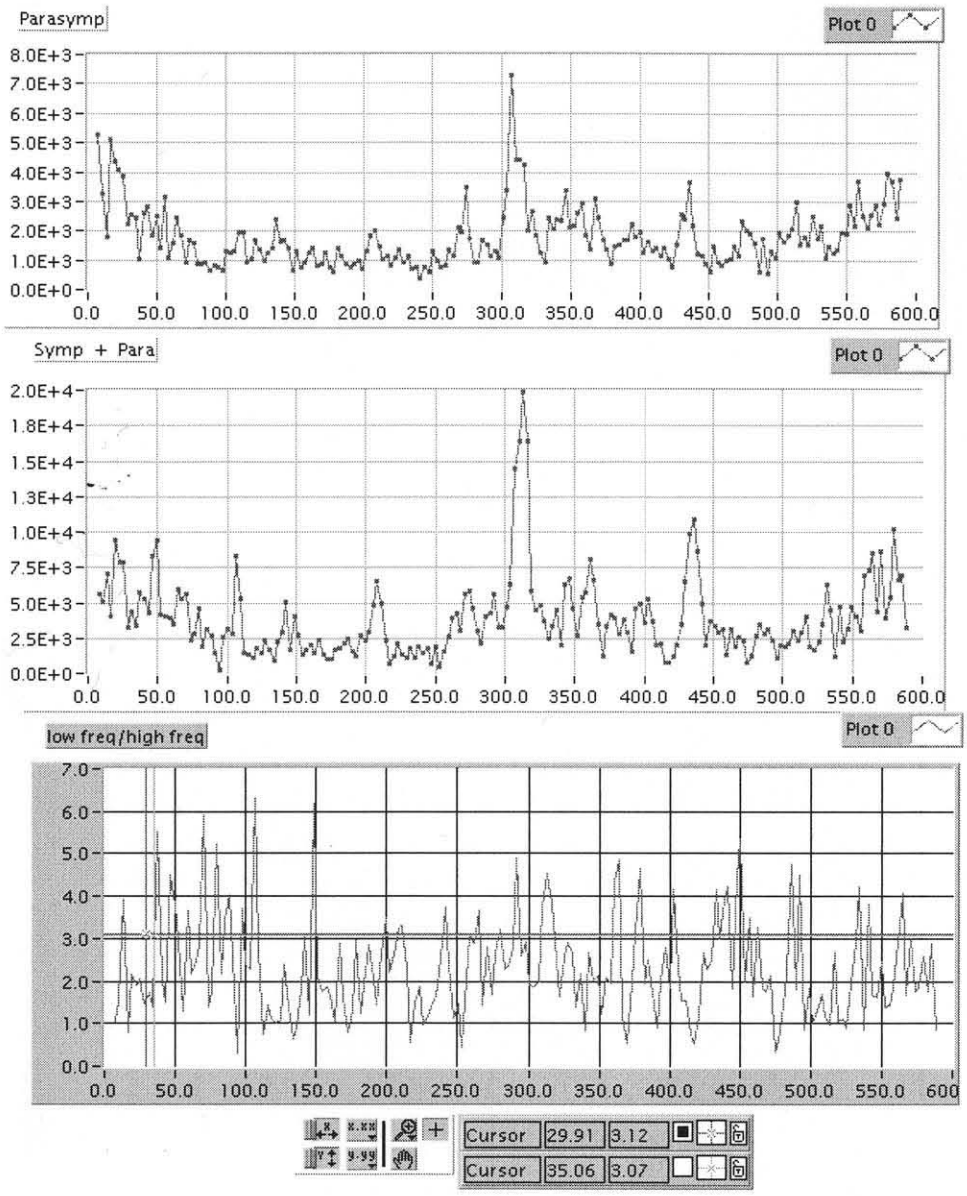
Parasymp
Plot 0
8.0E+3
7.0E+3
6.0E+3
5.0E+3
4.0E+3
3.0E+3
2.0E+3
1.0E+3
0.0E+0
0.0 50.0 100.0 150.0 200.0 250.0 300.0 350.0 400.0 450.0 500.0 550.0 600.0
Symp + Para
Plot 0
2.0E+4
1.8E+4
1.5E+4
1.3E+4
1.0E+4
7.5E+3
5.0E+3
2.5E+3
0.0E+0
0.0 50.0 100.0 150.0 200.0 250.0 300.0 350.0 400.0 450.0 500.0 550.0 600.0
low freq/high freq
Plot 0
7.0
6.0
5.0
4.0
3.0
2.0
1.0
0.0
0.0 50.0 100.0 150.0 200.0 250.0 300.0 350.0 400.0 450.0 500.0 550.0 600
Cursor 29.91 3.12
Cursor 35.06 3.07

V060

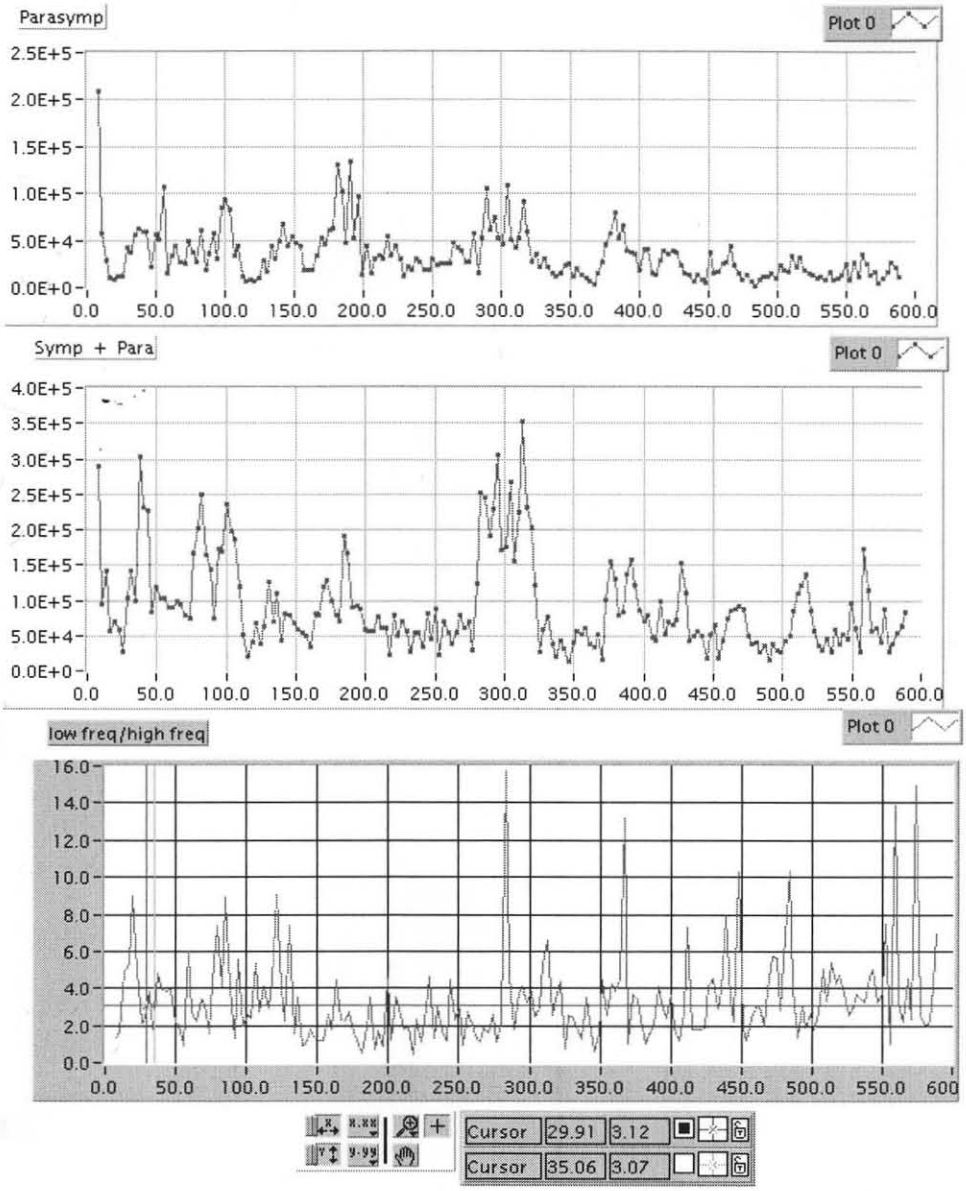
Parasymp
Plot 0
2.5E+5
2.0E+5
1.5E+5
1.0E+5
5.0E+4
0.0E+0
0.0 50.0 100.0 150.0 200.0 250.0 300.0 350.0 400.0 450.0 500.0 550.0 600.0
Symp + Para
Plot 0
4.0E+5
3.5E+5
3.0E+5
2.5E+5
2.0E+5
1.5E+5
1.0E+5
5.0E+4
0.0E+0
0.0 50.0 100.0 150.0 200.0 250.0 300.0 350.0 400.0 450.0 500.0 550.0 600.0
low freq/high freq
Plot 0
16.0
14.0
12.0
10.0
8.0
6.0
4.0
2.0
0.0
0.0 50.0 100.0 150.0 200.0 250.0 300.0 350.0 400.0 450.0 500.0 550.0 600
Cursor 29.91 3.12
Cursor 35.06 3.07

V064

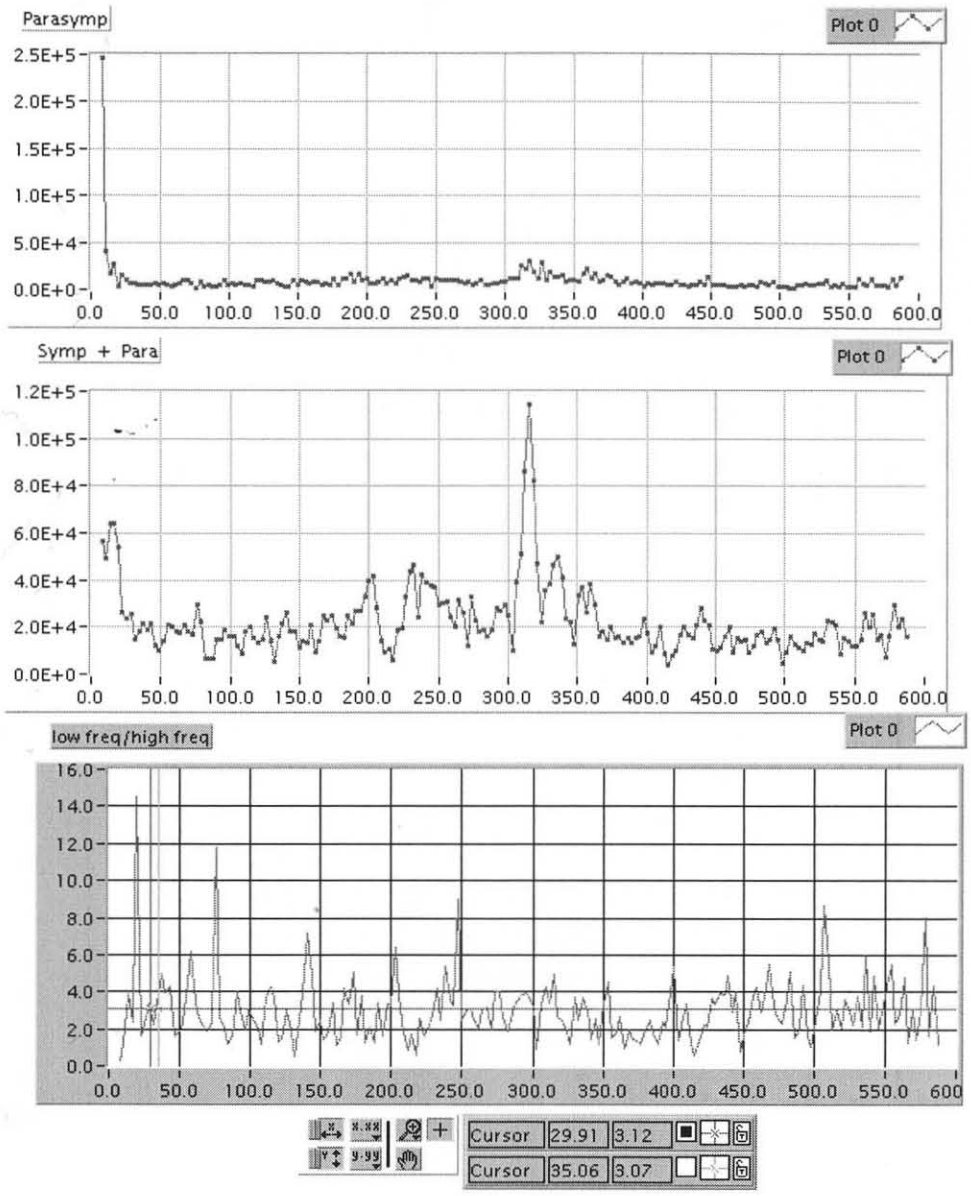
Parasymp
Plot 0
2.5E+5
2.0E+5
1.5E+5
1.0E+5
5.0E+4
0.0E+0
0.0 50.0 100.0 150.0 200.0 250.0 300.0 350.0 400.0 450.0 500.0 550.0 600.0
Symp + Para
Plot 0
1.2E+5
1.0E+5
8.0E+4
6.0E+4
4.0E+4
2.0E+4
0.0E+0
0.0 50.0 100.0 150.0 200.0 250.0 300.0 350.0 400.0 450.0 500.0 550.0 600.0
low freq/high freq
Plot 0
16.0
14.0
12.0
10.0
8.0
6.0
4.0
2.0
0.0
0.0 50.0 100.0 150.0 200.0 250.0 300.0 350.0 400.0 450.0 500.0 550.0 600
Cursor 29.91 3.12
Cursor 35.06 3.07

V067

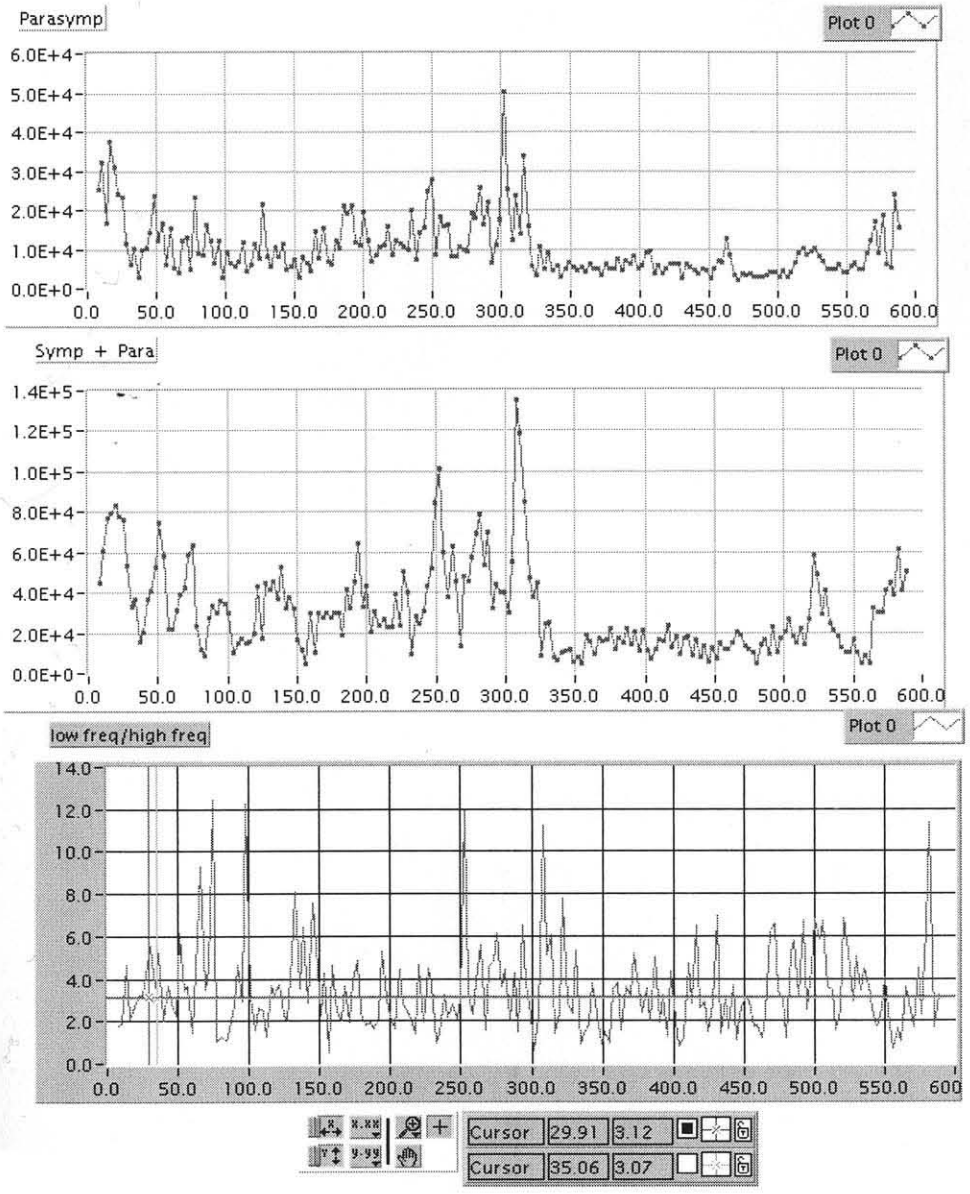
Parasymp
Plot 0
6.0E+4
5.0E+4
4.0E+4
3.0E+4
2.0E+4
1.0E+4
0.0E+0
0.0 50.0 100.0 150.0 200.0 250.0 300.0 350.0 400.0 450.0 500.0 550.0 600.0
Symp + Para
Plot 0
1.4E+5
1.2E+5
1.0E+5
8.0E+4
6.0E+4
4.0E+4
2.0E+4
0.0E+0
0.0 50.0 100.0 150.0 200.0 250.0 300.0 350.0 400.0 450.0 500.0 550.0 600.0
low freq/high freq
Plot 0
14.0
12.0
10.0
8.0
6.0
4.0
2.0
0.0
0.0 50.0 100.0 150.0 200.0 250.0 300.0 350.0 400.0 450.0 500.0 550.0 600
Cursor 29.91 3.12
Cursor 35.06 3.07

V082

APPENDIX C

PERL CODE

Perl code used to modify the files to get them in the proper format and split them into two. The duration from rest to tilt and the other from tilt to rest. Also it was used to remove unwanted trailing zeros.

```
#!/usr/bin/perl
$ARGV[0] || die "No data file specified\n";
$file = $ARGV[0];
open (junk, "tail -1 $file|");
while (<junk>)
{
    ($f, $s) = split ('\t', $_);
}
close junk;
open (junk, "< $file") || die "Cannot open input file\n ";
open (out, "> a.$file.ecg") || die "Cannot open output file one\n ";
open (out1, "> b.$file.ecg") || die "Cannot open output file two\n";
while(<junk>)
{
    ($first, $sec) = split ('\t', $_,2);
    if ($sec < 600)
{
        print out "$first\t$sec";
```

```
}
 if ($sec > $s - 600) {
open (out, "> a.$file.ecg") || die "Cannot open output file one\n ";
open (out1, "> b.$file.ecg") || die "Cannot open output file two\n";
while(<junk>)
{
      ($first, $sec) = split ('\t', $_,2);
      if ($sec < 600)
      {
     print out "$first\t$sec";
      }
      if ($sec > $s - 600)
         {
            print out1 "$first\t$sec";
         }
}
close out;
close out1;
close junk;
```

APPENDIX D

EXCEL MACRO

Excel Macro for removing the blank rows

The following subroutine opens the file in Excel and interchanges the rows and multiplies them by 200 the sampling frequency.

```
Sub complete()
'
' complete Macro
' Macro recorded 11/29/98 by Shrenik Dagli
'
' Keyboard Shortcut: Ctrl+c
'
ChDir "C:\LABVIEW\Temp1\original_data"
Workbooks.OpenText FileName:="C:\LABVIEW\Temp1\original_data\v082hrv.ecg", _
Origin:=xlWindows, StartRow:=1, DataType:=xlDelimited,
TextQualifier:=xDoubleQuote, ConsecutiveDelimiter:=False, Tab:=True,
Semicolon:=False, Comma:=False, Space:=False, Other:=False,
FieldInfo:=Array(Array(1, 1), Array(2, 1))
Application.Run "Book4.xls!nulldel"
Application.Run "Book4.xls!nulldel"
Columns("A:B").Select
Selection.Copy
```

```
Columns("D:E").Select
ActiveSheet.Paste
Columns("B:B").Select
Application.CutCopyMode = False
ActiveCell.FormulaR1C1 = "=RC[3]*200"
Range("B1").Select
' Application.Run "Book4.xls!complete"
Range("B1").Select
' Application.Run "Book4.xls!complete"
 Selection.Copy
 Columns("B:B").Select
 ActiveSheet.Paste
 Application.CutCopyMode = False
 Columns("B:B").Select
 Selection.Copy
 Columns("A:A").Select
 Application.CutCopyMode = False
 Columns("A:A").Select
 Selection.Delete Shift:=xlToLeft
 Columns("B:B").Select
 Selection.Delete Shift:=xlToLeft
 Range("D1").Select
```

```
ChDir "C:\LABVIEW\Temp1\original_data\original_data_text"
ActiveWorkbook.SaveAs FileName:=
"C:\LABVIEW\Temp1\original_data\original_data_text\v082hrv.ecg",
FileFormat:=xlText, CreateBackup:=False
ActiveWindow.Close
Workbooks.OpenText FileName:= _
"C:\LABVIEW\Temp1\original_data\original_data_text\v082hrv.ecg",
Origin:= xlWindows, StartRow:=1, DataType:=xlDelimited,
TextQualifier:=xlDoubleQuote, ConsecutiveDelimiter:=False, Tab:=True,
Semicolon:=False, Comma:=False, Space:=False, Other:=False, FieldInfo:=Array(1, 1)
Columns("C:C").Select
Selection.Delete Shift:=xlToLeft
ActiveWorkbook.SaveAs FileName:= _
"C:\LABVIEW\Temp1\original_data\original_data_text\v082hrv.ecg",
FileFormat:= xlText, CreateBackup:=False
ActiveWindow.Close
End Sub
```

The following subroutine removes the blank rows from datafile.

```
    Sub nulldel()
    '
```

```
'nulldel Macro
'Macro recorded 11/29/98 by Shrenik Dagli
,
'Keyboard Shortcut: Ctrl+n
,
For counter = 1 To 2000
  Set m = Worksheets("v082hrv").Cells(counter, 1)
  If m.Value = "" Then
   Rows(counter).Delete
   End If
   Next counter
End Sub

Sub convert()
,
'convert Macro
'Macro recorded 12/19/98 by Shrenik Dagli
,
'Keyboard Shortcut: Ctrl+q
,
LineNo% = 5
```

```
myfile$=
Dir("C:\LABVIEW\Temp1\original_data\original_data_text\results\r\a\laboutput\results\v
*_2")
        Do While myfile <> ""
        extn$                                                    =
"C:\LABVIEW\Temp1\original_data\original_data_text\results\r\a\laboutput\results\"
Name$ = extn$ + myfile$
Workbooks.OpenText  FileName:=Name$  _,  Origin:=xlWindows,  StartRow:=1,
DataType:=xlDelimited, TextQualifier_  :=xlDoubleQuote, ConsecutiveDelimiter:=False,
Tab:=True,  Semicolon:=  _False,  Comma:=False,  Space:=False,  Other:=False,
FieldInfo:=Array(1, 1)
   Range("A1").Select
        Workbooks("book1.xls").Activate
        Set m = ActiveSheet.Cells(LineNo%, 1)
        m.Value = myfile$
        Workbooks(myfile$).Activate
           Call rem0(LineNo%, myfile$)
           Workbooks(myfile$).Close SaveChanges:=False
        myfile$ = Dir
        LineNo% = LineNo% + 1
        Loop
        End Sub
```

```
Sub rem0(LineNo%, myfile$)
'
' rem0 Macro
' Macro recorded 12/19/98 by Shrenik Dagli
'
' Keyboard Shortcut: Ctrl+o
'

Name$ = "v004_4"
'Set m = Worksheets(Name).Cells(1, 1)
Set m = ActiveSheet.Cells(1, 1)
a1! = m.Value
'Set m = Worksheets(Name).Cells(2, 1)
Set m = ActiveSheet.Cells(2, 1)
a2! = m.Value

If a1! > a2! Then
t! = a1!
a1! = a2!
a2! = t!
End If
```

```
startl% = ((10 - a2) / a1) + 3

endl% = ((280 - a2) / a1) + 3


For counter = startl To endl


 ' Set m = Worksheets(Name).Cells(counter, 1)

  Set m = ActiveSheet.Cells(counter, 1)

  Sum = Sum + m.Value

  Next counter


'Set m = Worksheets("comparision.xls").Cells(LineNo$, 2)

Average! = Sum / (endl - startl)

Range("c1").Select

ActiveCell.FormulaR1C1 = Average!

Range("c2").Select

ActiveCell.FormulaR1C1 = startl%

Range("c3").Select

ActiveCell.FormulaR1C1 = endl%

Workbooks("book1.xls").Activate

Set m = ActiveSheet.Cells(LineNo%, 4)

m.Value = Average!
```

```
Workbooks(myfile$).Activate
startl% = ((315 - a2) / a1) + 3
endl% = ((580 - a2) / a1) + 3
For counter = startl To endl
' Set m = Worksheets(Name).Cells(counter, 1)
  Set m = ActiveSheet.Cells(counter, 1)
   Sum = Sum + m.Value
   Next counter
Set m = Worksheets("comparision.xls").Cells(lineno$, 5)
Average! = Sum / (endl - startl)
Range("d1").Select
ActiveCell.FormulaR1C1 = Average!
Range("d2").Select
ActiveCell.FormulaR1C1 = startl%
Range("d3").Select
ActiveCell.FormulaR1C1 = endl%
Workbooks("book1.xls").Activate
Set m = ActiveSheet.Cells(LineNo%, 8)
m.Value = Average!

End Sub
```

REFERENCE

[1] A .J. Vander , J.H. Sherman & D. S. Luciano, *Human Physiology*, NY, McGraw Hill Publishing Company, sixth edition 1994

[2] A C Guyon, *Text book of Medical Physiology*, Philadelphia, W. B. Saunders Company 8th Edition, 1991

[3] M.D. Kamath and E.L Fallen, "Power spectral analysis of heart rate variability: a noninvasive signature of cardiac autonomic function," *Crit. Rev. in Biomed Eng.*, vol.21, no. 3, pp. 245-311, 1993.

[4] G.G. Bemtwon, J.T. Cacioppo, and K.S. Quigley, "Respiratory sinus arrhythmia: Autonomic origins, physiological mechanisms, and psychophysiological implications," *Psychophysiology, Vol.* 30, pp. 183-196, 1993.

[5] S.J. Shin, W.N. Tapp, S.S. Reisman, and Natelson, "Assessment of autonomic regulation of heart rate variability by the method of complex demodulation," *IEEE Trans. on Biomed Eng.* 36, no. 2, pp 274-282, 1989.

[6] R. Saliba, S. Femando, and S.S. Reisman, "Autonomic nervous system evaluation using instantaneous frequency," *Proceedings of the 2lst IEE Annual Northeast Bioengineering Conference,* Maine, 1994.

[7] M. Pagani, F. Lombardi, S. Guzzetti, 0. Rimoldi, R. Furlan, P. Pizzinelli, Sandrone, G. Malfatto, S. Del' Orto, E. Picc.Vuga, M.,Ttiriel, G. Baselli, S. Cerutti, and A. Malliani, "Power spectral analysis of heart rate and arterial pressure variabilities as a marker of sympatho-vagal interaction in man and conscious dog," *Circulation Res.,* Vol. 59, pp. 178-93, 1986.

[8] P. Novak and V. Novak, "Time/frequency mapping of the heart rate, blood pressure and respiratory signals," *Medical & Biological Engineering & Computing,* Vol. 31, pp. 103-110, 1993.

[9] L. R. Rabiner and R. W. Schafer. *Digital Processing of Speech Signals* Englewood Cliffs, NJ: Prentice-Hall, 1978.

[10] A.S Gevins, "Analysis of the electromagnetic signals of human brain: Milestones, obstacles and goals," *IEEE Tans. on* Biomed. Eng., vol. 33, pp. 833-850,1984.

[11] L.G.Durand, A.P.Yoganathan, E.C.Harrison, and W.H.Corcoran, "A quantitative method for the in vitro study of sounds produced by prosthetic aortic heart valves," Parts 1-3. *Medical & Biological Engineering & Computing,* Vol. 22, pp. 32-54,1984.

[12] S, H. Nawab and T. F, Quatieri, "Short-time Fourier transform," in *Advanced Topics in Signal Processing,* J. S. Lim and A. V. Oppenheim, Eds. Englewood 1 Cliffs, NJ: Prentice-Hall, pp. 289-337, 1988.

[13] E. Wigner, "On the quantum correction for thermodynamic equilibrium," *Phys. Rev.,* Vol. 40, pp. 749-759, 1932

[14] J. Ville, "Theorie et applications de la notion de signal analytique," *Cables Transmiss.,* Vol. 20A, pp. 61-74,1948.

[15] W. Martin and P. Flandrin, "Wigner-Ville detection of changes of signal structure by using Wigner -Ville spectrum," *Sig. Proc.*, Vol. 8, pp. 215-233, 1985.

[16] R M. S S Abeysekera, , R. J. Bolton, L. C. Westphal, and B. Boashash, "Patterns ln Hilbert Transforms and Wigner-Ville distributions of electrocardiogram data," *Proc. IEEE ICASSP,* Tokyo, Vol. 34, pp. 1793-1796,1986.

[17] R. 1. Kitney and H. Talhami, "The zoom Wigner transform and its application to the analysis of blood velocity waveforms," *J. Theoret. Biol.,* vol. 129, pp. 395409, 1987.

[18] K. Kaluzynski, "Selection of a spectral analysis method for the assessment of velocity distribution based on the spectral distribution of ultrasonic Doppler signals," *Medical & Biological Engineering & Computing,* Vol. 27, pp. 463-469, 1989.

[19] J. J. Eggermont and G. M. Smith, "Characterising auditory neurons using the Wigner and Rihacek distribution: A comparison," *J. Acoust. Soc. Am.,* Vol. 87, pp. 246-259, 1990.

[20] D. T. Barry and N. M. Cole, "Muscle sounds are emitted at the resonant frequencies of skeletal muscle," *IEEE Trans. on BME,* Vol. 37, pp. 525-531, 1990.

[21] L. Cohen, "Time-Frequency Distributions - A Review," *Proceedings of the IEEE,* Vol. 77, no. 7, July 1989.

[22] B. Boashash. *Time-Frequency Signal Analysis Methods and Applications,* Wiley Halsted Press, NY, 1992.

[23] T.A.C.M. Classen and W.F.G. Mecklenbrauker. "The Wigner Distribution-a Tool for Time-Frequency Signal Analysis", *Philips J. Res.* 35, Part I, 217-250; Part II, 276-300; Part III 372-389, 1980.

[24] H. 1. Choi and W. J. Williams, "Improved time-frequency representation of multicomponent signals using exponential kernels, " *IEEE Trans. Acoust., Speech, Signal Processing,* vol. 37, no. 6, pp. 862-871, 1989.

[25] C. Zheng, A. Tornow, R. Kushwaha, and 1. C. Sackellares, "Time-frequency analysis of EEG recordings with the reduced interference distribution. " *Proc. 12th annu. Int. Conf. IEEE EMBS,* vol. 12, pp. 857,1990.

[26] H.P. Zaveri, W.J. Williams, and J.C. Sackellares, "Cross time-frequency representation of electrocorticograms in temporal lobe epilepsy," *Proc. 13th annu. Int. Conf. IEEE EMBS,* vol. 13, pp. 437-438, 1991.

[27] C. Zheng, S. E. Widmalm, and W. J. Williams, "New time-frequency analyses of EMO and TMJ sound signals," *Proc. 11th Annu. Int. Conf. IEEE EMBS,* vol. I 1, pp. 741-742, 1989.

[28] B. Sahiner and A. E. Yagle, "Application of time-frequency distributions to magnetic imaging of non-constant flow," *Proc. IEEE ICASSP,* pp. 1865-1868, 1990.

[29] J. Jeong and W. J. Williams. "Kernel design for reduced interference distributions", *IEEE Transactions on Signal Processing,* vol. 40, no. 2, February 1992.

[30] W. J. Williams, H. P. Zaveri, and J. C. Sackellares, "Time-frequency of Electrophysiology Signals in Epilepsy," *IEEE Engineering in Medicine & Biology,* pp. 133-143, March/April 1995.

[31] J. C. Wood and D. T. Barry, "Time-frequency analysis of the first heart sound," *IEEE Engineering in Medicine & Biology,* pp. 144-15 1, March/April 1995.

[32] R. F. Rushmer, "Structure and function of the cardiovascular system," in *Handbook of Research Methods in Cardiovascular Behavioral Medicine, N.* Schneiderman, S. M. Weiss, and P. G. Kaufmann, Plenum Press, NY, pp. 5-22, 1989.

[33] D. S. Krantz and J. Ratliff-Crain, "The social context of stress and behavioral medicine research," in *Handbook of research methods in cardiovascular behavioral medicine, N.* Schneiderman, S. M. Weiss, and P. G. Kaufmann, Plenum Press, NY, pp. 383-392, 1989.

[34] J. Mason, "Re-evaluation of the concept of non-specificity in stress theory," *Journal of Psychiatric Research,* vol. 8, pp. 323-333, 1971.

[35] G. R. Elliott and C. Eisdorfer. *Stress and Human Health,* Berlin: Springer, VA, 1982

[36] F. Cohen, M. Horowitz, R. Lazarus, R. Moos, L. Robins, R. Rose, and N. Rutter, "Panel report on psychosocial assets and modifiers of stress," in *Stress and human health,* G. Elliott and C. Eisdorfer, Berlin: Springer, pp. 147-288, 1982.

[37] R. S. Lazarus. *Psychological Stress and the Coping Process,* McGraw-Hill, NY, 1966.

[38] P. A. Obrist, C. J. Gaebelein, E. S. Teller, A. W. Langer, A. Grignolo, K. C. Light, and J. A McCubbin, "The relationship among heart rate, carotid dP/dt and blood pressure in humans as a function of the type of stress," *Psychophysiology,* vol. 15,pp. 102-115, 1978.

[39] S. B. Manuck, C .D. Corse, and P. A. Winkelmen, "Behavioral correlates of individual differences in blood pressure reactivity," *Journal of Psychosomatic Research,* 23, pp. 281-288, 1979.

[40] T. M. Dembroski, J. M. MacDougall, J. A. Herd, and J. C. Shields, "Effects of level of challenge on pressor and heart rate responses in type A and B subjects," *Journal of Applied Social Psychology,* vol. 9, pp. 209-228, 1979.

[41] D. C. Glass, L. R. Krakoff, R. Contrada, W. F. Hilton, K. Kehoe, E. G. Mannucci, C. Collins, B. Snow, and E. Elting, "Effect of harassment and competition upon cardiovascular and plasma catecholamine responses in Type A and Type B individuals," *Psychophysiology,* vol. 17, pp. 453-463, 1980.

[42] A. Szabo, F. Peronnet, G. Boudreau, L. Cote, L. Gauvin, and P. Seraganian, "Psychophysiological profiles in response to various challenges during recovery from acute aerobic exercise," *Intemational Joumal of Psychophysiology,* vol. 14, pp. 285-292, 1993.

[43] R. Saliba, "Bilinear time-frequency analysis," *Phd. Dissertation,* Dept. of Electrical Engineering, New Jersey Institute of Technology, Newark, New Jersey, October 1994.

[44] F. Hlawatsch and G. F. Boudreaux-Bartels. "Linear and Quadratic Time-Frequency Signal Representations", *IEEE Signal Processing Magazine,* pp. 21-67, April 1992.

[45] R. Ziemer, W. Tranter, and R. Fannin. *Signals and Systems: Continuous and Discrete.* Macmillan Publishing Company, New York. Second Edition. 1989.

[46] R. E. Ziemer and W. H. Tranter. *Principles of Communications.* Houghton Mifflin Company. Boston,Third Edition, 19-119, 1990.

[47] M. Amin, L. Cohen and W.J. Williams, "Methods and Applications for Time Frequency Analysis" *Conference Notes,* University of Michigan, Michigan, 1993.

[48] D. L. Jones and T. W. Parks, "A Resolution Comparison of Several TimeFrequency Representations", *IEEE Transactions on Signal Processing,* vol. 40, no. 2, February 1992.

[49] P. V. O'Neil. *Advanced Engineering Mathematics,* Wadsworth Publishing Company, Denver, Second Edition 575-585,1987.